Arch. Rational Mech. Anal. 166 (2003) 99–166
Digital Object Identifier (DOI) 10.1007/s00205-002-0216-7

Stability of Periodic Solutions of Conservation Laws with Viscosity: Analysis of the Evans Function

M. Oh & K. Zumbrun

Communicated by S. S. Antman

Abstract

Nonclassical conservation laws with viscosity arising in multiphase fluid and solid mechanics exhibit a rich variety of traveling-wave phenomena, including homoclinic (pulse-type) and periodic solutions along with the standard heteroclinic (shock, or front-type) solutions. Here, we investigate stability of periodic traveling waves within the abstract Evans-function framework established by R. A. Gardner. Our main result is to derive a useful *stability index* analogous to that developed by Gardner and Zumbrun in the traveling-front or -pulse context, giving necessary conditions for stability with respect to initial perturbations that are periodic on the same period T as the traveling wave; moreover, we show that the periodic-stability index has an interpretation analogous to that of the traveling-front or -pulse index in terms of well-posedness of an associated Riemann problem for an inviscid medium, now to be interpreted as allowing a wider class of measure-valued solutions, or, alternatively, in terms of existence and nonsingularity of a local "mass map" from perturbation mass to potential time-asymptotic T-periodic states. A closely related calculation yields also a complementary *long-wave stability criterion* necessary for stability with respect to periodic perturbations of arbitrarily large period NT, $N \to \infty$. We augment these analytical results with numerical investigations analogous to those carried out by Brin in the traveling-front or -pulse case, approximating the spectrum of the linearized operator about the wave.

The stability index and long-wave stability criterion are explicitly evaluable in the same planar, Hamiltonian cases as is the index of Gardner and Zumbrun, and together yield rigorous results of instability similar to those obtained previously for pulse-type solutions; this is established through a novel *dichotomy* asserting that the two criteria are in certain cases logically exclusive. In particular, we obtain results bearing on the nature and mechanism for formation of highly oscillatory Turing-like patterns observed numerically by Frid and Liu and Čanić and Peters in models of multiphase flow. Specifically, for the van der Waals model considered by Frid and Liu, we show instability of all periodic waves such that the period increases with

amplitude in the one-parameter family of nearby periodic orbits, and in particular of large- and small-amplitude waves; for the standard, double-well potential, this yields instability of all periodic waves. Likewise, for a quadratic-flux model like that considered by Čanić and Peters, we show instability of large-amplitude waves of the type lying near observed patterns, and of all small-amplitude waves; our numerical results give evidence that intermediate-amplitude waves are unstable as well. These results give support for an alternative mechanism for pattern formation conjectured by Azevedo, Marchesin, Plohr, and Zumbrun, not involving periodic waves.

1. Introduction

In this paper, we study stability of periodic traveling-wave solutions of *conservation laws with viscosity*,

$$u_t + f(u)_x = (B(u)u_x)_x, \tag{1.1}$$

$u, f \in \mathbb{R}^n$, $B \in \mathbb{R}^{n\times n}$, modeling flow in compressible media. Periodic solutions do not occur for classical systems (1.1) possessing a convex entropy in the sense of [Sm, Ka], for example, ideal gas dynamics or magnetohydrodynamics, being forbidden by energy considerations. However, they arise in a natural way in certain nonclassical systems modeling media with multiple phases, for example van der Waals gas dynamics and elasticity, or three-phase flow in porous media, in conjunction with a host of other complex phenomena not seen in classical conservation laws: in particular, hetero- and homoclinic cycles of traveling-front and -pulse type solutions, and associated nonuniqueness of Riemann solutions in the corresponding first-order system

$$u_t + f(u)_x = 0; \tag{1.2}$$

see, e.g., [Sl.1–Sl.5, Sh.1–Sh.3, AMPZ.1–AMPZ1.4, Z]. As discussed in [AMPZ.2], these features have the common seed of instability of constant solutions in certain regions of state space: in the case of phase-transitional models, regions that are "between phases". Such instability is frequently (but not always) associated with a change in type from hyperbolic to elliptic in the first-order system (1.2).

In the case of van der Waals gas and solid dynamics, there is a close relation between the mechanical model (1.1) and the variational Cahn-Hilliard model for phase transition; see Section 7 for further details. In particular, their stationary theories agree, reducing to the Euler-Lagrange equations for the associated van der Waals/Cahn-Hilliard energy: a planar Hamiltonian ordinary differential equation. Thus, it is no surprise that the mechanical model features the same rich solution structure found in the study of Cahn-Hilliard equations $u_{tt} + f(u) = u_{xx}$, or Allen-Cahn (reaction-diffusion) equations $u_t + f(u) = u_{xx}$ based on the same energy functional. Indeed, the existence of hetero-, homoclinic, and periodic cycles is already suggested by the planar Hamiltonian form of the stationary-wave ordinary differential equation.

On the other hand, the dynamics of these models are quite different, and so *a priori* it is not clear to what extent, or in what way, this stationary structure will be manifested in the asymptotic behavior of solutions. In particular, we would like to know whether the mechanical model (1.1) indeed supports persistent transition layers (fronts) between phases, and, more, whether it can successfully predict, at least at a qualitative level, the experimentally observed phenomena of nucleation (spontaneous formation of transition layers in previously smooth flow) and pattern formation (e.g., Martensitic crystal structure in stressed elastic solids). In the case of three-phase flow models commonly used in oil recovery simulation, with gas, water and oil treated as separate phases of a single fluid, both modeling and experimental data are less certain than in the case of the van der Waals model. Nonetheless, the same basic questions are of interest, now for purposes of experimental prediction and validation or invalidation of the mathematical model. These questions must be addressed in the context of the full, *dynamical* behavior of model (1.1), and ultimately involve the careful study of stability.

Stability and behavior of hetero- and homoclinic, or front- and pulse-type solutions of phase-transitional models have been investigated numerically and analytically in, e.g., [ZPM, AMPZ.1–AMPZ.3, LZ.1, LZ.2, GZ, Z.1, Z.2]. For both van der Waals and three-phase flow models, the picture that has emerged is that traveling-front solutions connecting one pure phase to another are stable, as are simple Riemann patterns involving two or more traveling fronts moving away from each other with nonzero speed, whereas traveling-pulse solutions connecting a single phase to itself, and therefore Riemann patterns in which they appear, are unstable. In terms of time-asymptotic dynamics, the latter seem to play the role of saddle points separating the basins of attraction of the former, attracting asymptotic states [AMPZ.1]. These studies essentially answer the first two questions posed above, showing that phase-transitional layers are indeed supported by the models, and can form spontaneously from smooth initial data. Moreover, the experiments of [AMPZ.1] show that a classical, stable small-amplitude Riemann pattern not involving phase transitions may bifurcate under an initial perturbation with compact support to a stable large-amplitude pattern involving two or more phase-transitional layers; this is a stronger sense in which nucleation is seen to occur.

The present investigation is motivated by the third question, concerning the possibility of *pattern formation* in models of form (1.1). Particularly intriguing are numerical experiments of Frid & Liu [FL.1, FL.2, LF] and Čanić & Peters [CP], in which Riemann solutions of various phase-transitional models were seen to exhibit highly oscillatory, Turing-like patterns reminiscent of Martensitic crystal structure or nucleation in phase-transitional elasticity. A natural conjecture, by analogy with similar phenomena in Cahn -Hilliard or reaction-diffusion equations, is that these are stable patterns consisting of fronts connecting various periodic or constant states: the classical mechanism for pattern formation.

Support for this point of view was given by recent investigations of Čanić [C] suggesting a connection with Hopf bifurcation and the appearance of limit cycles in the traveling-wave equations arising from the specific Riemann data associated with these phenomena. A closer look [AMPZ.4, AMPZ.5] reveals a rich global structure in the phase portraits of the associated traveling-wave ordinary differential

equations, which indeed feature large-amplitude periodic orbits resembling each of the observed oscillatory motifs. However, these periodic solutions appear in one-parameter families of varying wavelength, terminating in the infinite-wavelength limit at a hetero- or homoclinic cycle corresponding to a degenerate Riemann pattern of front- or pulse-type traveling-waves with common speed: a metastable, slowly interacting pattern of waves which by themselves would be stable. The criterion that would select a particular wavelength from among such a family is unclear. Moreover, in further numerical experiments [AMPZ.4, AMPZ.5], the patterns, though apparently robust, do not appear to settle down into a final, periodic configuration; rather, as conjectured in [AMPZ.4], they seem to be the result of complex metastable interactions of an infinite pattern of slowly interacting traveling fronts between pure phases, driven by linear instability in the limiting states at plus and minus spatial infinity (the "generalized Riemann data" in the sense of [AMPZ.1]).

More precisely, it appears that oscillations in phase originate at spatial infinity through a linear instability mechanism. A stationary phase calculation [AMPZ.5] reveals that the response under perturbation of the unstable constant states at infinity (i.e., the Green function of the constant-coefficient equations obtained by linearizing about constant solutions with those values) is well approximated by a sum of modulated, time-exponentially growing Gaussian wave-packets

$$\bar{\Psi}_j := \frac{e^{\mathrm{Re}\,\lambda(k_j^*)t}e^{ik_j^*(x-\alpha_j^* t)}e^{-(x-\alpha_j^* t)^2/4\beta_j^* t}}{\sqrt{4\pi\beta_j^* t}}\frac{r_j l_j^*}{\langle r_j, l_j\rangle}, \tag{1.3}$$

where k_j^* denotes the frequency for which the associated dispersion relation $\lambda_j(k)$ takes on its maximum real part (temporal growth rate), $i\alpha_j^* := -d\lambda_j/dk(k_j^*)$, $\beta_j^* := -(1/2)d^2\lambda_j/dk^2(k_j^*)$, and r_j, l_j denote right and left eigenvectors of the flux Jacobian $df(u)$ evaluated at the background constant state. The waves $\bar{\Psi}_j$ might be called *unstable linear diffusion waves*, by analogy with the picture given by LIU & ZENG [LZe] in the stable case. Their oscillations grow exponentially in amplitude until they reach the nonlinear regime, at which time they sharpen into slowly moving fronts connecting approximately pure phases and do not grow further.

Note that this process does not involve periodic waves, or even their infinite-wavelength heteroclinic-cycle limit. The average wavelength of the pattern is, rather, closely approximated by the characteristic wavelength of the *linear* oscillations originating at spatial infinity, i.e., the rate at which new waves are "born". Likewise, the "front" separating an oscillatory region from an unstable constant state is just the front edge of the linear Gaussian wave-packet, whose speed of propagation can be well approximated by tracking the point at which the Gaussian envelope reaches a fixed amplitude representing the transition to nonlinear dynamics. For more detailed discussion, and a derivation of (1.3), see Appendix B. This description, if correct, represents a novel and nonclassical mechanism for pattern formation, different from that seen in Cahn-Hilliard and reaction-diffusion models for phase transition. Indeed, it seems more related to certain models for turbulence, in which energy from high frequency modes drives the evolution of characteristic large-scale structures on a lower-dimensional attracting manifold.

It seems difficult to rigorously verify this picture of pattern formation, which by its nature lies outside the usual analytical frameworks. However, it is possible to give indirect support by eliminating the more usual scenario involving periodic waves. For, recall that the patterns of [FL.1, FL.2, LF, CP], consist of one or more oscillatory regions sandwiched between two unstable constant regions extending to plus and minus spatial infinity. If these oscillatory regions indeed represent pieces of different periodic solutions, then the most likely scenario is that at least one of these periodic solutions should be *stable*; the alternative, a stable pattern consisting entirely of unstable pieces, would represent a new type of dynamic stabilization for which we know of no possible mechanism. Thus, it is strong evidence against the classical scenario if we can show that there exist no large-amplitude stable periodic solutions lying near to the observed oscillatory patterns.

Motivated by these considerations, we here study the general question of stability of periodic solutions of conservation laws with viscosity. Of particular interest is the situation present in the above-mentioned numerical studies, of a planar, periodic family of solutions, originating from a nonlinear center and bounded by a limiting homoclinic or heteroclinic cycle, i.e., a typical (global) Hopf bifurcation [GH, HK].

Our analysis is by spectral Evans-function techniques, using an analytic framework developed by GARDNER [G.1–G.3]. Specifically, changing coordinates to a rest frame for the traveling wave $\bar{u}$, we obtain the linearized equation

$$v_t = Lv := (Bv_x)_x - (Av)_x, \tag{1.4}$$

about the (now stationary) wave $u = \bar{u}(x)$. We shall investigate stability of $\bar{u}$ by the study of the spectrum of the linearized operator L about the wave. More precisely, we investigate the *weak spectral stability* of $\bar{u}(\cdot)$ as a solution of (1.1), defined as

$$\sigma(L) \subset \{\mathrm{Re}\ \lambda \leqq 0\}, \tag{1.5}$$

i.e., nonexistence of time-exponentially unstable eigenmodes. Note that failure of (1.5) implies exponential linearized and (appropriately defined) nonlinear instability; hence, the study of spectral stability is appropriate for investigation of *instability phenomena*. (Linearized *stability* involves different issues, and will be discussed in a companion paper [OZ].)

Following GARDNER [G.1–G.3], we study the spectrum of L "directly", via the *periodic Evans function*, a determinant $D(k, \lambda)$ involving the monodromy matrix of the linearized eigenvalue equation

$$(L - \lambda)w = 0 \tag{1.6}$$

for L, whose zero set (k, λ) corresponds to bounded solutions $e^{ikx}w(x)$ of (1.6), with w periodic; for a detailed derivation, see Section 2. This approach has the advantage of generality, whereas more specialized analyses based on variational [M.1, M.2, LP] or Hamiltonian [Mi] structure may take better advantage of the specific structure of the underlying evolution model. For conservation laws (1.1), there does not seem to be any such useful structure to which we may appeal.

Evans-function techniques have been used successfully to study the stability of traveling-front and -pulse solutions; however, computations in the periodic case become considerably more complicated. Indeed, to our knowledge, ours is one of only three such explicit computations that have been carried out using Gardner's framework, the others being low-frequency expansion of the Evans function $D(k, \lambda)$ in the wave number k, carried out by ESZTER [Es] in a singularly perturbed limit and by SANDSTEDE & SCHEEL [SS.1] in the large-amplitude (long-period) limit. These previous analyses were obtained by different techniques, in the somewhat different reaction-diffusion setting, and under hypotheses that do not apply here: in particular, that zero be a simple eigenvalue of the linearized operator about the wave. However, the main distinction of the present analysis is that it is not in principle restricted to any type of limiting case, giving useful stability criteria for waves of arbitrary amplitude or type. (On the other hand, as we shall see, such limiting situations can be extremely helpful in the analytic evaluation of these criteria). This feature distinguishes our results also from those obtained in, e.g., [M.1, M.2, BMi.1, BMi.2, Mi] by other than Evans-function techniques, all of which concern the limiting cases of a large-amplitude bounding cycle or a small-amplitude constant solution.

Abstract result 1. Our main result is the development of a stability index analogous to that obtained by GARDNER & ZUMBRUN [GZ] in the traveling-front or -pulse context, relating evolutionary stability to the dynamics of the traveling-wave ordinary differential equation. Specifically, we show that

$$\Gamma = \operatorname{sgn} \gamma \Delta \det df(u_-) \gtrless 0 \tag{1.7}$$

is necessary for stability with respect to periodic perturbations of the same period as the background wave, where γ is a transversality coefficient for the traveling-wave ordinary differential equation

$$u' = B^{-1}(u)(f(u) - f(u_-) - s(u - u_-)), \tag{1.8}$$

$$\bar{u}(0) = \bar{u}(T) = u_0, \tag{1.9}$$

and $\Delta := \det(\partial \bar{u}_m / \partial u_-)$, where $\bar{u}_m$ denotes the mass over one period of the periodic profile $\bar{u}(\cdot)$ and $u_- \in \mathbb{R}^n$ is an artificial parameter. For a detailed derivation of (1.8), (1.9) and precise definitions of γ and Δ, see Sections 2 and 5, respectively.

Similarly as in the traveling-front or -pulse case [GZ, BSZ, ZS, Z.3], the coefficient Δ is seen to be related to well-posedness of an associated inviscid Riemann problem; however, this must now be interpreted in the context of measure-valued solutions appropriate for oscillatory solutions. Alternatively, $\Delta \neq 0$ may be viewed as expressing the existence and nonsingularity of a local "mass map" from perturbation mass to potential time-asymptotic T-periodic states, an evident necessary condition (by conservation of mass) for orbital stability of $\bar{u}$ with respect to nonzero mass perturbations within the class of T-periodic solutions of (1.1); for further discussion, see Section 5.

Abstract result 2. The stability index Γ detects strong (time-exponentially growing) instabilities analogous in the front or pulse case to an unstable point spectrum of the

linearized operator about the wave. By closely related computations, we derive also a complementary long-wave stability criterion detecting weak (time-algebraically growing) instabilities, analogous in the front or pulse case to an unstable essential spectrum, or linearized instability of the limiting, constant states connected by the profile of the traveling wave. Whereas the stability index concerns instability with respect to periodic perturbations with the same period as the background wave, the long-wave stability criterion concerns instability with respect to periodic perturbations on a different period, in the limit as this period goes to infinity: i.e., so-called "sideband instabilities". Specifically, in the "quasi-Hamiltonian" case, where the traveling-wave ordinary differential equation (1.8) has an integral of motion, we establish an illuminating small-frequency expansion

$$\begin{aligned} D(k,\lambda) = \gamma\lambda \det\big(-\lambda(\partial\bar u_m/\partial u_-)df(u_-)^{-1} - ikT\big) \\ + \mathcal{O}\big((|k|+|\lambda|)^{n+2}\big), \end{aligned} \tag{1.10}$$

of the Evans function, where γ and $(\partial\bar u_m/\partial u_-)$ are as described just above. This yields a distinguished dispersion relation

$$\lambda_0(k) = o(k) \tag{1.11}$$

and n dispersion relations

$$\lambda_j(k) = -ikT\alpha_j + O(k^2), \quad j = 1,\dots,n, \tag{1.12}$$

where α_j denote the eigenvalues of $(\partial\bar u_m/\partial u_-)^{-1}df(u_-)$. Relations (10.3) generalize those seen in the constant-coefficient case, for which $\partial\bar u_m/\partial u_-$ reduces to I; for further discussion see Example 3.4 and Remarks 3.5 and 5.10. In particular, they show that the "generalized hyperbolicity" requirement

$$\sigma\Big((\partial\bar u_m/\partial u_-)^{-1}df(u_-)\Big) \text{ real} \tag{1.13}$$

is necessary for long-wave stability.

Remark 1.1. There is a further analogy between conditions (1.7) and (1.13) and the stability index and long-wave stability conditions arising in the study of multi-dimensional planar viscous shock fronts [GZ, BSZ, ZS, Z.3], where, similarly, the stability index concerns strong instability with respect to planar perturbations respecting the symmetry of the background solution, while the long-wave stability condition concerns weak instability with respect to perturbations with small but nonzero transverse frequency. However, the origins of the long-wave dispersion relations are rather different in the two cases; in particular, (6.1) appears to be closely tied to the assumed quasi-Hamiltonian structure, whereas the corresponding expansion in the shock front case is completely general.

Numerical results. Along with these analytic tools, we develop also numerical techniques for approximating the spectrum of the linearized operator about the wave, analogous to those developed by Brin [Br.1, Br.2, BZ] and Brin & Zumbrun [BZ] in the traveling-front or -pulse case. Here, the issues are rather different.

For example, the evaluation of the Evans function in the periodic case is numerically straightforward, since it involves only integration of a well-behaved ordinary differential equation on a finite interval; by contrast, the traveling-front or -pulse case involves integration on an infinite interval, making the problem stiff. On the other hand, the location of the spectrum, that is, the zero set $(k, \lambda(k))$ of the Evans function $D(\cdot\,,\cdot)$ becomes considerably more complicated than in the traveling-front or -pulse case, for which the Evans function depends on a single argument only. In particular, it is quite difficult to resolve the $n+1$ curves (1.11), (10.3) bifurcating from the point $(k, \lambda) = (0, 0)$. Thus, our numerical techniques are effectively restricted to (k, λ) bounded away from the origin, and so are complementary to the analytical techniques described above, which include but are not limited to the Taylor expansion of D about the origin.

Applications. The stability index and long-wave stability criterion are explicitly *comparable* in the same "planar Hamiltonian" case for which the index of Gardner and Zumbrun was explicitly *evaluable* in the traveling-front or -pulse case, namely, the case for which the traveling-wave ordinary differential equation (1.8) is planar Hamiltonian for some distinguished speed; and together these yield rigorous results of instability similar to those obtained previously for pulse-type solutions in [GZ, Z.1] In this case, using a Poincaré-Bendixon argument similar to that used in [GZ], we may express the sign of the Melnikov integral γ appearing in the stability index in terms of the sign of the derivative dT/da of period T with respect to amplitude a in the embedding family of nearby periodic orbits of (1.8), i.e., as simply

$$\operatorname{sgn} \gamma = \operatorname{sgn} dT/da. \tag{1.14}$$

This reduces both stability conditions (1.7) and (1.13) to requirements on the derivative $\partial \bar{u}_m/\partial u_-$, a quantity which in the small-amplitude and the large-amplitude homoclinic limits approaches the identity.

In general (i.e., for intermediate-amplitude waves), $\partial \bar{u}_m/\partial u_-$ seems difficult if not impossible to evaluate analytically. Nonetheless, we are able to obtain rigorous instability results through a novel *dichotomy*, asserting that criteria (1.7) and (1.13) are in certain cases logically exclusive, based only on structure or symmetries of $\partial \bar{u}_m/\partial u_-$ rather than its precise value. The basic strategy is to show the matrix $df(u_-)(\partial u_m/\partial u_-)^{-1}$ to be trace-free, in which case its eigenvalues are real if and only if its determinant is negative and thus $\Gamma = -\operatorname{sgn} dT/da < 0$ if $dT/da > 0$. (Recall that $df(u_-)(\partial u_m/\partial u_-)^{-1}$ is 2×2 in the planar case we consider.) Specifically, we show that for the equations of van der Waals gas dynamics and elasticity there exist *no* stable periodic solutions, of any amplitude, with the property that period increases with amplitude in the one-parameter family of nearby periodic orbits: in particular that large-amplitude waves are unstable. A separate argument shows that small-amplitude solutions are unstable, due to Majda-Pego instability of the limiting constant state [MP]. In the case of a standard double-well potential, it can be shown that the period is everywhere monotone increasing (see Remark 7.2, below), and so *all periodic solutions are unstable*. Likewise, for the special (Hamiltonian) class of planar, quadratic-flux systems considered in [GZ] we establish instability of large-amplitude waves lying near the numerically observed patterns, and (by a separate, continuity argument) of small-amplitude solutions.

These two cases are quite relevant to the issue of pattern formation that originally motivated our investigations. The former equations, modeling phase-transitional fluids/solids, are precisely those that were seen to exhibit pattern formation in the numerical investigations of [FL.1]. The latter, which serve as qualitative models for multiphase flow in porous media, are prototypical for the other models in which pattern formation has been observed [FL.2, CP, AMPZ.4, AMPZ.5]. Indeed, taken together, our results are strongly suggestive of nonexistence of *any* stable periodic waves in the cases where oscillatory patterns have been observed. Further support for this conjecture is given by our numerical experiments, in which we find instability of periodic solutions across their entire (numerically determined) region of existence. Our results thus appear to eliminate from consideration the usual paradigm of multiple stable periodic states, pointing to a *different mechanism* for pattern formation in multiphase conservation laws than that typically seen in reaction-diffusion equations: for example, the one proposed in [AMPZ.4, AMPZ.5].

Besides the direct, physical interest of our conclusions, we point out an indirect contribution of this paper that is perhaps more important. Namely, we provide a useful, and *explicit* analogy between the Evans-function framework for the periodic case and that of the better-studied traveling-front or -pulse case, *different than the large-period limit* studied by GARDNER [G.1, G.2]. In the present paper, we have applied this analogy to the results of [GZ, Z.1, BSZ, ZS, Z.3] to obtain interesting instability results in the context of conservation laws with viscosity, i.e., *necessary* conditions for stability. A similar translation of the complementary pointwise semigroup methods developed in [ZH] yields interesting *sufficient* conditions for linearized stability; these results will be presented in the companion paper [OZ].

Discussion and open problems. The quasi-Hamiltonian assumption made in deriving (6.1) seems to be fundamental for the evaluation of the long-wave viscosity criterion. Besides appearing frequently in physical examples, quasi-Hamiltonian systems are shown in [OZ] to be the *only* type that can support periodic waves that are asymptotically stable in the usual, diffusive sense (see further discussion, beginning of Section 6).

A related assumption on the structure of stationary solutions is made by BRIDGES & MIELKE [BMi.2] in their powerful study, by quite different, center manifold techniques, of instability of *multi-dimensional* but small-amplitude periodic waves in the Cahn-Hilliard/Allen-Cahn setting

$$m\Psi_{tt} + d\Psi_t = \Psi_{xx} + \Psi_{yy} + dF(\Psi), \tag{1.15}$$

F, Ψ, $x \in \mathbb{R}$, $y \in [0, \pi]$ with periodic boundary, $m, d \geqq 0$. Namely, they assume that the center manifold of small bounded solutions of the stationary equation near some rest point is foliated by periodic solutions consisting of level sets of an appropriate "spatial" Hamiltonian: that is, it has the same solution structure as does the (planar Hamiltonian) one-dimensional stationary equation

$$\Psi_{xx} = dF(\Psi) \tag{1.16}$$

obtained formally by shrinking the y-dimension to zero in (1.15). Likewise, this structure is present, and used in an important way in the authors' (related) landmark

study of Benjamin-Feir instability in [BMi.1] and in MIELKE's characterization, using a Lyapunov-Schmidt type reduction, of linearized stability of roll-up solutions of the Swift-Hohenberg equation [Mi].

It is interesting to compare our results with those of BRIDGES & MIELKE in [BMi.2]. They derive a relation (see Lemma 4.1 of the reference)

$$\tilde{D}(k, \Lambda) = b_0(\Lambda - Ck^2) + O(|\Lambda|^2 + |k||\Lambda| + |k|^3) \tag{1.17}$$

similar to our (6.1), with

$$b_0 \neq 0, \quad \text{sgn } C = \text{sgn } dT/da. \tag{1.18}$$

Here, $\Lambda := m\lambda^2 + d\lambda$ is the generalized spectral parameter arising in the eigenvalue equation associated with the linearized stability problem, and $\tilde{D}$ is essentially an Evans function for the reduced eigenvalue equation they obtain by center manifold reduction. From (1.17), (1.18) there follows immediately the geometric necessary condition

$$dT/da < 0 \tag{1.19}$$

for stability that is their main result: equivalently, a sufficient condition $dT/da > 0$ for instability. It is to be noted that *this is a sideband-type instability condition, and not a stability index* in the sense of our condition (1.7).

This result generalizes well-known results in the one-dimensional case (obtained by dropping y in (1.15)) relating $dT/da > 0$ to instability, described, e.g., in [IR]. However, as pointed out in [BMi.2, discussion below (1.13)], $dT/da < 0$ in the one-dimensional case *also implies instability*, though of a different kind: strong (large λ) rather than sideband instability. Thus, it might well be that such instabilities occur also in the multi-dimensional case, even though they are not detected by the sideband instability analysis of Bridges and Mielke.

In this regard, it is interesting to consider the stability of periodic solutions of the one-dimensional version

$$m\Psi_{tt} + d\Psi_t = \Psi_{xx} + dF(\Psi) \tag{1.20}$$

of (1.15) from the point of view of this paper. By exactly the same calculations used to establish (1.7), (6.1), and (1.14), we obtain for this problem a low-frequency expansion

$$D(k, \Lambda) = \gamma\Lambda - T^2k^2 + O(|\Lambda|^2 + |k||\Lambda| + |k|^3) \tag{1.21}$$

and a stability index

$$\Gamma = \text{sgn } \gamma = \text{sgn } dT/da; \tag{1.22}$$

indeed, the calculations reduce substantially in this case. Here, D as usual denotes the Evans function for the full (unreduced) eigenvalue equation associated with linearized stability, and $\Lambda := m\lambda^2 + d\lambda$ as above denotes the generalized spectral parameter arising in that equation. Thus, we not only recover the sideband instability analysis (1.17)–(1.19) of [BMi], but, through the stability index, detect also

strong instabilities in case $dT/da < 0$. That is, we see a similar dichotomy in a substantially different setting to the one used here to show instability of solutions of (1.1); in fact, the absence of the "hyperbolic factor" $\Delta = \partial \bar{u}_m / \partial u_-$ in the formulae makes the argument much simpler to apply in this case, and leads to a stronger result (instability without regard to sgn dT/da). Note that there is no requirement here on the amplitude of solutions.

The above discussion suggests that an Evans-function analysis based on "spatial dynamics" might be a possible direction for generalization of the multi-dimensional analysis of Bridges and Mielke, both to the case $dT/da < 0$ and to the case of large-amplitude waves. The Evans function described by SANDSTEDE & SCHEEL [SS.2], based on the Galerkin approximation on finite subspaces, appears to be a natural candidate for such investigations. This would be an extremely interesting direction for further study.

The analysis of (1.20) also suggests interesting questions in the one-dimensional case. Our results for the vectorial van der Waals phase-transitional model are now seen to be natural, though somewhat weaker, generalizations of those for the scalar phase-transitional model (1.20). But this suggests that it might be possible to obtain a weakened version of these results also for the vector version $\Psi \in \mathbb{R}^n$ of (1.20). Indeed, for more general equations $mu_{tt} + du_t = u_{xx} + G(u)$, $u \in \mathbb{R}^n$, in the quasi-Hamiltonian case, a low-frequency expansion

$$D(k, \Lambda) = \gamma \Lambda - \delta T^2 k^2 + O(|\Lambda|^2 + |k||\Lambda| + |k|^3), \tag{1.23}$$

is obtained, and a stability index $\Gamma = \text{sgn } \gamma$, where the transversality coefficient γ no longer has a simple geometric interpretation, and the coefficient δ is no longer explicitly evaluable. Thus, we do seem to obtain a result of instability when $\delta > 0$, analogous to that obtained for the van der Waals model when $dT/da > 0$. However, it is not clear whether $\delta > 0$ can in fact occur; this would be another interesting issue for further investigation. Likewise, in the conservation law setting, it would be interesting to determine whether or not the results for the van der Waals model carry over to the general planar Hamiltonian case, or even to the vector quasi-Hamiltonian case, *without* further assumptions restricting the structure of the matrix $\partial \bar{u}_m / \partial u_-$. We suspect strongly that the answer is "no", but do not so far have any counterexamples.

Finally, we mention the related analysis carried out by LAUGESEN & PUGH [LP] using quite different, variational methods, of stability under periodic perturbations of periodic solutions (with the same period) of the thin-film evolution model

$$h_t = (f(h)h_{xx} + g(h)h)_{xx} + ah, \tag{1.24}$$

$h \in \mathbb{R}$, in the zero-gravity case $a = 0$, which as far as we know is the only other treatment of stability of periodic waves in the conservation law setting (they obtain results also for $a \neq 0$, but these are not relevant to our discussion). Here again the stationary-wave equation is a second-order nonlinear oscillator, so planar Hamiltonian, even though the general (nonzero speed) traveling-wave equation is third-order. Applying our methods to this problem, we conjecture that it should be possible to recover a partial version of their results, namely a stability index

of $\Gamma = \text{sgn}\,(dT/da)$, where the derivative dT/da is taken with the area under h (i.e., the mass) held fixed, yielding instability whenever $dT/da < 0$.[1] (Laugesen and Pugh in fact *characterize* stability by this condition, obtaining positive stability results as well.) What is more interesting is that it might equally well be possible to carry out a low-frequency expansion analogous to (6.1), to obtain conditions for sideband instability as well. These were not treated in [LP], and do not seem to be accessible by their methods.

Remark 1.2. The planar Hamiltonian structure of (1.20) is what makes possible the explicit evaluation in (1.21) of the coefficient of the quadratic term in k. For systems of general type, this can usually be done only in some asymptotic limit; see for example the analyses of [Es, SS.1] in the large-amplitude limit.

Plan of the paper. In Section 2, we frame the problem, describing the equations and assumptions under consideration, and deriving traveling-wave and eigenvalue ordinary differential equations. In Sections 3 and 4, we define the Evans function, following [G.1, G.2], and recall a result of [G.2] relating the spectra of periodic waves in the large-amplitude (large-period) limit to that of a bounding homoclinic solution; we also explore briefly the more elementary small-amplitude limit, in which periodic waves approach a limiting, constant solution. In Section 5, we define a periodic-stability index analogous to that of the traveling-front or -pulse case, and establish the fundamental relation (1.7). In Section 6, restricting our attention to the quasi-Hamiltonian case, we derive by similar techniques the small-frequency expansion (1.10). This yields, in particular, an appealing formula for the "averaged", or effective constant-coefficient equation governing behavior under perturbation, and also gives further details completing the description of large-amplitude behavior given by GARDNER in [G.2]. Finally, restricting ourselves further to the planar Hamiltonian case, and applying a Poincaré-Bendixon argument similar to that used in [GZ], we obtain the sign of the Melnikov integral γ appearing in the stability index in terms of the sign of the derivative dT/da of period T with respect to amplitude a in the embedding family of nearby periodic orbits. In Section 7, we use the analytic tools developed in Sections 5 and 6 to establish rigorous instability results for the two classes of example systems described above. In Appendix A, we describe a numerical algorithm for location of the spectrum, and carry out systematic numerical experiments for the same two classes of example system; these support and in some cases extend our earlier analytical results. Finally, in Appendix B, we describe in detail the alternative mechanism for pattern formation proposed in [AMPZ.4, AMPZ.5], based on metastable configurations of slowly interacting fronts, driven by linear instability in the constant states at spatial infinity. As described in the appendix, these could be thought of as unstable nonlinear diffusion waves generalizing the stable versions described in [LZe].

[1] The situation here is somewhat degenerate due to the fact that the traveling-wave equation reduces in order at speed zero; indeed, condition (H3) of Section 2 is violated. However, the computation can still be carried out, as discussed in Remark 5.3 below.

2. Preliminaries

Consider a conservation law (1.1) and a periodic traveling-wave solution $u = \bar{u}(x - st)$, of period T, satisfying the traveling-wave ordinary differential equation

$$(B(u)u')' = f(u)' - su', \tag{2.1}$$

with initial conditions

$$\begin{aligned} \bar{u}(0) &= \bar{u}(T) =: u_0, \\ \bar{u}'(0) &= \bar{u}'(T) =: u_1. \end{aligned} \tag{2.2}$$

Here, and elsewhere, $'$ denotes $\partial/\partial x$. Integrating (2.1) from 0 to x, we obtain a first-order dynamical system

$$u' = B^{-1}(u)(f(u) - su - q), \tag{2.3}$$

$$\bar{u}(0) = \bar{u}(T) = u_0, \tag{2.4}$$

parametrized by $(q, s) \in \mathbb{R}^{n+1}$, where the "total flux"

$$\begin{aligned} q &:= B(u)u' - f(u) + su \\ &\equiv B(u_0)u_1 - f(u_0) + su_0 \end{aligned}$$

is a constant of motion. Notice that the map $(u_0, u_1) \to (u_0, q)$ is locally invertible so long as $\det B(u_0) \neq 0$, by the Inverse Function Theorem, hence we have lost no information by this reparametrization.

To emphasize the connection with the traveling-front or -pulse case, we assume further that there exists some rest point u_- of (2.3), i.e., $q = f(u_-) - su_-$, so that we can rewrite (2.3), (2.4) in the final form (1.8), (1.9) given in the introduction. We shall use this form of the equations throughout the paper. Recall that (1.8) is exactly the equation satisfied by a front- or pulse-type traveling-wave solution

$$u = \bar{u}(x - st), \quad \lim_{x \to \pm\infty} \bar{u} = u_\pm, \tag{2.5}$$

allowing the convenient comparison of front- or pulse-type and periodic solutions within the same dynamical system framework. Note, in the planar case of our main interest, that such a rest point always exists within the region bounded by a periodic wave, so there is no loss of generality in changing to the new coordinates; moreover, provided that u_- is a nondegenerate rest point, $\det(df(u_-) - sI) \neq 0$, the map $u_- \to q$ is again locally invertible.

We make the following nondegeneracy assumptions, analogous to those made in [GZ,ZH] for the traveling-front or -pulse case:

(H0) $f, B \in C^2$;
(H1) $\operatorname{Re} \sigma(B(\bar{u}(x))) > 0$ for all x;
(H2) $df(u_-) - sI$ invertible.
(H3) The traveling-wave profile $\bar{u}$ is a transversal orbit of traveling-wave equation (1.8) augmented with $s' = 0$, under periodic boundary conditions $u(0) = u(T)$; in particular, for fixed u_-, $\bar{u}$ is, locally, the unique T-periodic solution of (1.8) up to translation, even allowing variation in the speed of propagation s.

As mentioned above, (H2) concerns nondegeneracy of the parametrization (u_0, u_-, s) of (1.8), and thus is not strictly necessary for our analysis of periodic waves below; a similar analysis without this assumption can be carried out in (u_0, q, s) coordinates, with only minor expositional changes.

Note that assumption (H3) *does not preclude* the interesting case of a planar Hamiltonian ordinary differential equation possessing a family of nested periodic solutions, since generically the orbits of the periodic family have distinct periods; this will in fact be the main source of our examples in Sections 6 and 7.

Now, assume without loss of generality that speed $s = 0$, i.e., $u \equiv \bar{u}(x)$ is a *stationary* solution of (1.1). Linearizing (1.1) about $\bar{u}(\cdot)$, we obtain the usual linearized equation (1.4), where now A, B are *periodic*, rather than asymptotically constant as in the traveling-front or -pulse context. The eigenvalue equation for L is likewise

$$(Bw')' = (Aw)' + \lambda w, \tag{2.6}$$

where again '$'$' denotes $\partial/\partial x$, or, written as a first-order system:

$$W' = \mathbb{A}(\lambda, x)W, \tag{2.7}$$

where $W := (w, w')^t$ and coefficient

$$\mathbb{A} := \begin{pmatrix} 0 & I \\ B^{-1}(\lambda I + A') & B^{-1}(A - B') \end{pmatrix} \tag{2.8}$$

is a periodic $2n \times 2n$ matrix.

Through a study of the eigenvalue equations, we shall investigate the *weak spectral stability* of $\bar{u}(\cdot)$ as a solution of (1.1), as defined in (1.5). That is, we shall investigate whether or not the linearized operator L possesses unstable eigenmodes λ : $\mathrm{Re}\,\lambda > 0$. Failure of (1.5) implies *exponential linear instability* with respect to test-function initial data, as measured in any norms whatsoever; this can be seen by applying the evolution operator to $\phi\chi^M$ for M sufficiently large, where ϕ is a (merely bounded) unstable mode and $\chi^M(x) := \chi(x/M)$, with χ a smooth cutoff function that is 1 on $[-1, 1]$ and vanishes off $[-2, 2]$. By the "almost-finite propagation speed" property of (1.4), we find that the amplification of the resulting solution $v(t)$ in going from time zero to time t is of order

$$\|v(t)\|_{L^p}/\|v(0)\|_{L^q} \sim t^{1/p-1/q} e^{\mathrm{Re}\,\lambda t} \to \infty$$

as $t \to \infty$, precluding uniform $L^q \to L^p$ stability for any choice of p and q.

Remark 2.1. It is shown in [OZ] that *strong spectral stability*, defined as (1.5) augmented with appropriate nondegeneracy conditions (conditions (D1)–(D3) of [OZ]), implies linearized $L^1 \to L^p$ asymptotic stability for all $p > 1$, with uniform rates of decay equal to those for the standard heat equation.

3. The Evans function and the Spectrum of L

A brief calculation reveals that L has no point spectrum in L^p, $p < \infty$. Following [G.1, G.2], we introduce the *monodromy matrix*

$$M(\lambda) := \Psi(T, \lambda), \tag{3.1}$$

where $\Psi(\cdot, \lambda)$ is the fundamental solution of (2.7), i.e.,

$$\Psi' = \mathbb{A}(\lambda, x)\Psi, \quad \Psi(0, \lambda) = I \tag{3.2}$$

and T is the period of the coefficients. Then,

$$W(NT) = M(\lambda)^N W(0) \tag{3.3}$$

for any integer N, for any solution W of the eigenvalue equation (2.7), whence W can be at most bounded and not decaying at $\pm\infty$. Indeed, we have:

Proposition 3.1. *The spectrum $\sigma(L)$ consists, for all L^p, precisely of L^∞ eigenvalues, i.e., λ such that*

$$\det(M(\lambda) - \gamma) = 0, \quad |\gamma| = 1. \tag{3.4}$$

Proof. If $M(\lambda)$ has no eigenvalue of modulus 1, then there exist k "stable", i.e., with modulus less than 1, eigenvalues, and $2n - k$ "unstable", or with modulus greater than 1, eigenvalues, the associated normal modes decaying exponentially at $+\infty$ and $-\infty$ respectively, and linearly independent. We can thus construct a Green function G_λ, as in the asymptotically constant case, to obtain a bounded resolvent, hence $\lambda \in \rho(L)$. For further details, see [He, Z.3, Z.4, OZ].

On the other hand, L^∞ eigenvalues can be shown to lie in any L^p spectrum, by a standard limiting argument: specifically, by showing that

$$\|\chi^M \phi\|_{L^p} / \|(L - \lambda)\chi^M \phi\|_{L^p} \to \infty$$

as $M \to \infty$ for any bounded ϕ such that $(L - \lambda)\phi = 0$, where $\chi^M(x) := \chi(x/M)$ for any C^∞ cutoff function χ that is 1 on $[-1, 1]$ and vanishes off $[-2, 2]$. □

Loosely following [G.1, G.2], we define the *Evans function*

$$D(k, \lambda) := \det\left(M(\lambda) - e^{ikT}\right) \tag{3.5}$$

for any $(k, \lambda) \in \mathbb{R} \times \mathbb{C}$. Note that $D(k, \lambda)$ is clearly jointly analytic in k and λ on all of $\mathbb{R} \times \mathbb{C}$; thus, it is somewhat better behaved than the corresponding object in the traveling-front or -pulse case, see [GZ, ZH] for further discussion. From Proposition 3.1, we have immediately:

Corollary 3.2. *The spectrum of $\sigma(L)$ consists of the set of all λ such that $D(k, \lambda)$ vanishes for some k.*

In the terminology of [G.1, G.2], points λ satisfying (3.4) are called γ-eigenvalues; we will call them k-eigenvalues, where $\gamma = e^{ikT}$. The parametrization by k gives a more transparent analogy to the analysis by Fourier transform of the constant-coefficient case, see Example 3.4 just below (or, see [OZ] or [S.1–S.3] for a deeper discussion of this analogy).

Remark 3.3. More generally,

$$M(\lambda) = \widetilde{\Psi}(L)\widetilde{\Psi}^{-1}(0) \tag{3.6}$$

for any matrix $\widetilde{\Psi}$ of solutions of (2.7). The coordinate-independent representation (3.6) is quite useful in computations. Likewise, $D(\cdot\,,\cdot)$ is invariant under linear changes of coordinates,

$$\Psi \to P(x)\Psi, \tag{3.7}$$

with P periodic. (Note that this includes changes of coordinates at the level of (2.6), but also more general ones at the level of phase coordinates, (2.7).)

It is interesting to compare this to the spectrum of L considered as an operator on periodic functions $L^2[0, T]$. Necessarily discrete, the spectrum of L acting on the bounded interval $[0, T]$ corresponds precisely to the set of $(k = 0)$-eigenvalues of L acting on the unbounded domain; conversely, $(k = 0)$-stability corresponds to stability with respect to periodic perturbations of period T. More generally, $(k = 2\pi m/n)$-stability corresponds to stability with respect to perturbations that are periodic with period nT; letting $n \to \infty$, we recover stability with respect to *general perturbations*. Applying the Implicit Function Theorem to (3.4), we find that the spectrum of L on the real line consists typically of *curves* of k-spectra, given by the closure of the spectra of L considered as an operator on periodic functions over all multiple intervals $[0, nT]$, n an integer.

Example 3.4. In the constant-coefficient case, $Lv := Bv_{xx} - Av_x$ with A, B identically constant, an elementary computation yields

$$D(k, \lambda) = \Pi_{j=1}^{2n}(e^{\mu_j(\lambda)T} - e^{ikT}),$$

where μ_j, $j = 1, \ldots, 2n$ denote the roots of the characteristic equation

$$\det(B\mu^2 - A\mu - \lambda) = 0 \tag{3.8}$$

associated with eigenvalue equation (2.7). On the set of λ such that $\mathbb{A}$ is diagonalizable, this is easily seen by changing coordinates to a basis in which it is diagonal, see Remark 3.3; recalling that this set is dense, we obtain the full result by continuity. Thus, the zero set of D consists of all k, λ such that

$$\mu_j(\lambda) = ik \pmod{2\pi i/T} \tag{3.9}$$

for some j. Setting $\mu = ik$ in (3.8), we obtain the dispersion relation

$$\det(\lambda - ikA - k^2B) = 0, \tag{3.10}$$

recovering the standard characterization of $\sigma(L)$ by Fourier transform.

Note that $D(0,0) = 0$ in the example above, for any choice of A, B, since $\mu = 0$ is an n-fold root of (3.8) at $\lambda = 0$; we shall see later that this holds also in the general variable-coefficient case. An obvious necessary condition for stability is thus:

$$(\partial/\partial k)\lambda_*(0) \quad \text{is imaginary,} \tag{3.11}$$

where $\lambda_*(k)$ is any smooth root of $D(k, \lambda_*(k)) \equiv 0$ bifurcating from $\lambda_*(0) = 0$. For, otherwise there would exist exponentially unstable modes $\lambda = \lambda_*(k)$ for k sufficiently small (in fact for all $k > 0$ or all $k < 0$, depending on sgn Re $(\partial/\partial k)\lambda_*(0)$). We shall make essential use of this simple observation later on.

Remark 3.5. In the constant-coefficient case, relation (3.10) yields expansions

$$\lambda_j(k) = 0 - ia_jk + \cdots, \quad j = 1, \ldots, n, \tag{3.12}$$

for the n roots bifurcating from $\lambda(0) = 0$, where a_j denote the eigenvalues of A. Thus, we obtain the necessary stability condition of *hyperbolicity*, $\sigma(A)$ real.

4. A result of Gardner

Before beginning our main analysis, we recall an interesting related result of GARDNER [G.2] concerning a particular (rather typical) kind of large-amplitude limit for a family of periodic waves. Specifically, consider the situation of a family of periodic traveling waves $\{\bar{u}^\varepsilon\}$, approaching as $\varepsilon \to 0$ a limiting homoclinic, or "pulse-type", solution $\bar{u}^0$, the vertex of which is a nondegenerate (i.e., hyperbolic) rest point of the associated traveling-wave ordinary differential equation. Here, $\bar{u}^\varepsilon$ may be taken without loss of generality to be stationary (i.e., zero speed), and the partial differential equations they solve to vary smoothly with ε, so long as $\varepsilon \to 0$ is a regular perturbation, with all ε-equations parabolic of some fixed order. Included in this framework is the usual case of traveling-wave solutions of the *same* (parabolic) partial differential equation, with possibly differing speeds, approaching a homoclinic separatrix in the $\varepsilon \to 0$ limit.

In this scenario, as $\varepsilon \to 0$, the period T^ε of $\bar{u}^\varepsilon$ goes to infinity, while the profile on a single period $[0, T^\varepsilon]$ approaches uniformly an appropriate shift of the homoclinic profile $\bar{u}^0$, without loss of generality to $\bar{u}^0(x - T/2)$. Thus, it is natural to ask whether the stability properties of periodic waves may be related in the large-period limit to those of the limiting homoclinic wave. The following result of Gardner shows that this is indeed correct.

Assume as is standard [GZ, ZH] that the linearized operator L^0 about the homoclinic wave $\bar{u}^0$ has an essential spectrum contained in Re $\lambda \leqq 0$, so that the point spectrum determines spectral stability, (1.5). This point spectrum may be detected by the vanishing of a traveling-front-type Evans function

$$D(\lambda) := \det(\phi_1^-, \ldots, \phi_k^-, \phi_{k+1}^+, \ldots, \phi_N^+), \tag{4.1}$$

where $\{\phi_1^-, \ldots, \phi_k^-\}$ and $\{\phi_{k+1}^+, \ldots, \phi_N^+\}$ are appropriately chosen bases of the subspaces of decaying solutions at $-\infty$ and $+\infty$ respectively, of the eigenvalue

equation (2.7). This can be constructed in a way that is analytic in λ on all of $\{\lambda : \text{Re}\,\lambda > 0\}$; for details, see [GZ, ZH].

Then, we have:

Proposition 4.1 ([G.2]). *The homoclinic limit $\bar{u}^0$ is weakly spectrally stable if and only if the family of periodic waves $\{\bar{u}^\varepsilon\}$ is "weakly spectrally stable in the limit", in the sense that the spectra of the associated linearized operators L^ε about $\bar{u}^\varepsilon$ satisfy*

$$\sigma(L^\varepsilon) \subset \{\lambda : \text{Re}\,\lambda \leqq \eta(\varepsilon)\},$$

with $\eta \to 0$ as $\varepsilon \to 0$. In particular, if the homoclinic $\bar{u}^0$ is spectrally unstable, then so are all $\bar{u}^\varepsilon$ for ε sufficiently small.

More precisely:

Proposition 4.2 ([G.2]). *Let $\Lambda \subset \mathbb{C}$ be compactly contained in $\{\lambda : \text{Re}\,\lambda > 0\}$, with $\partial\Lambda$ contained in the resolvent set of L^0. Then, for ε sufficiently small, the number of zeros in Λ of the periodic Evans function $D(\cdot, k)$, for any fixed k, is equal to the number of zeros of the front-type Evans function $D(\cdot)$.*

Proposition 4.1 is an immediate consequence of Proposition 4.2 together with standard sectorial bounds [Pa, He, Z.3, Z.4] restricting the spectra of elliptic operators in $\{\lambda : \text{Re}\,\lambda \geqq 0\}$ to a bounded domain. Proposition 4.2 is of more general application, applying (under suitable, mild assumptions) also to evolution equations that are not parabolic. From Proposition 4.2 we obtain the revealing picture that eigenvalues of L^0, as ε increases from zero, unfold into loops of the (essential) spectrum of L^ε; looking in reverse, we see that, as $\varepsilon \to 0$, the radius of the corresponding spectral loop decreases to zero (*Proof.* Denoting the eigenvalue in question as λ_*, apply Proposition 4.2 on balls $B(\lambda_*, r)$, with $\varepsilon(r) \to 0$ as $r \to 0$.)

In [G.2], (an equivalent version of) Proposition 4.2 was established using the topological index (Chern number) construction introduced in [AGJ]. Here, we sketch an alternative, more elementary proof. On an initial reading, the reader may wish to skip this proof, which is independent from and uses a different set of techniques than the analysis in the rest of the paper.

Proof of Proposition 4.2. We sketch the proof in the context of (1.1), in which case $k = n$ and $N = 2n$ in (4.1), where n as in (1.1) is the dimension of u. Analogous computations hold in the general case. Since both periodic- and front-type Evans functions are analytic in λ on $\bar{\Lambda} \subset \{\lambda : \text{Re}\,\lambda > 0\}$ the result will follow (using Rouché's Theorem) by a winding number calculation about the contour $\Gamma = \partial\Lambda$, provided we establish:

Assertion. On any compact subset Γ of the resolvent set of L^0 intersect $\{\lambda : \text{Re}\,\lambda > 0\}$,

$$e^{-\alpha_- T^\varepsilon}(-e^{ikT^\varepsilon})^n D(k, \lambda_*) \to C(k, \lambda) D(\lambda_*)$$

as $\varepsilon \to 0$, uniformly in k, λ, where $C(k, \lambda)$ is a nonvanishing (jointly) analytic function, $\alpha_-(\lambda)$ is analytic, and n as above is the dimension of u.

Proof of Assertion. By the general theory of [AGJ, GZ, ZH], the basis elements ϕ_j^+ and ϕ_j^- approach exponentially, as $x \to +\infty$ and $-\infty$ respectively, the stable and

unstable subspace of the limiting coefficient matrix $\mathbb{A}_\infty := \mathbb{A}(\pm\infty)$ of (2.7) (recall that in the homoclinic case coefficients are not periodic, but approach limiting values at the same rate as does the background wave $\bar{u}^0$: exponential, in the case assumed here that $\bar{u}^0(\pm\infty)$ is a nondegenerate rest point of the traveling-wave ordinary differential equation). More precisely,

$$\phi_1^- \wedge \cdots \wedge \phi_n^- \sim \bar{\phi}_1^- \wedge \cdots \wedge \bar{\phi}_n^-$$

and

$$\phi_{n+1}^+ \wedge \cdots \wedge \phi_{2n}^+ \sim \bar{\phi}_{n+1}^+ \wedge \cdots \wedge \bar{\phi}_{2n}^+,$$

where $\cdot \wedge \cdots \wedge \cdot$ denotes an n-fold exterior algebraic product, or minor, and $\bar{\phi}_j^\pm$ denote basis elements for the manifolds of decaying solutions at $\pm\infty$ of the limiting, constant-coefficient equations

$$W' = \mathbb{A}_\infty W$$

at infinity. In turn, we have

$$\begin{aligned}\bar{\phi}_1^- \wedge \cdots \wedge \bar{\phi}_n^- &= e^{\alpha_- x} V_1^- \wedge \cdots \wedge V_n^-,\\ \bar{\phi}_{n+1}^+ \wedge \cdots \wedge \bar{\phi}_{2n}^+ &= e^{\alpha_+ x} V_{n+1}^+ \wedge \cdots \wedge V_{2n}^+,\end{aligned}$$

where vectors V_j^- and V_j^+ respectively span the unstable and stable subspaces of $\mathbb{A}_\infty$, and α_- and α_+ denote the trace of $\mathbb{A}_\infty$ on these respective subspaces.

Now, let the matrix of solutions $\tilde{\Psi}$ in (3.6), Remark 3.3, be chosen by

$$\tilde{\Psi}(0) := (\tilde{\psi}_1^-(0), \ldots, \tilde{\psi}_n^-(0), \tilde{\psi}_{n+1}^+(+T/2), \ldots, \tilde{\psi}_{2n}^+(+T/2)),$$

where $\tilde{\psi}_j^\pm$ are determined by

$$\tilde{\psi}_j^-(0) := \bar{\phi}_j^-(-T/2), \qquad \tilde{\psi}_j^+(T) := \bar{\phi}_j^+(+T/2).$$

Then, the standard estimates of [GZ, ZH] show that $\det \tilde{\Psi}(\lambda, T/2) \to D(\lambda)$ uniformly in λ as $\varepsilon \to 0$.

Moreover, since $D(\lambda)$ was assumed not to vanish on Γ, we have

$$\phi_1^-(x) \wedge \cdots \wedge \phi_n^-(x) \sim C_-(\lambda) e^{\alpha_+ x} V_{n+1}^+ \wedge \cdots \wedge V_{2n}^+$$

as $x \to +\infty$, which says that decaying solutions at $-\infty$ must be growing at $+\infty$, and likewise

$$\phi_{n+1}^+(x) \wedge \cdots \wedge \phi_{2n}^+(x) \sim C_+(\lambda) e^{\alpha_- x} V_{n+1}^+ \wedge \cdots \wedge V_{2n}^+$$

as $x \to -\infty$; the transmission coefficients $C_\pm$ as in [ZH] are determined by solving appropriate systems of linear equations with analytic coefficients, whose respective determinants factor as $D(\lambda)$ times a nonvanishing analytic function. Therefore,

$$\tilde{\psi}_1^-(T) \wedge \cdots \wedge \tilde{\psi}_n^-(T) \sim C_-(\lambda) e^{\alpha_+ T/2} V_{n+1}^+ \wedge \cdots \wedge V_{2n}^+, \tag{4.2}$$

and likewise

$$\tilde{\psi}^+_{n+1}(0) \wedge \cdots \wedge \tilde{\psi}^+_{2n}(0) \sim C_+(\lambda) e^{-\alpha_- T/2} V_1^- \wedge \cdots \wedge V_n^-. \tag{4.3}$$

Using the representation $D(k,\lambda) = \det\big(\tilde{\Psi}(T) - e^{ikT}\tilde{\Psi}(0)\big)/\det\tilde{\Psi}(0)$ afforded by Remark 3.3, combined with (4.2), (4.3) and the fact that $\alpha_+ < 0 < \alpha_-$ (more precisely, $\phi_1^+, \dots, \phi_n^+$ decay exponentially, while $\phi_{n+1}^-, \dots, \phi_{2n}^-$ grow exponentially), we therefore obtain

$$\begin{aligned} D(k,\lambda) &\sim \det(\tilde{\psi}_1^-(T), \dots, \tilde{\psi}_n^-(T), -e^{ikT}\tilde{\psi}_{n+1}^+(0), \dots, -e^{ikT}\tilde{\psi}_{2n}^+(0))/\det\tilde{\Psi}(0) \\ &\sim C_- C_+ (-e^{ikT})^n e^{(\alpha_- - \alpha_+)T}/C_+ e^{-\alpha_+ T} \\ &= C_-(-e^{ikT})^n e^{\alpha_- T}. \end{aligned} \tag{4.4}$$

On the other hand, Abel's formula and the exponential convergence $\mathbb{A} \to \mathbb{A}_\infty$ as $x \to \pm\infty$ imply that

$$\begin{aligned} D(\lambda) &\sim \det\tilde{\Psi}(T/2) \\ &= C_0 e^{-(\alpha_- + \alpha_+)(T/2)} \det\tilde{\Psi}(T) \\ &\sim C_0 C_- \det(V_1^+, \dots, V_n^+, V_{n+1}^-, \dots, V_{2n}^-), \end{aligned} \tag{4.5}$$

where

$$C_0(\lambda) := e^{\int_0^\infty (\mathrm{Tr}\ \mathbb{A}_\infty(\lambda) - \mathrm{Tr}\ \mathbb{A}(\lambda,x))dx} = \mathcal{O}(1).$$

Comparing (4.4) and (4.5), we obtain the result, with

$$C(k,\lambda) := \big(C_0 \det(V_1^+, \dots, V_n^+, V_{n+1}^-, \dots, V_{2n}^-)\big)^{-1}. \qquad \square$$

Remarks. 1. As noted above, the calculation in the proof of Proposition 4.2 also shows explicitly that the k-loops of the spectrum shrink as $T \to \infty$ to single eigenvalues, thus illuminating the passage from continuous to point spectrum as the period T goes to infinity. Though we did not do it here, we could have quantified the rate of shrinking by a more careful version of the same argument.

2. The final assertion of Proposition 4.1 (the one that mainly concerns us here) is intuitively clear from consideration of a small multiple of an unstable eigenfunction of the homoclinic wave given as initial perturbation of a periodic wave – this will grow exponentially for some time, by the property of "almost finite propagation speed", or approximate localization of behavior.

3. In the more general case where the family of orbits corresponding to $\{\bar{u}^\varepsilon\}$ converges as $\varepsilon \to 0$ to a heteroclinic cycle, we can carry out an entirely similar analysis to show that the k-spectra of the periodic operators L^ε, for k fixed, ε sufficiently small, correspond approximately to the *union* of the spectra of the linearized operators about each of the heteroclinic traveling waves in the limiting cycle. (This computation is in the spirit of "multi-bump" calculations carried out for multiple traveling-pulse solutions in models of nerve-impulse and optical transmission.)

Applications. In [GZ], there was derived a *stability index* suitable for the evaluation of stability of traveling-front- or -pulse-type solutions of conservation laws. Precisely, this index yields the parity of the number of unstable eigenvalues λ such that $\mathrm{Re}\,\lambda > 0$ of the linearized operator about the wave; evidently odd parity establishes instability, while even parity is consistent with stability but inconclusive. This index was explicitly evaluated in [GZ] for the class of planar, Hamiltonian quadratic-flux models, and later in [Z.1] for the equations of van der Waals gas dynamics: precisely the models we will study here in connection with pattern formation. In both cases, homoclinic, or pulse-type, solutions were found to have odd index, implying instability, while heteroclinic, or front-type, solutions were found to have even index, consistent with stability. Though the latter result is inconclusive, there is substantial evidence from other quarters [AMPZ.1, LZ.1, LZ.2] that the heteroclinic waves are indeed stable.

Combining these results with the result of Proposition 4.1, we find for these models that periodic solutions approaching a bounding homoclinic solution must be *unstable in the large-period limit*, an observation that was already made in [GZ]. This is suggestive, but not conclusive evidence regarding the nature of numerically observed pattern formation. For, though numerically observed patterns do appear to lie near limiting separatrices [AMPZ.5], the distance relative to the requirements of the abstract theory is difficult to quantify. Also, in both cases, the patterns appear to lie near not only homoclinic but also heteroclinic cycles: 3- and 2-cycles, respectively. Presuming, as evidence suggests, that the component heteroclinic fronts of such a limiting cycle are stable, we find from Remark 3 above that the approaching periodic waves are at worst *weakly unstable*, in the sense that unstable eigenvalues must have vanishingly small real part as $\varepsilon \to 0$. Thus, the question of stability is in this case much more sensitive. Indeed, our numerical experiments in Appendix A indicate that such periodic waves are in the large-amplitude (i.e., large-period) limit *stable* with respect to period-$T/(k = 0)$ perturbations, but *unstable* with respect to perturbations of some other periods/values of k, whereas, recall, the methods of this section do not distinguish between different k-values. Similar considerations hold in the small-amplitude limit; see Remark 4.5 below.

These difficulties motivate us to develop, in the following sections, a more direct and general approach to stability of periodic waves. First, rather than using the front or pulse stability index to obtain information in the large-period limit, we will define an analogous stability index in the periodic case, and compute this directly, thus obtaining, at least in principle, information about small- and intermediate- as well as large-amplitude waves. This corresponds essentially to determining the Taylor expansion in λ of the Evans function at the origin $(k, \lambda) = (0, 0)$. Next, performing a similar but less generally applicable Taylor expansion in the variable k, we will obtain a complementary, "long-wave" stability criterion differentiating between different values of k. Together, these will turn out to be sufficient to obtain rigorous instability results relevant to the pattern formation phenomena discussed above: in particular, in the case of the van der Waals equations, for waves of *arbitrary* amplitude.

Remark 4.3. At least formally,[2] the same kind of "multi-bump" analysis as sketched in Remark 3, above, suggests that, for a family of homoclinic orbits $\{\bar{u}^\varepsilon\}$ converging to a 2-cycle limit $\bar{u}^0$, the spectra of the associated linearized operators L^ε should converge as $\varepsilon \to 0$ to approximately the union of the spectra of the component heteroclinic waves in the 2-cycle. We have conjectured that these heteroclinic waves are stable, in which case their point spectra consist, in the set $\{\lambda : \operatorname{Re}\lambda \geqq 0\}$, of single translational eigenvalues at $\lambda = 0$. Pursuing this line of reasoning, we deduce that the approaching homoclinic solutions should have, besides the obligatory translational eigenvalue at $\lambda = 0$, a second eigenvalue of vanishingly small real part, the sign of which determines stability or instability. Thus, the stability of homoclinic solutions would be quite sensitive in the limit as they approach a 2-cycle, a result consistent with the sensitive stability we have deduced for their nearby periodic waves (which must with them approach the same 2-cycle).

Remark 4.4. It is interesting also to consider the opposite situation from that studied by Gardner, namely the *small-amplitude limit* as a family of periodic waves $\{\bar{u}^\varepsilon\}$ shrinks to a single point, or nonlinear center u_c. Specifically, let us consider the typical situation of a Hopf bifurcation, for which the linearization

$$v' = B^{-1}A(u_c)v \tag{4.6}$$

of the traveling-wave ordinary differential equation $Bu' = Au$ about u_c possesses a two-dimensional center manifold corresponding to a single pair of complex eigenvalues $\alpha_\pm := \pm i\tau$ of the coefficient matrix $B^{-1}A(u_c)$. In this scenario, the period T^ε of $\bar{u}^\varepsilon$ converges as $\varepsilon \to 0$ to $T^0 := 2\pi/\tau$, while the amplitude shrinks to zero.

Likewise, the eigenvalue equation (2.7) converges as $\varepsilon \to 0$ to a constant-coefficient equation as considered in Example 3.4, with $A \equiv A(u_c)$ and $B \equiv B(u_c)$. Referring to (3.8), we find that, for $\lambda = 0$, there is an n-fold root $\mu = 0$ and n remaining roots μ consisting of the eigenvalues of $B^{-1}A$. Consulting (3.9), and noting that roots $\pm i\tau$ are by definition equal to $\pm 2\pi i/T^0$, we find, fixing $k = 0$, that $\lambda = 0$ is an $(n+2)$-fold root of $D(0,\cdot) = 0$, while all other roots are far from the origin, and may in fact be stable: this is the case, for example, when $B = I$. Thus, stability with respect to periodic perturbations of period T, corresponding to stability/instability of the roots of the restricted Evans function $D(0,\cdot)$, may be quite sensitive in the small-amplitude limit. On the other hand, waves are usually quite *unstable* with respect to perturbations on different periods, corresponding to

[2] There is a technical difficulty associated with the accumulation of the essential spectrum at the imaginary axis of the linearized operators about these waves; in particular, note that the argument of Proposition 4.1 makes essential use, specifically in the derivation of the crucial estimate (4.4), of the fact that $\phi_1^+, \dots, \phi_n^+$ are exponentially decaying for x near $+\infty$, while $\phi_{n+1}^-, \dots, \phi_{2n}^-$ are exponentially growing for x near $-\infty$ (which is to say they decay as $x \to -\infty$). It is a standard fact (see, e.g. [He, GZ, ZH]) that this property is equivalent to the assumption that λ lie uniformly to the right of the essential spectrum boundary of L. On the other hand, the more general bundle construction of [AGJ, G.1, G.2] should still go through, in conjunction with analytic continuation into the essential spectrum of the traveling-front- or -pulse-type Evans function using the Gap Lemma of [GZ, KS]; see, for example, the related analysis in [DGK].

zeros of $D(k,\cdot)$ with $k \neq 0$: for example, in the case where $B = I$, A has imaginary eigenvalues $\pm i\tau$, and so hyperbolicity, hence also (3.11), is violated.

5. The stability index

Motivated by the discussion of the previous section, we now define directly a stability index for periodic waves analogous to the one defined in [GZ] for traveling-front- or -pulse-type solutions. This index, being designed to identify *strong* instabilities, concerns only ($k = 0$)-eigenvalues, i.e., instability with respect to periodic perturbations of the same period T as the background solution $\bar{u}$. For this purpose the choice of k is expected to be somewhat arbitrary (by continuity; see also the large-period analysis of the previous section). And, this allows us to make a link to the previous analyses of heteroclinic waves, for which the Evans function has only the argument λ.

As in the analysis of [GZ] in the traveling-front or -pulse case, our goal is to relate sgn $D(0,\lambda)$ for λ near $+\infty$ to sgn $D(0,\lambda)$ for λ near 0, for λ restricted to the real axis, and, in turn, to relate the latter to the dynamics of the traveling-wave ordinary differential equation. This approach, introduced by EVANS in the pioneering papers [E.1–E.4], and widely generalized in, e.g., [J, AGJ, PW], has proved to be a powerful tool in the stability analysis of traveling-front or -pulse type solutions. However, until now it does not seem to have been carried out in the periodic case.

Large-λ behavior. We begin with the large-λ limit, which admits a particularly simple treatment.

Lemma 5.1. *As $\lambda \to +\infty$ along the real axis,* sgn $D(0,\lambda) \to (-1)^n$, *where n as in* (1.1) *is the dimension of u.*

Proof. By standard Gärding-type (i.e., sectorial) energy estimates, L has no spectrum in Re $\lambda \geqq 0$ for $|\lambda|$ sufficiently large. Moreover, the Evans function varies continuously with respect to continuous changes in the coefficients of L, by continuous dependence with respect to initial data of solutions of ordinary differential equation. Thus, the quantity

$$\lim_{\lambda \to +\infty} \text{sgn } D(0,\lambda), \tag{5.1}$$

with λ restricted to the real axis, is both well-defined and invariant under homotopy in L within the class of strictly elliptic operators with periodic coefficients of period T. Deforming L to the Laplacian $\bar{L} := (\partial/\partial_x)^2$ via the homotopy

$$\theta \bar{L} + (1-\theta)L,$$

θ going from 0 to 1, we may thus evaluate (5.1) by an explicit and elementary computation, which we omit. This could alternatively be carried out directly, for the original operator L, using a rescaling argument as in [GZ]. A related, but much more complicated, homotopy argument was used in [BSZ] to treat the traveling-front or -pulse case. □

Remark 1. Note that in this periodic context, the sign of (5.1) is an absolute quantity, and does not depend on any choice of coordinates. Likewise, in the homoclinic case, there is a natural choice of coordinates by which the sign may be made absolute (namely, choosing initializing bases of the stable subspace at $+\infty$ and the unstable subspace at $-\infty$ that together form a basis of $\mathbb{R}^{2n}$ with the standard orientation; see construction of the front- or pulse-type Evans function in the previous section). By contrast, a significant difficulty confronted in [GZ] for the traveling-front case was to relate the sign at infinity to the normalization chosen at $\lambda = 0$. Indeed, this limited the original analysis of [GZ] to the case $n = 2$; for the extension to the general case, see [BSZ, Z.3].

Small-λ behavior. We next address the crucial small-λ case. By analogy with the traveling-front or -pulse case, we seek to relate small-λ behavior to the dynamics of the traveling-wave ordinary differential equations (1.8), (1.9).

Notice, in the present periodic context, that (1.8), (1.9) involve $2n+1$ parameters (u_-, u_0, s) rather than the $n+1$ parameters (u_-, s) of the traveling-front or -pulse case, since the choice of initial condition u_0 is completely independent of the critical point u_-. For each choice of parameters, there is a unique solution $\bar{u}^{(u_-,u_0,s)}(x)$ of (1.8). We can thus define the *special separation function*

$$d(u_-, u_0, s) := \bar{u}^{(u_-,u_0,s)}(x)|_0^T. \tag{5.2}$$

Note that this is a bit different from the usual separation function in that the vanishing of $d(\cdot)$ corresponds to existence of a periodic solution of *precisely period* T. A standard Melnikov function would be based, rather, on the Poincaré return map; here, however, we are concerned only with period T.

Variations

$$w_j := \partial\bar{u}/\partial u_0 \cdot e_j, \quad j = 1, \dots, n, \tag{5.3}$$

satisfy the linearized traveling-wave equation

$$Bw' = Aw, \quad w(0) = e_j. \tag{5.4}$$

Without loss of generality, take coordinates such that

$$\bar{u}_x(0) = e_1; \tag{5.5}$$

hence

$$w_1 = \bar{u}_x. \tag{5.6}$$

Likewise, the variation

$$\widetilde{z}_1 := -\partial\bar{u}/\partial s \tag{5.7}$$

satisfies

$$Bz' = Az + (\bar{u} - u_-), \quad z(0) = 0, \tag{5.8}$$

while

$$w_{n+j} := (\partial \bar{u}/\partial u_-) \cdot e_j, \quad j = 1, \cdots n, \tag{5.9}$$

satisfy

$$Bw' = Aw - f'(u_-)e_j, \quad w(0) = 0. \tag{5.10}$$

We thus have relations

$$(\partial d/\partial u_0) \cdot e_j = [w_j], \tag{5.11}$$

$$-\partial d/\partial s = [\widetilde{z}_1], \tag{5.12}$$

$$(\partial d/\partial u_-) \cdot e_j = [w_{n+j}], \tag{5.13}$$

where e_j denotes the jth standard basis element in $\mathbb{R}^n$.

With these definitions, we may restate (H3) in the more quantitative form:

(H3′) $\partial d/\partial(u_0, s) = ([\widetilde{z}_1], [w_1], \ldots, [w_n])$ is full rank,

i.e., (recalling that $[w_1] = [\bar{u}_x] = 0$)

$$\gamma := \det([\widetilde{z}_1], [w_2], \ldots, [w_n]) \neq 0. \tag{5.14}$$

That is, for a fixed period T and equilibrium u_-, the orbit $\bar{u}(\cdot)$ is locally unique up to translations, even allowing variation in s; moreover, it corresponds to a transverse intersection of the tangent manifolds at $\bar{u}(0)^{(u_-,u_0,s)}$ and $\bar{u}(T)^{(u_-,u_0,s)}$ with respect to variations in (u_0, s).

Then, by the Implicit Function Theorem, there is an $(n+1)$-dimensional surface

$$(u_-, u_0^1) \to (u_-, u_0, s) \tag{5.15}$$

in parameter space for which $\bar{u}^{(u_-,u_0,s)}(\cdot)$ has period T, where $u_0^1 := u_0 \cdot e_1$ denotes the component of u_0 in the $e_1 = \bar{u}_x(0)$ direction. Fixing u_0^1 to factor out translation invariance and fix the phase, we find n directions in which connections persist. We can thus uniquely specify n variations in $\bar{u}^{(u_-,u_0,s)}$,

$$\widetilde{w}_{n+j} \in w_{n+j} \oplus \mathrm{Span}(\widetilde{z}_1, w_2, \cdots w_n), \tag{5.16}$$

by the requirement

$$[\widetilde{w}_{n+j}] = 0. \tag{5.17}$$

Finally, we define the "zero-viscosity stability coefficient":

$$\Delta := \det\left(\int \widetilde{w}_{n+1}, \cdots, \int \widetilde{w}_{2n}\right) = \det(\partial \bar{u}_m/\partial u_-), \tag{5.18}$$

where $\int \widetilde{w}_{n+j}$ denotes $\int_0^T \widetilde{w}_{n+j}(y)dy$ and

$$\bar{u}_m(u_-, u_0^1) := \int_0^T \bar{u}^{(u_-,u_0,s)}(y)dy \tag{5.19}$$

denotes the mass over one period of the solution $\bar{u}^{(u_-,u_0,s)}$ determined by (u_-, u_0^1) via map (5.15); note that this does not depend on u_0^1, since it is invariant under phase shifts. The condition $\Delta \neq 0$ corresponds to the requirement that there exist no nearby periodic orbits of period T that have the same mass as does $\bar{u}(\cdot)$, at least up to linear order in the perturbation of (u_-, u_0, s). This has an interesting heuristic interpretation in the spirit of [FL.1, FL.2] as linearized well-posedness within a special class of measure-valued solutions, in the limit of zero viscosity, of an associated *Riemann problem* having left and right states both equal to the average value of $\bar{u}$ over one period: namely, the class of measure-valued solutions for which the associated limiting sequence consists of periodic functions with a fixed ratio between period and viscosity. (Note that average value is preserved both under compact perturbations of $\bar{u}(\cdot)$ and, by conservation of mass, under the nonlinear flow of (1.1).) The latter restriction comes from the fact that we are here considering stability only within the class of periodic functions of fixed period T; its somewhat awkward form reflects the link via rescaling between the long-time and small-viscosity limits. For a careful description of measure-valued solutions and their relation to asymptotic behavior of (1.1), we refer the reader to [FL.1, FL.2].

Alternatively, $\Delta \neq 0$ may be viewed as the requirement that, near $\bar{u}$, there is a unique periodic orbit of period T having a given mass $\bar{u}_m$ over one period: that is, the "mass map" from perturbation mass to possible time-asymptotic (periodic) states is both well defined and nonsingular. Since mass per period is preserved under the flow of (1.1) with periodic boundary conditions, this condition is clearly necessary for orbital stability of $\bar{u}$ within the class of T-periodic solutions, under perturbations with nonzero mass.

In this sense, Δ is precisely analogous to the corresponding one-dimensional zero-viscosity stability coefficient $\Delta(0, 1)$ defined in [ZS, Z.3][3] for the traveling-front or -pulse case, which has the same relations to linearized well-posedness of the Riemann problem and nonsingularity of the mass map. With these definitions, we have the following fundamental relation, analogous to the one described in [GZ, ZS, BSZ, Z.3] for the traveling-front or -pulse case.

Proposition 5.2. *Let* (H0)–(H3) *hold. Then*

$$D(0, \lambda) = \lambda^{n+1}(-1)^n \det\left(df(u_-)^{-1}\right)\gamma\Delta + \mathcal{O}(\lambda^{n+2}), \tag{5.20}$$

or, equivalently,

$$(\partial/\partial\lambda)^k D(0, 0) = 0, \quad 0 \leqq k \leqq n, \tag{5.21}$$

and

$$(\partial/\partial\lambda)^{n+1} D(0, 0) = (-1)^n (n + 1)! \det df(u_-)^{-1}\gamma\Delta, \tag{5.22}$$

where γ is the transversality coefficient defined in (5.14) *and $\Delta = \det(\partial\bar{u}_m/\partial u_-)$ is the inviscid stability coefficient defined in* (5.18), (5.19).

[3] The relation between the stability index, linearized well-posedness of the Riemann problem, and the mass map was first noted in [GZ], in slightly less explicit form; see [FreZ] for related applications.

Remark 5.3. In the case where $\gamma = 0$, but $\partial d/\partial(u_0, u_-, s)$ is still of full rank, a similar calculation gives

$$(\partial/\partial\lambda)^{n+1} D(0,0) = (-1)^n (n+1)! \det df(u_-)^{-1} \gamma_1 \Delta,$$

where γ_1 now denotes the determinant of an appropriately chosen alternative transverse set of vectors, and Δ is as in (5.18), with $\widetilde{w}_{n+1}, \dots, \widetilde{w}_{2n}$ chosen again to span the tangent manifold to the family of nearby periodic orbits, modulo translation, i.e., satisfying (5.17). (Of course, these cannot now be defined as in (5.16).) Thus, we see precisely the same relation to linearized well-posedness of Riemann problems as found in the case of Lax and undercompressive shock waves in [GZ, ZS, BSZ, Z.3].

Remark 5.4. It may happen that $\gamma \to 0$ but Δ remains bounded as (u, u_-, s) and T approach certain limiting values. In this case, we may conclude that $\Gamma = 0$ for the limiting periodic orbit, since D, as the uniform limit of analytic functions, has continuous partial derivatives as well. For example, $\gamma = 0$ in the small-amplitude, constant-coefficient limit described in Remark 4.4, since in this case there is a one-parameter family of periodic orbits with period $T = T^0$, but also $\partial \bar{u}/\partial u_- \to I$ as this limit is approached; see Remark 5.10, below. Thus, we may conclude that $\Gamma = 0$ in the constant-coefficient case. This is consistent with our previous observation, obtained by direct calculation, that $D(0, \cdot)$ must vanish in this case to order $(n+2)$ and not $(n+1)$.

Proof of Proposition 5.2. Defining the fundamental set of solutions $W_1, \dots, W_{2n}$ of eigenvalue ordinary differential equation (2.7) by initialization

$$(W_1, \dots, W_{2n})(0) = \begin{pmatrix} I & 0 \\ B^{-1}A & -B^{-1} df(u_-)_{|0} \end{pmatrix}, \tag{5.23}$$

and writing $W_j =: (w_j, w_j')^t$, we obtain by Remark 3.3 the representation

$$\begin{aligned} D(0,\lambda) &= \det([W_1], \dots, [W_{2n}]) / \det(W_1(0), \dots, W_{2n}(0)) \\ &= (-1)^n \det \begin{pmatrix} [w_1], \dots, [w_{2n}] \\ [w_1'], \dots, [w_{2n}'] \end{pmatrix} / \det \left(B^{-1}(u_0) df(u_-) \right). \end{aligned} \tag{5.24}$$

With this choice of coordinates, the $w_j(\lambda)$ defined here agree at $\lambda = 0$ with the traveling-wave ordinary differential equation variations w_j defined in (5.4), (5.9), satisfying the (second-order) linearized traveling-wave ordinary differential equation

$$(Bw')' = (Aw)'. \tag{5.25}$$

Likewise, variations $z_j := w_{j\lambda}$ are seen at $\lambda = 0$ to satisfy

$$(Bz')' = (Az)' + w_j, \quad z(0) = z'(0) = 0, \tag{5.26}$$

and $y_j := w_{j\lambda\lambda}$ to satisfy

$$(By')' = (Ay)' + 2z_j, \quad y(0) = y'(0) = 0. \tag{5.27}$$

In particular, z_1 satisfies

$$(Bz')' = (Az)' + \bar{u}_x, \quad z(0) = 0, \tag{5.28}$$

hence

$$Bz' = Az + (\bar{u} - u_0), \quad z(0) = 0. \tag{5.29}$$

Comparing (5.29) with (5.8), (5.10), we find that

$$z_1 = \widetilde{z}_1 \quad \text{modulo span } (w_{n+1}, \cdots w_{2n}). \tag{5.30}$$

Next, integrating (5.25) from 0 to T, we find that, at $\lambda = 0$,

$$B(u_0)[w_j'] = [Bw_j'] = [Aw_j] = A(u_0)[w_j]; \tag{5.31}$$

hence

$$[w_j'] - B^{-1}A(u_0)[w_j] = 0 \tag{5.32}$$

for all $1 \leqq j \leqq 2n$. Likewise, integrating (5.26) and (5.27) gives

$$[z_j'] - B^{-1}A(u_0)[z_j] = B^{-1}(u_0)\int_0^T w_j, \tag{5.33}$$

$$[y_j'] - B^{-1}A(u_0)[y_j] = 2B^{-1}(u_0)\int_0^T z_j, \tag{5.34}$$

respectively. In the special case $j = 1$, (5.33) gives

$$[z_1'] - B^{-1}A(u_0)[z_1] = B^{-1}(u_0)\int_0^T \bar{u}_x = \bar{u}|_0^T = 0. \tag{5.35}$$

Now, Taylor expanding formula (5.24) about $\lambda = 0$, we obtain, for small λ,

$$\begin{aligned} D(0,\lambda) &= (-1)^n \det\left(df(u_-)^{-1}B(u_0)\right) \\ &\quad \times \det\begin{pmatrix} [w_1] + \lambda[z_1] + \frac{1}{2}\lambda^2[y_1] + \cdots, & \ldots, & [w_{2n}] + \lambda[z_{2n}] + \cdots \\ [w_1'] + \lambda[z_1'] + \frac{1}{2}\lambda^2[y_1'] + \cdots, & \ldots, & [w_{2n}'] + \lambda[z_{2n}'] + \cdots \end{pmatrix}. \end{aligned} \tag{5.36}$$

Subtracting $B^{-1}A(u_0)$ times the first row from the second, and using (5.33), (5.34) and $\int w_1 = [w_1] = [w_1'] = 0$, we obtain

$$\begin{aligned} D(0,\lambda) &= (-1)^n \det\left(df(u_-)^{-1}B(u_0)\right) \\ &\quad \times \det\begin{pmatrix} \lambda[z_1] + \cdots, & [w_2] + \cdots, & \ldots, & [w_{2n}] + \cdots \\ \lambda^2 B^{-1}\int z_1 + \cdots, & \lambda B^{-1}\int w_2 + \cdots, & \ldots, & \lambda B^{-1}\int w_{2n} + \cdots \end{pmatrix} \\ &= \lambda^{n+1}(-1)^n \det\left(df(u_-)^{-1}\right) \det\begin{pmatrix} [z_1], & [w_2], & \ldots, & [w_{2n}] \\ \int z_1, & \int w_2, & \ldots, & \int w_{2n} \end{pmatrix} \\ &\quad + \mathcal{O}(\lambda^{n+2}), \end{aligned} \tag{5.37}$$

where $\int$ denotes $\int_0^T$. Applying now appropriate column operations, we obtain from (5.16), (5.17), (5.30) that

$$\begin{aligned} D(0,\lambda) &= \lambda^{n+1}(-1)^n \det\big(df(u_-)^{-1}\big) \\ &\quad \times \det\begin{pmatrix} [\widetilde{z}_1], & [w_2], \dots, [w_n], & 0, & \dots, & 0 \\ \int \widetilde{z}_1, & \int w_2, \dots, \int w_n, & \int \widetilde{w}_{n+1}, & \dots & \int \widetilde{w}_{2n} \end{pmatrix} \\ &\quad + \mathcal{O}(\lambda^{n+2}) \\ &= \lambda^{n+1}(-1)^n \det\big(df(u_-)^{-1}\big) \\ &\quad \times \det([\widetilde{z}_1], [w_2], \dots, [w_n]) \det\Big(\int \widetilde{w}_{n+1}, \dots, \int \widetilde{w}_{2n}\Big) \\ &\quad + \mathcal{O}(\lambda^{n+2}) \\ &= \lambda^{n+1}(-1)^n \det\big(df(u_-)^{-1}\big)\gamma\Delta + \mathcal{O}(\lambda^{n+2}), \end{aligned} \tag{5.38}$$

as claimed. □

Remark 5.5. The solutions $w_{n+1}, \dots, w_{2n}$, satisfy the inhomogeneous equations

$$Bw'_{n+j} = Aw_{n+j} - df(u_-)e_j, \quad w_{n+j}(0) = 0. \tag{5.39}$$

Thus, they also can be expressed in terms of the fundamental solution $\psi(x)$ of the n-dimensional linearized traveling-wave equation

$$Bw' = Aw \tag{5.40}$$

(different from the fundamental solution Ψ of the $2n$-dimensional eigenvalue ordinary differential equation (2.7)) via Duhamel's principle:

$$w_{n+j}(x) = -\Big(\int_0^x \psi(x)\psi(y)^{-1}dy\Big)df(u_-)e_j, \tag{5.41}$$

and therefore

$$\begin{aligned} [w_{n+j}] &= w_{n+j}(T) \\ &= \Big(\psi(T)\int_0^T \psi(y)^{-1}dy\Big)df(u_-)e_j. \end{aligned} \tag{5.42}$$

Likewise,

$$[w_j] = (\psi(T) - \psi(0))e_j, \tag{5.43}$$

$$\int w_j = \Big(\int_0^T \psi(y)dy\Big)e_j, \tag{5.44}$$

$$[\widetilde{z}_1] = \psi(T)\int_0^T \psi(y)^{-1}(\bar{u}(y) - u_-)dy. \tag{5.45}$$

That is, formula (5.18) for Δ can be interpreted as a sort of Melnikov integral, like the corresponding object in the homoclinic (undercompressive) case of the traveling-front or -pulse theory [GZ, Z.1].

Remark 5.6. The quantity $[z_1]$ can clearly be substituted for $[\tilde{z}_1]$ in (5.14), since the two quantities are equal, modulo $\mathrm{Span}(w_{n+1}, \dots, w_{2n})$.

The stability index. With these preparations, we now define the *stability index*:

$$\Gamma := \mathrm{sgn}\ (\partial/\partial\lambda)^{n+1} D(0,0) D(0,+\infty). \tag{5.46}$$

We have immediately:

Proposition 5.7. *Let* (H0)–(H3) *hold. Then, the parity of the number of unstable eigenvalues of L, considered as an operator on the space of functions periodic on $[0,T]$ is even if Γ is positive, and odd if Γ is negative. In particular, $\Gamma \geqq 0$ is necessary for weak spectral stability as defined in* (1.5).

Proof. Evidently, $D(0,\lambda)$ is invariant with respect to complex conjugation, i.e., $D(0,\bar{\lambda}) = \bar{D}(0,\lambda)$, by the definition of $D(\cdot,\cdot)$. This yields the familiar fact that the eigenvalues of the real-valued operator L, considered as acting on the periodic functions on $[0,T]$, are either real or else belong to complex conjugate pairs, whence the parity of the number of unstable eigenvalues is equal to the parity of the number of unstable *real* eigenvalues. But, this is clearly determined by Γ in the manner stated. □

Remark 5.8. The strict inequality $\Gamma > 0$ is necessary for *strong spectral stability* as defined in [OZ]. In particular, it is necessary for $L^1 \to L^p$ linearized stability for any $p < \infty$, by Proposition 1.5 and condition (D̃3)(i) of [OZ] combined with (5.46), (5.10) above. This is analogous to the situation in the traveling-front or -pulse case; see discussion, Section 11 [ZH], of the "neutrally stable case".

Combining the results of Lemma 5.1, Proposition 5.2, and Proposition 5.7, we obtain the main result of this section, an expression for Γ involving only geometry of the phase space of the traveling-wave ordinary differential equation:

Theorem 5.9. *Let* (H0)–(H3) *hold. Then,*

$$\Gamma = \mathrm{sgn}\ \gamma\, \Delta \det df(u_-), \tag{5.47}$$

where γ and $\Delta = \det(\partial \bar{u}_m/\partial u_-)$ are as defined in (5.14) *and* (5.18), (5.19), *respectively. In particular,*

$$\mathrm{sgn}\ \gamma\, \Delta \det df(u_-) \geqq 0 \tag{5.48}$$

is necessary for weak spectral stability of $\bar{u}$.

Remark 5.10. In the small-amplitude limit discussed in Remark 4.4, recall that $D(0,\cdot)$ typically has $n+2$ zeros lying near the origin $\lambda = 0$, and the rest lying in the strictly stable complex half-plane $\mathrm{Re}\,\lambda < 0$. By Propositions 5.2 and 5.7, $n+1$ of these in fact lie precisely at $\lambda = 0$, with the remaining small eigenvalue being stable, unstable, or zero according as the stability index Γ is positive, negative, or zero. Therefore, in this case, $\Gamma \geqq 0$ is *necessary and sufficient* for weak spectral stability with respect to periodic perturbations of period T.

Remark 5.11. With appropriate choice of the rest point u_-, it can be shown that the key quantity $(\partial \bar{u}_m/\partial u_-)$ in (5.10) approaches the identity in both the small-amplitude and the large-amplitude homoclinic limits considered earlier. For the small-amplitude limit described in Remark 4.4, we may choose u_- to be the rest point lying near the nonlinear center u_c to which the family of periodic orbits converges; for the homoclinic limit, we choose u_- to be the rest point lying near the vertex of the homoclinic orbit. We omit the standard, but somewhat involved calculations giving these results.

This has an interesting implication in the planar case, $n = 2$. For, in the simplest case, where γ is nonvanishing for the entire family of periodic waves, we find by Theorem 5.9 that the sign of Γ depends entirely on sgn $\det(df(u_-))$. The latter is negative when u_- is set equal to a homoclinic vertex, since this is a saddle of the traveling-wave ordinary differential equation, so that $\det(B^{-1}df(u_-))$, and thus also $\det(df(u_-)) = \det B \det(B^{-1}df(u_-))$, is negative, as the product of a positive and a negative eigenvalue. But, by similar reasoning, it is positive when u_- is set equal to a nonlinear center, since then the eigenvalues of $\det(B^{-1}df(u_-))$ are complex conjugates. Thus, combining this observation with that of Remark 5.10 just above, we find that if large-amplitude waves are spectrally unstable with respect to period-T perturbations, then small-amplitude waves are necessarily *stable* in this sense. Regarding period-T perturbations, we thus have the global picture of a single, small real eigenvalue detaching from the origin at amplitude zero and initially moving into the stable complex half-plane, later crossing zero again at some critical intermediate amplitude to become unstable thereafter; this picture is borne out by our numerical investigations in Appendix A. On the other hand, we see that the stability index by itself is not likely to be effective across the range of all amplitudes, even when it is useful in the large-amplitude limit, and for small amplitudes is usually *not* useful.

Remark 5.12. By calculations similar to those in the proof of Assertion 4 (see proof of Proposition 4.2), the expression for γ given in (5.14) may, in the large-amplitude homoclinic limit discussed in Section 4, be related to a corresponding quantity arising in the study of stability of homoclinic, or pulse-type, traveling waves. For $n = 2$, this is the quantity Γ defined in (3.18), Lemma 3.4 of [GZ]; a similar quantity arises in the general case [BSZ, Z.3]. Combining this observation with that of Remark 5.11 above, we can show that the sign of the periodic stability index converges in the large-amplitude homoclinic limit, to the sign of the traveling-pulse-type index for the limiting homoclinic wave. We omit the associated calculations as lying too far from the direction of our main interest; however, see the related, explicit computation (6.26) in Section 6 below.

6. The quasi-Hamiltonian case

We next restrict attention to the case where the traveling-wave ordinary differential equation (1.8) is "quasi-Hamiltonian" in the sense that it admits an integral of motion for each (u_-, u_0), with s held fixed at the base value under consideration,

without loss of generality $s = 0$. This situation arises in some physical applications; see Section 7. Furthermore, it has a particular mathematical interest; as shown in [OZ], this is essentially the only circumstance under which we can expect standard "diffusive", or asymptotic $L^1 \to L^p$ linearized stability of periodic solutions: in the generic case, linearized $L^1 \to L^p$ stability can hold only for $p = \infty$, and is bounded at best; see [OZ], Proposition 1.5 and discussion surrounding condition ($\tilde{\text{D}}3$).

With this additional structure, we may determine not only the low-frequency behavior of the Evans function with respect to λ, but (to lowest order) the Taylor expansion with respect to (k, λ):

Theorem 6.1. *Let* (H0)–(H3) *hold, and suppose in addition that the traveling-wave ordinary differential equation* (1.8) *is quasi-Hamiltonian for the value of s associated with solution $\bar{u}$. Then, for k, λ sufficiently small,*

$$\begin{aligned} D(k,\lambda) = \gamma\lambda \det\big(&- \lambda(\partial\bar{u}_m/\partial u_-)df(u_-)^{-1} - ikT\big) \\ &+ \mathcal{O}\big((|k| + |\lambda|)^{n+2}\big), \end{aligned} \tag{6.1}$$

where γ and $(\partial\bar{u}_m/\partial u_-)$ are as defined in (5.14) *and* (5.18), (5.19), *respectively.*

Proof. By assumption, (1.8) admits an integral of motion $H(u_-, u)$ for each (u_-, u_0), i.e.,

$$H(u_-, u(t)) \equiv H(u_-, u_0) \tag{6.2}$$

for all solutions $u(t)$, where s is held fixed. Then, perturbing the periodic orbit $\bar{u}$ with respect to these parameters, we find that variations

$$[w_j] := (\partial/\partial u_0)\big(\bar{u}^{(u_-,u_0,s)}(T) - \bar{u}^{(u_-,u_0,s)}(0)\big), \tag{6.3}$$

$$[w_{n+j}] := (\partial/\partial u_-)\big(\bar{u}^{(u_-,u_0,s)}(T) - \bar{u}^{(u_-,u_0,s)}(0)\big) \tag{6.4}$$

must have range lying tangent to the hypersurface $H(u_-, u) \equiv H(u_-, u_0)$ at the base values of (u_-, u_0) associated with $\bar{u}$, i.e., orthogonal to $\nabla_u H(u_-, u_0)$. For, differentiating $H(u_-, \bar{u}(T)) - H(u_-, \bar{u}(0)) = 0$ with respect to u_0 yields

$$0 = \nabla_u H(u_-, u_0)[\partial\bar{u}/\partial u_0], \tag{6.5}$$

where, as usual, $[f]$ denotes $f(T) - f(0)$; likewise, differentiating with respect to u_- yields

$$\begin{aligned} 0 &= \nabla_u H(u_-, u_0)[\partial\bar{u}/\partial u_-] + \nabla_{u_-} H(u_-, u_0)I - \nabla_{u_-} H(u_-, u_0)I \\ &= \nabla_u H(u_-, u_0)[\partial\bar{u}/\partial u_-]. \end{aligned} \tag{6.6}$$

Moreover, $w_1 := \bar{u}_x(0)$ is also orthogonal to $\nabla_u H(u_-, u_0)$, since

$$0 = (d/dx)H\big(u_-, \bar{u}(0)\big) = \nabla_u H(u_-, u_0)\bar{u}_x(0). \tag{6.7}$$

Noting that $[w_2], \ldots, [w_n]$ must be independent, by (H3′), we thus find that they are by themselves a basis for

$$\text{Span}\,\{[w_j]\} \oplus \text{Span}\,(w_1), \tag{6.8}$$

with $[\widetilde{z}_1]$ not required. This simply reflects the fact that, by the Implicit Function Theorem, the full $(n+1)$-parameter family of nearby periodic orbits of period T can be generated with s held fixed; for, thanks to (6.2), only $n-1$ conditions must be satisfied to obtain existence.

Defining $W_1, \dots, W_{2n}$ again as in (5.23), but allowing k to vary, we obtain in place of (5.24) the representation:

$$\begin{aligned} D(k,\lambda) = {} & \det\big(-df(u_-)^{-1}B(u_0)\big) \\ & \times \det\big([W_1]-(e^{ikT}-I)W_1(0),\dots,[W_{2n}]-(e^{ikT}-I)W_{2n}(0)\big). \end{aligned} \tag{6.9}$$

Taylor expanding this about $(k,\lambda)=(0,0)$, we thus find for small k, λ that

$$\begin{aligned} & D(0,\lambda) = \det\big(-df(u_-)^{-1}B(u_0)\big) \\ & \times \det\begin{pmatrix} [w_1]+\lambda[z_1]-ikTw_1(0)+\cdots, \dots, [w_{2n}]+\lambda[z_{2n}]-ikTw_{2n}(0)+\cdots \\ [w_1']+\lambda[z_1']-ikTw_1'(0)+\cdots, \dots, [w_{2n}']+\lambda[z_{2n}']-ikTw_{2n}'(0)+\cdots \end{pmatrix}. \end{aligned} \tag{6.10}$$

Recalling (5.4), (5.9), we find that

$$\begin{aligned} \big(w_j' - B^{-1}Aw_j\big)(0) &= 0, \\ \big(w_{n+j}' - B^{-1}Aw_{n+j}\big)(0) &= -B^{-1}(u_0)df(u_-)e_j \end{aligned}$$

for $j=1,\dots,n$. Thus, subtracting $B^{-1}A(u_0)$ times the first row from the second, we obtain as in (5.37) the expression

$$\begin{aligned} D(k,\lambda) = {} & \det\big(-df(u_-)^{-1}\big) \\ & \times \det\begin{pmatrix} \lambda[z_1]-ikTw_1(0), & [w_2], & \dots, & [w_{2n}] \\ \lambda^2\int\widetilde{z}_1, & \lambda\int w_2, & \dots, & \lambda\int w_{2n}+ikTdf(u_-)e_n \end{pmatrix} \\ & + \mathcal{O}\big((|k|+|\lambda|)^{n+2}\big) \\ = {} & \det\big(-df(u_-)^{-1}\big) \\ & \times \det\begin{pmatrix} \lambda[z_1], & [w_2], & \dots, & [w_{2n}] \\ \lambda^2\int\widetilde{z}_1, & \lambda\int w_2, & \dots, & \lambda\int w_{2n}+ikTdf(u_-)e_n \end{pmatrix} \\ & + \mathcal{O}\big((|k|+|\lambda|)^{n+2}\big), \end{aligned} \tag{6.11}$$

where in the final equality we have used (6.8) to eliminate term $ikTw_1(0)$. Applying column operations as in (5.38), we thus obtain

$$\begin{aligned} D(k,\lambda) = {} & \det\big(-df(u_-)^{-1}\big)\det\begin{pmatrix} \lambda[\widetilde{z}_1], & [w_2],\dots,[w_n], & 0 \\ \int\widetilde{z}_1, & \int w_2,\dots,\int w_n, & M(k,\lambda) \end{pmatrix} \\ & + \mathcal{O}\big((|k|+|\lambda|)^{n+2}\big), \end{aligned} \tag{6.12}$$

where the $n \times n$ block M is given by

$$M(k,\lambda) := \Big(\int \widetilde{w}_{n+1} + ikTdf(u_-)e_1, \dots, \int \widetilde{w}_{2n} + ikTdf(u_-)e_n \Big) \\ = (\partial \bar{u}_m/\partial u_-) + ikTdf(u_-)I. \tag{6.13}$$

Finally, factoring the determinant on the right-hand side of (6.12) using its block triangular form yields

$$D(k,\lambda) = \gamma\lambda \det\Big(\lambda(\partial \bar{u}_m/\partial u_-) + ikTdf(u_-)\Big) \det\Big(- df(u_-)^{-1}\Big) \\ + \mathcal{O}\big((|k| + |\lambda|)^{n+2}\big). \tag{6.14}$$

Rearranging (6.14), we obtain (6.1). □

Notice that result (6.1) is consistent with our previous result (3.3). As an immediate consequence, we obtain:

Corollary 6.2. *Let* (H0)–(H3) *hold, and suppose in addition that the traveling-wave ordinary differential equation* (1.8) *is quasi-Hamiltonian for the value of s associated with solution $\bar{u}$. If $\Delta := \det(\partial \bar{u}_m/\partial u_-) \neq 0$, then, for k, λ sufficiently small, the spectrum of L consists of $(n+1)$ smooth curves:*

$$\lambda_0(k) = o(k), \tag{6.15}$$

$$\lambda_j(k) = -i\alpha_j kT + o(k), \quad j = 1, \dots, n, \tag{6.16}$$

where α_j denote the eigenvalues of

$$df(u_-)(\partial \bar{u}_m/\partial u_-)^{-1}, \tag{6.17}$$

and where $(\partial \bar{u}_m/\partial u_-)$ is as defined in (5.18), (5.19). *In particular, the "effective hyperbolicity" condition*

$$\sigma\big(df(u_-)(\partial \bar{u}_m/\partial u_-)^{-1}\big) \text{ real} \tag{6.18}$$

is necessary for weak spectral stability of $\bar{u}$.

If $\Delta = 0$, then (6.15) *holds as before. Likewise,* (6.16) *holds with $\alpha_j := \beta_j^{-1}$, where β_j denote the eigenvalues of $(\partial \bar{u}_m/\partial u_-)df(u_-)^{-1}$, for all j such that $\beta_j \neq 0$. Associated with vanishing β_j, however, are nonsmooth curves*

$$\lambda(k) \sim k^{p/q},$$

p/q not an integer; in particular, $\det(\partial \bar{u}_m/\partial u_-) = 0$ implies spectral instability.

Remark. Note that $\Gamma = 0$ in this (quasi-Hamiltonian) case implies spectral, i.e., *exponential* instability, since then $\det(\partial \bar{u}_m/\partial u_-) = 0$ by (5.10) together with (H2) and (H3'). This is to be compared with the (apparently) more subtle situation of the general case; see Remark 5.8.

The formulae of Corollary 6.2 may be regarded as the natural generalizations of the constant-coefficient formulae of Remarks 3.5 and 4.4. In particular, comparing (6.16), (6.17) to (3.12), we see that $df(u_-)(\partial\bar{u}_m/\partial u_-)^{-1}$ plays in the quasi-Hamiltonian case the role played in the constant-coefficient case $\bar{u} \equiv u_0 = u_-$ by $A := df(u_-)$. That is, $df(u_-)(\partial\bar{u}_m/\partial u_-)^{-1}$ may be regarded as an "averaged" or "effective" convection matrix for the variable-coefficient case (indeed, this is shown in [OZ] to hold true in a very strong sense). Note, further, that $df(u_-)(\partial\bar{u}_m/\partial u_-)^{-1}$ converges in the small-amplitude limit to $df(u_-)$, since, as pointed out in Remark 5.11, $(\partial\bar{u}_m/\partial u_-) \to I$.

Likewise, in the large-amplitude, homoclinic limit considered by Gardner, we find again (Remark 5.11) that $df(u_-)(\partial\bar{u}_m/\partial u_-)^{-1}$ converges to $df(u_-)$, where u_- now denotes the vertex of the homoclinic orbit, i.e., the limiting state of the homoclinic wave as $x \to \pm\infty$. Thus, the spectral curves described in (6.16), (6.17) correspond to first order in k with the spectral curves of this limiting, constant state, which are in turn curves of essential spectrum for the linearized operator about the homoclinic wave: for a detailed discussion, see the introduction of [OZ]. The remaining curve (6.15) corresponds to the translational (continuous) eigenfunction at $\lambda = 0$ associated with the spatial derivative $\bar{u}^\varepsilon$ of the profile under consideration.

This extends to the small-frequency regime the picture described by Gardner (Section 4) in the large-amplitude homoclinic limit. It can be shown by an argument similar to that of Section 4 (together with the observations made in the introduction of [OZ] regarding structure of the resolvent set of the limiting homoclinic profile) that the former curves in fact *globally* approach the essential spectrum curves of the limiting homoclinic wave, in the sense that they approach on a ball of radius going to infinity with the period; thus, they extend arbitrarily far as the homoclinic limit is approached. We conjecture without proof that the latter curve belongs to a closed loop of spectra, shrinking in the large amplitude limit to the eigenvalue $\lambda = 0$ associated with the translational eigenfunction $\bar{u}_x^0$ of the limiting, homoclinic wave.

Remark. The Taylor expansion of D can likewise be carried out in the general (non-quasi-Hamiltonian) case, but does not seem amenable to any such simple interpretation.

The planar Hamiltonian case. Finally, we consider the planar case, $n = 2$, under the assumption that the traveling-wave ordinary differential equation (1.8) is in fact Hamiltonian for all u_-, with s held fixed at the base speed associated with $\bar{u}$, i.e.,

$$0 = \operatorname{Tr} d_u\big(B^{-1}(u)(f(u) - f(u_-) - s(u - u_-))\big). \tag{6.19}$$

This is the class from which we will take our example systems in the following section. Note that, for $B \equiv$ constant, condition (6.19) reduces to

$$0 = \operatorname{Tr}\big(B^{-1}(df(u) - sI)\big), \tag{6.20}$$

which is evidently independent of u_-; with this observation, it is straightforward to construct examples.

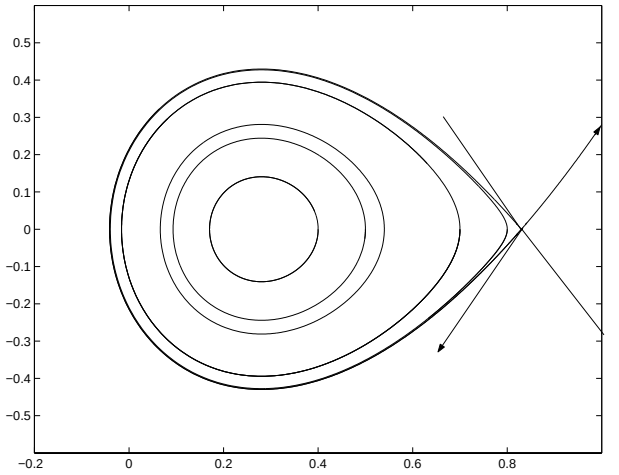

Fig. 1. The planar Hamiltonian case: bounding homoclinic cycle.

From (6.19), we find that the traveling-wave equation may be expressed as a Hamiltonian system

$$u' = B^{-1}(u)(f(u) - f(u_-) - s(u - u_-)) = \nabla_s u^\perp H(u, u_-), \tag{6.21}$$

for an appropriate Hamiltonian $H(u, u_-)$, whence $H(u(t), u_-)$ is an integral of motion; in particular, we see that the planar Hamiltonian systems are a subclass of the quasi-Hamiltonian systems defined above.

Existence of an integral of motion in the planar case implies considerable structure of the phase portrait of the traveling-wave ordinary differential equation. For example, in the situation we consider, where the phase portrait contains a heteroclinic poly-cycle, we find that the interior of the cycle must be entirely filled with cycles, either periodic or heteroclinic. In the simplest case, where there is only a single nonlinear center u_c enclosed, the interior must be made up entirely of periodic orbits; see, for example, the depiction of the homoclinic case in Fig. 1. In this situation, we may globally parametrize these orbits by amplitude a, defined as distance from center u_c along some (fixed) curve of steepest descent if u_c is a local maximum, or ascent if u_c is a minimum. In more general situations, we may still define a *local* parametrization in this way, in the vicinity of any fixed periodic orbit $\bar{u}$.

Let us consider the period T as a function of amplitude, $T = T(a)$. Then, we have:

Lemma 6.3. *Let* (H0)–(H3) *hold, and suppose in addition that the traveling-wave ordinary differential equation* (1.8) *is planar Hamiltonian for the value of s associated with solution $\bar{u}$, with $B \equiv$* constant. *Then,*

$$\text{sgn } \gamma = \text{sgn } (dT/da) \tag{6.22}$$

for $\gamma := \det([\widetilde{z}_1], [w_2])$ *as in* (5.14).

Proof. Let w_1, w_2 denote the variations defined in (5.4), (5.9), as usual normalizing $w_1 = \bar{u}_x(0) = e_1$. We may locally parametrize amplitude by location of u_0 along a curve tangent to the outward normal $\eta = \pm e_2$ at $\bar{u}(0)$ to the orbit $\{\bar{u}(x)\}$, so that

$$da/du_0 = \eta$$

at $\bar{u}(0)$, where $a(u_0)$ is the amplitude of the orbit corresponding through u_0, with (u_-, s) held fixed. Differentiating the identity

$$\bar{u}^{(u_-,u_0,s)}(T(a(u_0))) - \bar{u}^{(u_-,u_0,s)}(0) \equiv 0$$

with respect to u_0 in direction e_2, we thus obtain

$$[w_2] + \bar{u}_x(T)(dT/da)(\eta \cdot e_2) = 0,$$

or

$$[w_2] = C\bar{u}_x(0) = C\bar{u}_x(T) = Ce_1, \tag{6.23}$$

with

$$\text{sgn } (C) = \text{sgn } (dT/da)\text{sgn } \det(\eta, \bar{u}_x(0)). \tag{6.24}$$

The quantity

$$\gamma = \det([\widetilde{z}_1], [w_2]) = C \det(\widetilde{z}_1(T), \bar{u}_x(T)) \tag{6.25}$$

can therefore be conveniently calculated, using the inhomogeneous Abel's equation/Duhamel principal as a Melnikov integral:

$$\begin{aligned} \gamma &= C \int_0^T e^{\int \text{Tr } (B^{-1}A)} \det(B^{-1}(\bar{u} - \bar{u}_-), \bar{u}_x) dx \\ &= C \int_0^T \det(B^{-1}(\bar{u} - u_-), \bar{u}_x) dx, \end{aligned} \tag{6.26}$$

where in the second equality we have used the Hamiltonian property $\text{Tr } (B^{-1}A) \equiv$ constant. More precisely, this is found by setting $\gamma(t) := C \det(\widetilde{z}_1(t), \bar{u}_x(t))$ and observing that γ satisfies

$$\gamma' = \text{Tr } (B^{-1}A)\gamma + C \det(B^{-1}(\bar{u} - u_-), \bar{u}_x), \quad \gamma(0) = 0$$

by (5.4) and (5.7), (5.8); for similar calculations in the traveling-front or -pulse case, see [GZ].

But, (6.26), as in [GZ], may be viewed as a contour integral and explicitly evaluated using the Gauss-Green formula as

$$\begin{aligned} \gamma &= C\text{sgn } \det(\eta, \bar{u}_x) \int_{\partial\Omega} B^{-1}(u - u_-) \cdot \eta \, ds \\ &= C\text{sgn } \det(\eta, \bar{u}_x) \int_{\Omega} \text{div}\big(B^{-1}(u - u_-)\big) \, du \\ &= C\text{sgn } \det(\eta, \bar{u}_x) |\Omega| \text{Tr } (B^{-1}), \end{aligned} \tag{6.27}$$

where Ω is the region bounded by the orbit $\bar{u}(\cdot)$, and η denotes the outward unit normal. Recalling that $\text{Tr } B^{-1} > 0$ by (H1), and combining with (6.25), we are done. □

Remarks. 1. Formulae (6.26), (6.27) clearly show that

$$\det([z_1], [w_2]) = \det([\tilde{z}_1], w_2),$$

as asserted in Remark 5.6, since substitution of u_0 for u_- leaves the result unchanged.

2. Comparison of formula (6.26) to that given for Γ in (3.18), Lemma 3.4 of [GZ] shows explicitly the convergence described in Remark 5.12, since the two formulae are formally identical, differing only in the choice of profile $\bar{u}$.

3. Near a bounding poly-cycle, it is clear that $dT/da > 0$, indeed $dT/da \to +\infty$ as the boundary is approached. Thus, $\gamma > 0$, and in combination with the observation of Remark 5.11 that $(\partial \bar{u}_m/\partial u_-) \to I$ and $\det df(u_-) < 0$ in the homoclinic case, we find that $\operatorname{sgn} \Gamma < 0$, recovering the result of instability obtained by Gardner's technique together with the homoclinic instability results of [GZ, Z.1].

It is interesting to note that our periodic instability result for the homoclinic limit makes no requirement on the shape of the limiting homoclinic orbit, whereas the general homoclinic instability results of [GZ] require that the orbit be *convex* in the vicinity of its vertex. Indeed, in the nonconvex case, the stability index of the homoclinic orbit is positive, consistent with stability, an apparent contradiction with Remark 2 just above. In the quadratic-flux case considered in [GZ], it was shown that all homoclinic orbits are (globally) convex, hence this situation does not arise. Likewise, it does not arise in the van der Waals models studied in [Z.1] (described in the following section, just below), for which orbits are graphs over the v axis. However, it can certainly arise in more general situations; see [Z.4].

A closer inspection quickly resolves this apparent paradox. For, it is readily seen that a planar homoclinic orbit that is nonconvex at its vertex saddle must enclose a *second*, interior poly-cycle, containing the interior branches of its stable and unstable manifolds. Periodic orbits are thus bounded by *both* the interior poly-cycle and the exterior homoclinic orbit, so that the argument for Remark 2 does not apply. Indeed, considering the simplest case that the interior poly-cycle is a second, locally convex homoclinic orbit, and applying the "multi-bump" heuristics of Remark 4.3 and Remark 3 above it, we obtain, formally, the correct prediction of an *odd* multiplicity of unstable eigenvalues for the periodic orbit, as the sum of even and odd multiplicities.

Combining the results of Theorem 5.9, Corollary 6.2, and Lemma 6.3, we obtain, finally, the composite stability test:

Corollary 6.4. *Let* (H0)–(H3) *hold, and suppose also that the traveling-wave ordinary differential equation* (1.8) *is planar Hamiltonian for the value of s associated with solution $\bar{u}$, with $B \equiv$ constant. Then, provided that $(\partial \bar{u}_m/\partial u_-)$ is invertible, both*

$$\operatorname{sgn}\left(dT/da\right) \det\left(df(u_-)(\partial \bar{u}_m/\partial u_-)^{-1}\right) \geqq 0 \tag{6.28}$$

and

$$\sigma\left(df(u_-)(\partial \bar{u}_m/\partial u_-)^{-1}\right) \text{ real} \tag{6.29}$$

are necessary for weak spectral stability of $\bar{u}$, where dT/da is the rate of change of period with respect to amplitude, with amplitude measured in the direction of the outward normal to the orbit $\{\bar{u}(x)\}$. If $\det(\partial \bar{u}_m/\partial u_-) = 0$, *on the other hand, then $\bar{u}$ is spectrally unstable. (Recall, $dT/da \neq 0$ by* (H3′) *combined with Lemma 6.3.)*

7. Calculations for example systems

Using the complementary stability conditions of Corollary 6.4, we now derive instability results for the two classes of model, planar Hamiltonian systems that were considered in [Z.1] and [GZ]: van der Waals gas dynamics with artificial dispersion-viscosity, and the class of planar Hamiltonian models with quadratic flux functions. These are directly relevant to the issue of oscillatory pattern formation, being prototypes for the two kinds of systems in which these patterns have been observed numerically.

Van der Waals gas dynamics. The viscous-capillary p-system,

$$\begin{aligned} v_t - u_x &= \varepsilon_1 v_{xx}, \\ u_t + p(v)_x &= \varepsilon_2 u_{xx}, \end{aligned} \tag{7.1}$$

with nonmonotone stress relation p, has been studied by several authors as a model for dynamical phase transitions in compressible van der Waals fluids/solids undergoing isothermal motion (see, for example, [Ja,Sh.1–Sh.3,Sl.1–Sl.5,ST]). Here, $\varepsilon_1 > 0$ and $\varepsilon_2 > 0$ are related to the coefficients of viscosity and capillarity of the medium ($\varepsilon_1 + \varepsilon_2$ and $\varepsilon_1\varepsilon_2$, respectively), v denotes specific volume/strain, $\tilde{u} := u + \varepsilon_1 v_x$ is the velocity of the medium, and $p(v)$ denotes pressure/stress. A typical stress relation is $p = -W'(v)$, where

$$W(v) = \tfrac{1}{2}(1 - v^2)^2 \tag{7.2}$$

is the standard "double-well" potential.

In physical, $(v, \tilde{u})$ coordinates, equations (7.1) take the form

$$\begin{aligned} v_t - \tilde{u}_x &= 0, \\ \tilde{u}_t + p(v)_x &= (\varepsilon_1 + \varepsilon_2)\tilde{u}_{xx} - (\varepsilon_1\varepsilon_2)v_{xxx}, \end{aligned} \tag{7.3}$$

which is sometimes more natural for computations.

Existence. The traveling-wave ordinary differential equation associated with (7.1) (for periodic and front- or pulse-type waves alike) is

$$\begin{pmatrix} v \\ u \end{pmatrix}' = \begin{pmatrix} \frac{1}{\varepsilon_1} & 0 \\ 0 & \frac{1}{\varepsilon_2} \end{pmatrix} \left[\begin{pmatrix} -u + u_- \\ p(v) - p(v_-) \end{pmatrix} - s \begin{pmatrix} v - v_- \\ u - u_- \end{pmatrix} \right], \tag{7.4}$$

where s denotes the speed of propagation of the wave. For speed $s = 0$, this becomes a Hamiltonian system with Hamiltonian

$$H(v, u, v_-, u_-) := \frac{1}{2\varepsilon_1}(u - u_-)^2 - \frac{1}{\varepsilon_2}P(v)$$
$$= \frac{1}{2\varepsilon_1}(u - u_-)^2 - \frac{1}{\varepsilon_2}\big(W(v_-) - W(v) + W'(v_-)(v - v_-)\big), \tag{7.5}$$

where

$$P(v) := \int_{v_-}^{v} \big(p(v_-) - p(z)\big)\, dz. \tag{7.6}$$

For nonmonotone p, the orbits of (7.4), corresponding to level sets of H, will on some range of v_- include one-parameter families of periodic orbits bounded by heteroclinic or homoclinic cycles. For example, in the case of (7.2), there appears for $v_- = \pm 1$ a 2-cycle of heteroclinic orbits connecting (v_-, u_-) to $(-v_-, u_-)$ in either direction, respecting the vertical symmetry of H about the line $u = u_-$; within this cycle is a one-parameter family of periodic orbits converging in the small-amplitude limit to the nonlinear center $(0, u_-)$. For v_- in the range $[0.55, 1)$ or $(-1, -0.55]$, there appears a single homoclinic orbit with vertex at v_-, likewise enclosing a one-parameter family of periodic orbits about a nonlinear center (v_c, u_-). Together, these constitute all periodic solutions of (7.4) with $s = 0$ for the double-well case (7.2).

We may deduce by energy considerations that traveling periodic solutions of (7.1) must in fact be stationary, so that the Hamiltonian solutions just described constitute *all* periodic solutions of the van der Waals system (7.1). For, as noted in [Se.1, Se.2], the flow of (7.1), for periodic solutions of period T, serves to decrease the mechanical energy

$$\tilde{E}(v) := E(v) + \int_0^T \tfrac{1}{2}\tilde{u}^2\, dx = E(v) + \int_0^T \tfrac{1}{2}(u + \varepsilon_1 v_x)^2\, dx, \tag{7.7}$$

where

$$E(v) := \int_0^T \Big(\frac{\varepsilon_1\varepsilon_2}{2}|v'|^2 + P(v)\Big)\, dx \tag{7.8}$$

denotes the Cahn-Hilliard/van der Waals energy for the associated equilibrium problem. More precisely,

$$d\tilde{E}/dt = -(\varepsilon_1 + \varepsilon_2)\int_0^T |\tilde{u}_x|^2 dx, \tag{7.9}$$

as may easily be derived from (7.3). Thus, we may deduce that $\tilde{u} \equiv$ constant for any periodic traveling-wave solution of (7.1), from which we immediately obtain $0 \equiv v_t = -sv_x$. It follows that either v is identically constant, in which case u is as well, or else $s = 0$; in either case, we find as asserted that the wave must be stationary.

Moreover, we readily find for $\tilde{u}_x = 0$ that any solution of (7.3) must satisfy the Euler-Lagrange equations

$$\varepsilon_1\varepsilon_2 v_{xx} = p(v_-) - p(v) \tag{7.10}$$

for the equilibrium variational problem

$$\min_v E(v), \tag{7.11}$$

yielding back the stationary-wave ordinary differential equation (7.4) with $s = 0$.

Stability. Using the result of Corollary 6.4, we readily obtain:

Theorem 7.1. *Periodic orbits of* (7.1) *are unstable whenever* $dT/da > 0$, *in particular, in the large-amplitude limit as they approach either a bounding homoclinic orbit or two-cycle. Orbits for which* $dT/da < 0$ *are unstable if the spectrum of* $(\partial\bar{u}_m/\partial u_-)^{-1}df(u_-)$ *is nonreal. In the small-amplitude limit as orbits approach a nonlinear center, they are unstable regardless of the value of* sgn dT/da.

Proof. Clearly, (H0)–(H2), hold, whence the results of Corollary 6.4 apply whenever (H3′) holds, or $dT/da \neq 0$. By the final assertion of Corollary 6.4, we may without loss of generality take $\det(\partial\bar{u}_m/\partial u_-) \neq 0$. The second assertion then follows by either of (6.28), (6.29), the former because in this case the determinant of the real matrix $(\partial\bar{u}_m/\partial u_-)^{-1}df(u_-)$ must be positive, as the product of complex conjugates. To establish the first assertion, we make use of the structure of equations (7.1).

By direct computation, we obtain

$$df(u_-, v_-) = \begin{pmatrix} 0 & -1 \\ p'(v_-) & 0 \end{pmatrix}. \tag{7.12}$$

Moreover, from translational invariance of (7.1) with respect to u, in combination with the reflective symmetry $u \to -u$, $x \to -x$, we find without any computation that $\partial\bar{u}_m/\partial u_-$ must be of diagonal form

$$\begin{pmatrix} \alpha & 0 \\ 0 & 1 \end{pmatrix}, \tag{7.13}$$

with a single undetermined quantity $\alpha \neq 0$. Thus, assuming that $\det(\partial\bar{u}_m/\partial u_-) \neq 0$, or $\alpha \neq 0$, we find that the matrix

$$(\partial\bar{u}_m/\partial u_-)^{-1}df(v_-, u_-) = \begin{pmatrix} 0 & -1/\alpha \\ p'(v_-) & 0 \end{pmatrix} \tag{7.14}$$

is trace-free, whence we may conclude that its spectrum is real if and only if its determinant is negative. But, this implies that (6.28) and (6.29) are mutually exclusive when $dT/da > 0$, yielding spectral instability.

Finally, the third assertion follows simply by continuity of the Evans function, without invoking (H3′) or Corollary 6.4, once we observe that the limiting, constant-coefficient equations at a nonlinear center are always unstable, since the trace-free real matrix $df(v_c, u_c)$ must necessarily have pure imaginary eigenvalues (or else (v_c, u_c) would instead be a saddle). □

Remark 7.2. In the special case of the double-well potential (7.2), monotonicity $dT/da > 0$ holds for *all* periodic van der Waals orbits. This follows as a straightforward application of a monotonicity theorem of Schaaf (see [Sc, p. 102], or [LP, Theorem 7.1, p. 331]), which asserts that monotonicity holds for the nonlinear oscillator

$$v'' + \mu(v) = 0, \tag{7.15}$$

provided: (i) $\mu' > 0$ implies $5(\mu'')^2 - 3\mu'\mu''' > 0$; and, (ii) $\mu' = 0$ implies $\mu\mu'' < 0$. Noting that the van der Waals traveling-wave ordinary differential equation is of form (7.15), with $\mu(v) = p(v) - p(v_-)$, we readily verify (i) and (ii) in the double-well case $p(v) = 2v(1 - v^2)$, by direct computation. In particular, note that (i) follows simply from the fact that $p'''(v) = -12v < 0$. This finding is quite significant, since it shows that there is at least one model exhibiting oscillatory pattern formation for which no stable periodic waves exist, thus indicating the presence of some alternative mechanism for the formation of oscillatory patterns.

Remark 7.3. By Remark 5.10, in conjunction with Lemma 6.3, we find that small-amplitude periodic waves are *stable with respect to periodic perturbations* (of the same period T) if and only if $dT/da > 0$; in particular, they are stable for the double-well potential, as discussed just above. Likewise, numerical evaluation of $\partial\bar{u}_m/\partial u_-$ for large-amplitude waves in the two-cycle configuration yields $\Gamma > 0$, suggestive of stability under T-periodic perturbation, a conjecture that is further supported by numerical approximation of the $(k = 0)$-spectrum of L; see Appendix A. On the other hand, we have already seen analytically that large-amplitude waves in the homoclinic case are *unstable* with respect to T-periodic perturbations.

These results are quite interesting from the point of view of the associated variational problem (7.11). They imply that periodic solutions may or may not be stable critical points of the energy E, depending on the details of their structure. This is in sharp contrast to the results of [CGS.1, CGS.2, GM] for the same problem with Neumann in place of periodic boundary conditions, in which critical points are seen to be stable if and only if they are *monotone*. In both cases, stability is interpreted with respect to perturbations conserving mass. Note, in the conservation law setting, that stability is at best *orbital*, in the sense of convergence to the three-parameter family of nearby periodic solutions of the same period T, with the two conserved quantities given by the mass of the perturbed solution determining the limiting solution up to phase shift (translation).

To put things slightly differently, stability in the periodic setting is not determinable as in the Neumann setting by Sturm-Liouville-type considerations alone, but must indeed be estimated by some such computation as we have carried out. Similarly, stability for the variational problem on the whole line is more subtle than that for the (Neumann) problem on the bounded interval, requiring further analysis as in [Z.1].

Quadratic-flux models. Planar systems (1.1) with quadratic flux f have been studied as qualitative models for multiphase flow in porous media near an "elliptic boundary" where characteristics of the flux Jacobian $df(u)$ coalesce; see, e.g.,

[SSh,SSMP,MP]. Here, following [GZ], we consider the restricted class of 2×2 systems with f quadratic and B constant for which, additionally, the traveling-wave ordinary differential equation

$$u' = B(u)^{-1}[f(u) - f(u_-) - s(u - u_-)]$$

is *Hamiltonian*, i.e.,

$$\operatorname{tr}(B^{-1}(f'(u) - sI)) \equiv 0$$

for some choice of s. This is a codimension-2 subclass of the quadratic-flux models, as parametrized by the coefficients of B and f.

Generically, such systems can be reduced by an affine change of variables to the canonical form

$$\begin{pmatrix} u \\ v \end{pmatrix}_t + B \begin{pmatrix} \frac{\varepsilon}{2}v^2 - \frac{1}{2}u^2 + v \\ uv \end{pmatrix}_x = B \begin{pmatrix} u \\ v \end{pmatrix}_{xx} \tag{7.16}$$

where $\varepsilon = \pm 1$. For $\varepsilon = 1$ and $s = 0$, the traveling-wave ordinary differential equation then reduces to the Hamiltonian system

$$\begin{pmatrix} u \\ v \end{pmatrix}' = \begin{pmatrix} \frac{1}{2}v^2 - \frac{1}{2}u^2 + v \\ uv \end{pmatrix} - \begin{pmatrix} \frac{1}{2}v_-^2 - \frac{1}{2}u_-^2 + v_- \\ u_- v_- \end{pmatrix}, \tag{7.17}$$

with Hamiltonian

$$H(u, v) = \tfrac{1}{2}(\tfrac{1}{3}v^3 - u^2 v + v^2) - (\tfrac{1}{2}v_-^2 v - \tfrac{1}{2}u_-^2 v + v_- v - u_- v_- u) \equiv H(u_0, v_0) \tag{7.18}$$

preserved along orbits [GZ].

Explicit computation of the phase portrait of (7.17) using (7.18) reveals the existence of a unique three-cycle configuration for the special parameter values

$$(u_-, v_-) = (\pm\sqrt{3}/2, 0),\ (0, -1.5),\ (0, -.5), \tag{7.19}$$

corresponding, respectively, to the three saddle equilibria at the vertices of the three-cycle, and the single nonlinear center contained within. Enclosed within the three-cycle is a nested one-parameter family of periodic orbits. The heteroclinic orbits making up the three-cycle lie on straight lines, forming an equilateral triangle; in fact the entire phase portrait has the same triple symmetry about the center as does the bounding triangle. The three states (7.19) at the vertices of the triangle may be regarded as analogous to *pure phases* in physical models for three-phase flow, and the interior of the triangle to the physical state space of volume fractions thereof [AMPZ.3].

This configuration bifurcates as (u_-, v_-) is varied into various one- and two-cycle configurations, each cycle likewise enclosing a nested one-parameter family of periodic orbits. Where $dT/da \neq 0$, these are the only nearby periodic orbits to be found in parameter space, where s is now allowed to vary; however, we have not so far been able to rule out the possibility of further periodic orbits with large speed s.

In numerical experiments carried out in [AMPZ.5], systems (7.16) were seen to exhibit the same sort of oscillatory pattern formation discussed in [FL.1, FL.2, CP], with patterns composed of motifs with (u, v) profiles lying near either the three-cycle, or the various two-, and one-cycle configurations that bifurcate from it as (u_-, v_-) is varied from (7.19). Thus, the relevant issue from the point of view of pattern formation seems to be the stability or instability of large-amplitude periodic waves for parameters near the three-cycle values (7.19). Regarding this problem, we have a complete solution; indeed, the additional symmetries of the three-cycle case allow us to obtain results for *general amplitude* waves:

Theorem 7.4. *For B constant, symmetric, and positive-definite, periodic orbits of* (7.16) *are unstable for (u_-, v_-) lying near the three-cycle values* (7.19)*, independent of amplitude, provided that $dT/da \neq 0$. Likewise, so long as $dT/da \neq 0$, large-amplitude waves are unstable for (u_-, v_-) corresponding to a homoclinic configuration in the phase portrait of* (7.17)*; moreover, small-amplitude waves are unstable for any phase configuration.*

Proof. Clearly, (H0)–(H2) hold, whence, again, the results of Corollary 6.4 apply whenever (H3′) holds, or $dT/da \neq 0$. Taking (u_-, v_-) to be the nonlinear center $(u_c, v_c) = (0, -0.5)$, we find using the triple symmetry of the phase portrait that $\partial(\bar{u}_m, \bar{v}_m)/\partial(u_-, v_-)$ must be a multiple of the identity, for any periodic orbit whatsoever. More precisely, we note that, for $(u_-, v_-) = (u_c, v_c) = (0, -0.5)$, the traveling-wave ordinary differential equation (7.17) has reflective symmetry about each of the lines from (u_c, v_c) through the vertices of the surrounding three-cycle; moreover, each individual symmetry is preserved as (u_-, v_-) is varied along the respective line of symmetry. It follows that, under perturbations of (u_-, v_-) in direction ν, where ν is the direction vector of a line of symmetry, $(\bar{u}_m, \bar{v}_m)$ must be confined to the same line of symmetry, i.e., the resulting perturbation of the mean $(\bar{u}_m, \bar{v}_m)$ must lie in the same direction ν, for any choice of initial periodic orbit $(\bar{u}, \bar{v})$. In other words, each of the direction vectors of the three lines of symmetry is an eigenvector of $\partial(\bar{u}_m, \bar{v}_m)/\partial(u_-, v_-)$, whence $\partial(\bar{u}_m, \bar{v}_m)/\partial(u_-, v_-)$ must be a (real) multiple of the identity.

Thus,

$$df(u_-, v_-)\partial(\bar{u}_m, \bar{v}_m)/\partial(u_-, v_-)^{-1}$$

is simply a real multiple of

$$df(u_-, v_-) = B \begin{pmatrix} 0 & 0.5 \\ -0.5 & 0 \end{pmatrix}. \tag{7.20}$$

But, this matrix is similar to the anti-symmetric matrix

$$B^{1/2} \begin{pmatrix} 0 & 0.5 \\ -0.5 & 0 \end{pmatrix} B^{1/2},$$

hence must have a pure imaginary spectrum. (Note: in particular, it is again trace-free, as in the proof of Theorem 7.1.) We thus obtain instability by (6.29), for waves of arbitrary amplitude. The result for (u_-, v_-) near $(0, -0.5)$ follows by the same argument, together with continuity of $\partial(\bar{u}_m, \bar{v}_m)/\partial(u_-, v_-)$.

The large-amplitude homoclinic result has been established already by several different techniques. Likewise, the small-amplitude result follows from the instability of the constant-coefficient limit, as discussed previously in Remark 4.4. □

Remark 7.5. The proof of Theorem 7.4 shows also that, for (u_-, v_-) near the 3-cycle values (7.19) and $dT/da > 0$ – in particular, for large-amplitude periodic orbits approaching the 3-cycle, the stability index Γ is *positive*, suggestive of stability with respect to T-periodic perturbations. This conjecture is supported by numerical approximation of the $(k = 0)$-spectrum, which also indicates stability with respect to T-periodic perturbations of large-amplitude periodic solutions in the 2-cycle limit; see Appendix A. This is in contrast to the T-periodic *instability* observed in the large-amplitude homoclinic limit for both van der Waals and quadratic flux models.

Remark 7.6. The general features of the global phase portrait structure described above for the Hamiltonian models considered here have been shown in [AMPZ.4] to hold, more generally, for all 2×2 quadratic-flux models of type I under the viscous classification scheme of Hurley [HP]. In particular, there exist unique (u_-, v_-, s) such that the phase portrait of the traveling-wave ordinary differential equation contains a three-cycle, of which the connecting heteroclinic orbits must lie along straight lines; moreover, it can be shown by affine reduction to canonical form that the corresponding ordinary differential equation is quasi-Hamiltonian [CL]. It follows that the three-cycle encloses a nested one-parameter family of periodic orbits, as in the "pure" Hamiltonian case considered above. Likewise, formation of oscillatory patterns has been observed numerically for such systems [AMPZ.5], with patterns again lying near the special three-cycle configuration.

Appendix A. Numerical experiments

In this appendix, we describe numerical methods for the location of the zero set of the periodic Evans function $D(k, \lambda)$, or equivalently the spectrum of a linear operator L with periodic coefficients, and, in particular, the well-conditioned *numerical verification of instability*. We demonstrate these methods for the example systems considered in Section 7, amplifying and (in the case of the quadratic-flux models) extending the analytical results there obtained. The real advantage of the numerical approach, of course, is that it is applicable to general models.

The algorithm. We use the following basic strategy for numerical verification of instability:

1. Determine the range of existence of periodic orbits, and (numerically) solve for a representative sampling of profiles.

For each profile:

2. Find spectral curves $\lambda(k)$, i.e., zero-level sets of $D(\lambda, k)$.
3. Choose $k = k^*$ giving a maximum (positive) value of Re $(\lambda(k))$ and a numerically advantageous closed contour Γ contained in the strictly positive half-plane Re $\lambda > 0$ and containing $\lambda(k^*)$.

4. Perform a winding-number calculation in λ, with $k = k^*$ held fixed, to establish that there indeed lies a root of $D(k^*, \cdot)$ in the vicinity of the original numerical approximation of $\lambda(k^*)$ in steps 2 and 3.

The point of steps 3 and 4 is that the curves found in step 2 are "graphical" approximations of the zero-level sets, which, though extremely illuminating, do not give conclusive information about existence of zeros. Step 4 by contrast is both accurate and well-conditioned, and could be used as the basis for numerical proof; however, it requires an *a priori* guess for k^*, $\lambda(k^*)$.

Choosing k^* and Γ. By a standard Gärding-type energy estimate on (2.6), the zeros of the Evans function must lie in the truncated wedge

$$V = \{\lambda \in \mathbb{C} : \text{Im } (\lambda) + \text{Re } (\lambda) \leqq r, \text{Im } (\lambda) - \text{Re } (\lambda) \geqq -r, \text{Re } (\lambda) \leqq r/4\}$$

where $r = \|f(\xi)\|_\infty^2 / \|B\|_2$, $f(\xi) = \|A(\xi)\|_2$. Obviously, this is not a bounded region but it does give us a bound on the unstable zeros of D. We find spectral curves/zero sets of D numerically and observe that those are contained in V. We can see also agreement between our numerics and the analysis in Sections 1–7 (see discussion under *Applications*, below).

It is more tricky to find the zero sets of the two-parameter periodic-type Evans function than of the one-parameter front-type Evans function. Adding to the difficulty is the fact that $D(\lambda, k)$ vanishes to $(n+1)$th order in λ at $(0, 0)$, where n is the dimension of variable u, so that there are $n+1$ spectral curves bifurcating through the origin. The apparently straightforward step 2 in the algorithm is thus in fact a tricky problem in graphical display. To find spectral curves/zero sets of D, we use Müller's method which can approximate complex roots and converges to the root for any initial approximation choice. We also use deflation to achieve a reasonable result near the bifurcation point $(k, \lambda) = (0, 0)$.

Since the argument principle will be used to count the zeros inside some contour Γ, care must be taken that Γ itself does not contain any zeros. We avoid the origin and high multiplicities by looking at $k \neq 0$. A natural choice is to choose the value of k which gives the maximum value of the positive Re (λ) from the spectral curves, and for simplicity choose Γ as the rectangle whose center is that maximum positive value of Re (λ) in the right half-plane. In this process, we find that a practical upper bound on the size of the contour is enforced by the need to obtain good error estimates, which degrade rapidly for high frequencies. This particular k allows good numerics. When the computed winding number exceeds zero, the wave being tested is unstable; otherwise the wave is stable.

Applying the Argument Principle. Here we follow the approach of [Br.1, Br.2]. The first problem in calculating the winding number of $D[\Gamma]$ lies in evaluating $D(\lambda, k)$ for a fixed value of k. We use the maximal value $k = k^*$ described above. The second problem lies in partitioning Γ into subcontours Γ_i such that $D[\Gamma_i]$ lies in a slit plane; a slit plane being a subset of $\mathbb{C}$ of the form $\mathbb{C}\backslash\{r\alpha : 0 \neq \alpha \in \mathbb{C}, 0 \leqq r \in \mathbb{R}\}$. This will ensure that the calculated winding number is correct. We partition Γ so that $D[\Gamma_i]$ is contained in a half plane whose boundary passes through the origin.

For $w, z \in \mathbb{C}$, define $\langle w, z\rangle$ to be the dot product between the real 2-vectors (Re (w), Im (w)) and (Re (z), Im (z)):

$$\langle w, z\rangle = \text{Re}\,(w)\text{Re}\,(z) + \text{Im}\,(w)\text{Im}\,(z). \tag{8.1}$$

If $\Gamma(s_i)$ is the starting point of Γ_i, it suffices to find s_{i+1} and $\beta \in [0, 1)$ such that

$$\langle D(s_i + \Delta s), D(s_i)\rangle > \beta |D(s_i)| \tag{8.2}$$

for $0 \leqq \Delta s \leqq s_{i+1} - s_i$. In other words, the component of $D(s_i + \Delta s)$ in the direction of $D(s_i)$ should be a positive multiple of $D(s_i)$. Strictly speaking, the right side of inequality (8.2) could simply be 0 in practice. However, to allow for numerical error, a positive value of β should be chosen. We choose $\beta = 1/2$ over all. This condition allows checking whether a given partition is appropriate.

Error Estimates. In contrast to the front case [Br.1, Br.2], computation of D for moderate values of $|\lambda|$, given exact values for coefficients of L, is straightforward and numerically well-conditioned, and for practical purposes may be regarded as exact. The main approximation error comes rather from the computation of coefficients A and B in (1.4) through solution of the traveling-wave ordinary differential equation (1.8), which is likewise a standard and relatively well-conditioned problem; here we use a fourth-order Runge-Kutta method, for which analytical error estimates may be found, for example, in [SB]. For large $|\lambda|$, it is rather the $\mathcal{O}(|\lambda|)$ exponential growth rate in the eigenvalue ordinary differential equation that dominates the growth of errors; indeed, it is this consideration that effectively limits the size of our contours in the winding-number calculations described above. However, again, the relevant analytic error bounds are standard and straightforward.

We therefore omit the discussion of analytical error estimates, instead carrying out a numerical convergence study. Specifically, we use Richardson extrapolation to compute "exact values" to which we compare when we calculate relative errors and to check the convergence of D as the step size h becomes small. The resulting estimated errors are seen to be quite small, consistent with the above discussion.

Numerical experiments. We now describe the results of our numerical experiments for the two classes of systems discussed in Section 7.

Van der Waals gas or solid mechanics. Our first set of experiments is for the viscous-capillary p-system (7.1) with standard double-well potential (7.2). As discussed in Section 7, periodic solutions of this model are of necessity stationary, satisfying the Hamiltonian system (7.4) with $s = 0$, and this system features for $v_- = \pm 1$ a one-parameter family of heteroclinic two-cycles, indexed by u_- due to Galilean invariance in the speed u, in which there lie nested families of periodic orbits. Likewise, there exists a two-parameter family of homoclinic cycles for v_- in range $[0.55, 1)$, and u_- again arbitrary by Galilean invariance, in which there lie nested families of periodic orbits. Without loss of generality (using translation invariance), we may fix $u_- = 0$, reducing our study to a single 2-cycle and a one-parameter family of homoclinic orbits, and their enclosed periodic orbits, see Figs. 6 (top) and 6 (bottom) below.

First, we use a fourth-order Runge-Kutta method to get a profile (v, u) by solving the Hamiltonian system. By plotting v versus u, we can see clearly there exist

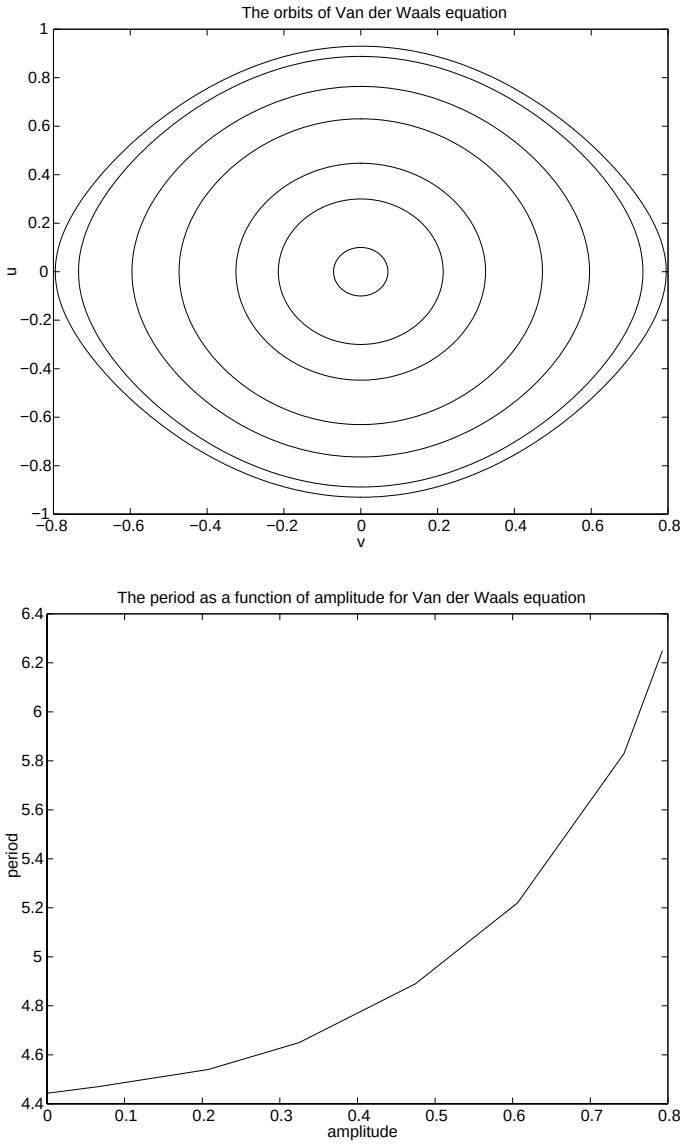

Fig. 2. Existence of periodic orbits (*top)*; Period as a function of amplitude (*bottom)*.

periodic orbits (Fig. 2 (top)) inside the two cycle. From these orbits, we observe a monotone relationship between the periods and the amplitudes (Fig. 2 (bottom)). Second, we use the method again to solve (2.7). Finally, we use the LU decomposition method to get a value of D. We also find periodic orbits and the monotone relationship inside the homoclinic orbit numerically. We study several periodic orbits in each cycle.

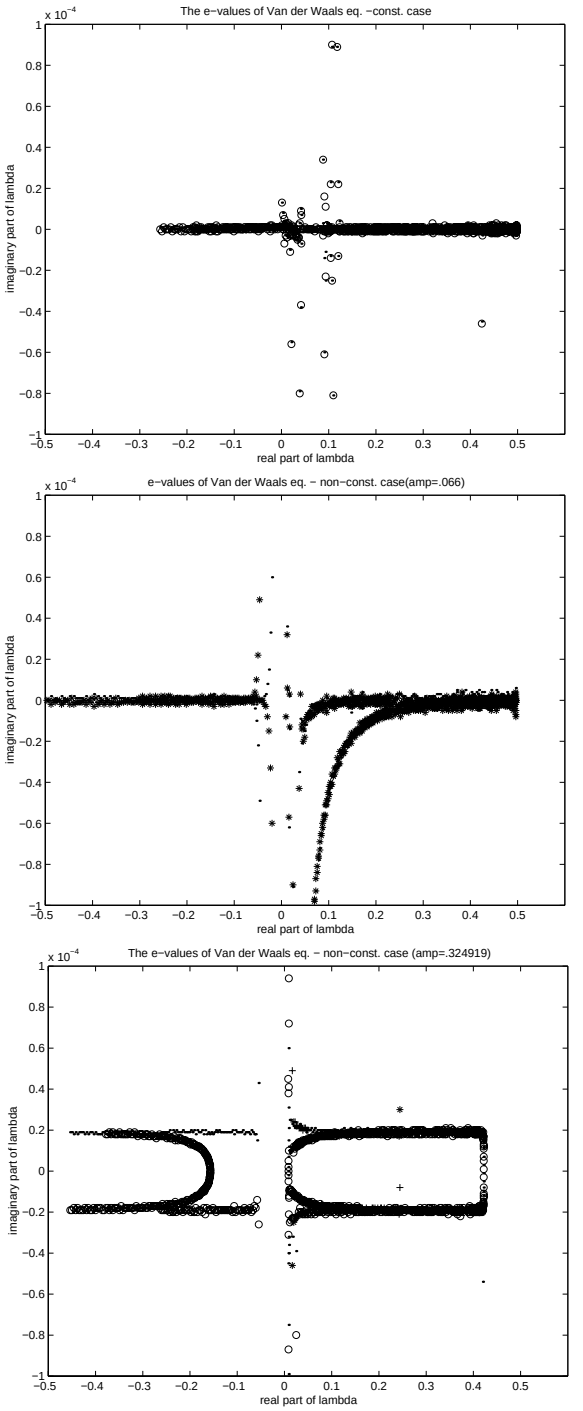

Fig. 3. Spectral curves of the Evans function D; Part I.

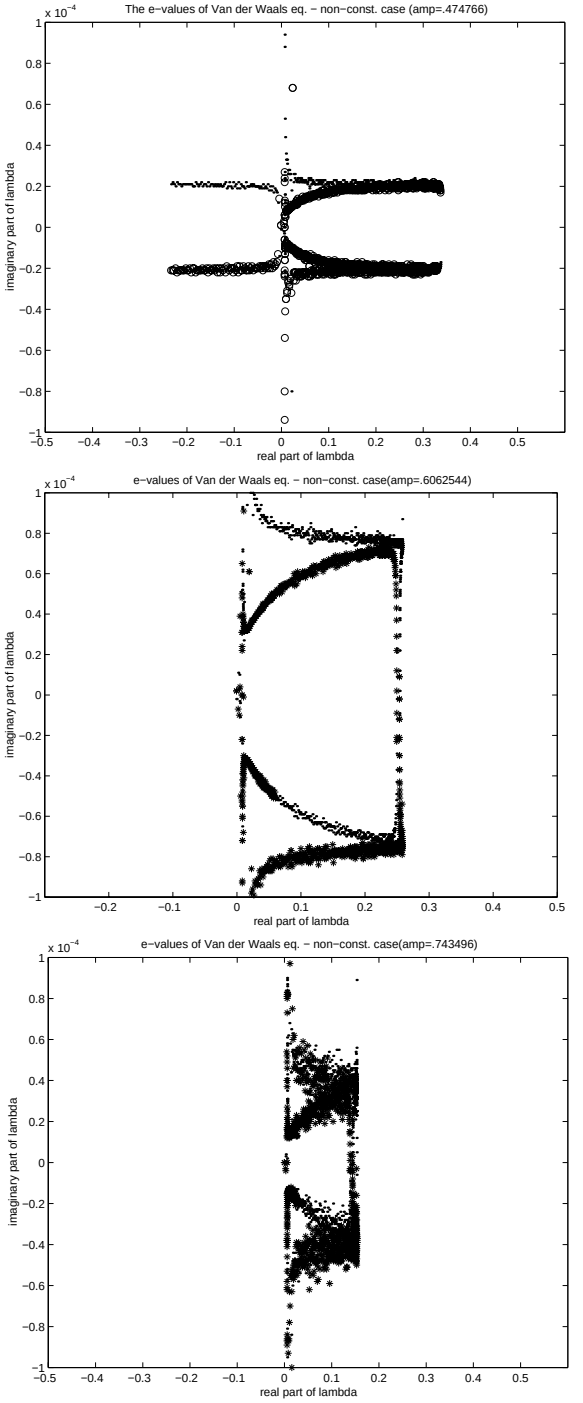

Fig. 3. Spectral curves of the Evans function D; Part II.

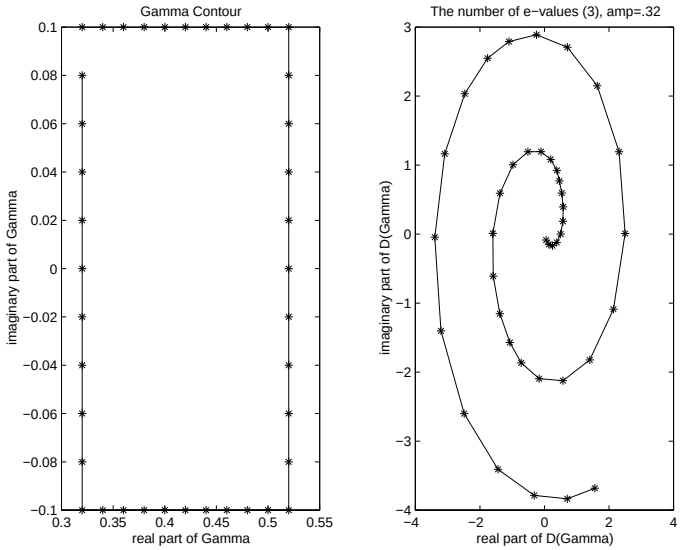

Fig. 4. The number of unstable eigenvalues in the two-cycle case.

Figure 3 shows spectral curves of L, or zero sets of D, for various periodic orbits within the 2-cycle depicted in Fig. 2 (top), starting with the (zero amplitude) constant-coefficient case and shows how the spectral curves are changed as the amplitude becomes large. We see what differences are made by change of amplitudes. These figures are extremely illuminating, showing in a way that calculations cannot, the detailed evolution of the spectrum as the amplitude of the underlying periodic orbit is varied from zero (constant-coefficient case) to the limiting amplitude as orbits approach their bounding poly-cycle. They both verify and amplify the observations obtained earlier by Evans function calculations. In particular, we immediately see that instability is rather dramatic, whereas the analytical results via Taylor expansion about the origin imply only that there exist infinitesimally unstable spectra; moreover, this instability is not confined to small- or large-amplitude limits, but persists across all amplitudes.

This suggests the strategy described above for numerical verification of instability; namely, to fix k at the value k^* corresponding to the maximally unstable spectrum $\lambda^* = \lambda(k^*)$ obtained by graphical examination, then perform a winding-number calculation on a well-chosen contour about λ^*.

As for stability results, Figs. 4 and 5 show Γ and $D[\Gamma]$ for periodic waves inside a two cycle and a homoclinic orbit respectively. Here, $D[\Gamma]$ is normalized by the mapping $D \longmapsto 0.1 * (i + 1) * D/|D|$ for $i = 0, 1, \ldots, 39$ (i is the index of λ on the contour Γ). The winding numbers are greater than 1 in both cases so the periodic waves are unstable.

We next perform the error analysis that was mentioned earlier. There is no analytic solution of the eigenvalue ordinary differential equation (2.7) for the van der Waals equations. We have to rely entirely on numerical estimates to gauge the

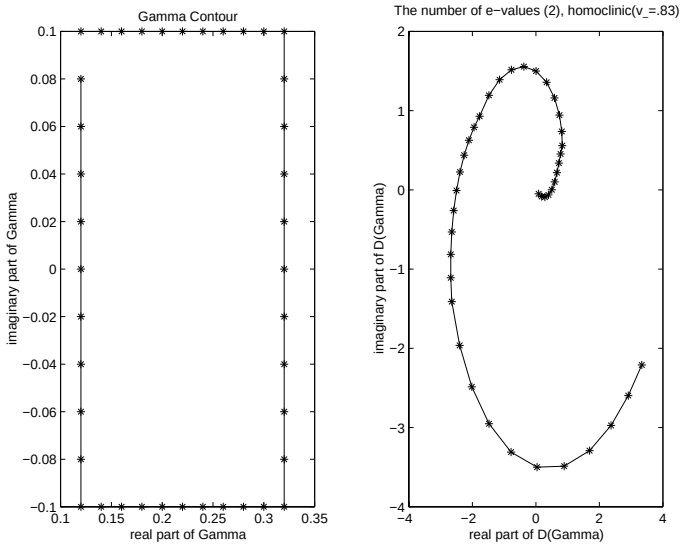

Fig. 5. The number of unstable eigenvalues in the two-cycle case.

accuracy of the Evans function method. In the tables below, third-order polynomial extrapolation was used to compute the values for $\tau = 0$ where τ is a local truncation error depending on the step size h, i.e., $\tau := Ch^4$ for some positive constant C (recall that the error to lowest order comes from solution of the profile equation by the fourth-order Runge-Kutta scheme).

Starting with the extrapolation results, examine Tables 1 and 2, which describe an illustrative calculation when the amplitude of periodic orbit is 0.32. The values chosen for λ are the points on Γ closest to and furthest from the center of Γ; in practice, these are found to give the extrema of errors. The extrapolated values are used as exact values in computing extrapolated relative errors. Note that $\tau = 10^{-6}$ is sufficient for calculating $D(\lambda, k)$ with approximate estimated accuracy 0.05.

Table 1. $D(0.32)$ for the van der Waals equations

τ	$D(0.32)$	Extrapolated Relative error
10^{-5}	3.358392	0.0121955
10^{-6}	3.358958	0.0120290
10^{-7}	3.359097	0.0119882
10^{-8}	3.399841	0.0000041
.	.	
.	.	
.	.	
0	3.399855	

Table 2. $D(0.52 - 0.1i)$ for the van der Waals equations

τ	$D(0.52 - 0.1i)$	Extrapolated Relative error
10^{-5}	$-4.636345 - 12.13182i$	0.0082597282
10^{-6}	$-4.636959 - 12.13066i$	0.0082772553
10^{-7}	$-4.637134 - 12.13046i$	0.0006327496
10^{-8}	$-4.722007 - 12.19752i$	0.0000185195
.	.	
.	.	
.	.	
0	$-4.721931 - 12.19775i$	

Similar calculations were carried out for all mesh points λ on the contours for each periodic orbit under consideration. For example, in the two-cycle case, we tested all periodic orbits indicated in Fig. 6 (top). The points in the figure represent the amplitudes of each periodic orbit. *Note: translation invariance greatly reduces the dimension of the problem.* Likewise we considered homoclinic profiles with vertices $v_- \in [0.55, 1)$ with vertex mesh 0.05 (see Fig. 6 (bottom)). For each homoclinic case, we then computed periodic orbits with amplitude mesh $O(0.01)$ where amplitude $\in [0, O(0.1)]$. In each case, the winding number was found to be greater than 1. The bounds for the winding-number calculations were found conservatively to be of order 10^{-2}, i.e., the worst-case Rouché error over all calculations was

$$\max \frac{|\triangle D|}{|D|} \leqq C10^{-2} << 1/2,$$

for some constant C (Table). This is comfortably below the bound 1 needed to apply Rouché's Theorem. Thus, we have numerical instability across the whole parameter range of existence.

As discussed in the main body of the paper, there are various interesting transitions of the number of unstable 0-eigenvalues of the periodic waves with respect to different amplitude. Recall that the small-amplitude limit is the constant-coefficient case. For fixed $k = 0$, the Evans function has four roots at the origin if the amplitude is zero, and three roots at zero otherwise when $n = 2$; see Remark 4.4. But, we can track a fourth small root of D as the amplitude changes. When the amplitude is small, the fourth root is typically in the left half-plane of Re (λ) (Remark 4.4). In the homoclinic case, as the amplitude becomes large, the fourth root moves from the left to the right half-plane crossing the origin (Fig. 7); see Remark 5.11. For the two-cycle case, no such transition occurs.

The quadratic-flux models. We next consider the class of quadratic-flux models (7.16) with identity viscosity matrix $B = I$, applying the same methods that we used for the van der Waals equations. First, we get a profile (u, v) by solving (7.17). By plotting u versus v, we can see clearly that there exist periodic orbits (Fig. 8 (top)). From these orbits, we observe that there is a monotone relationship between the

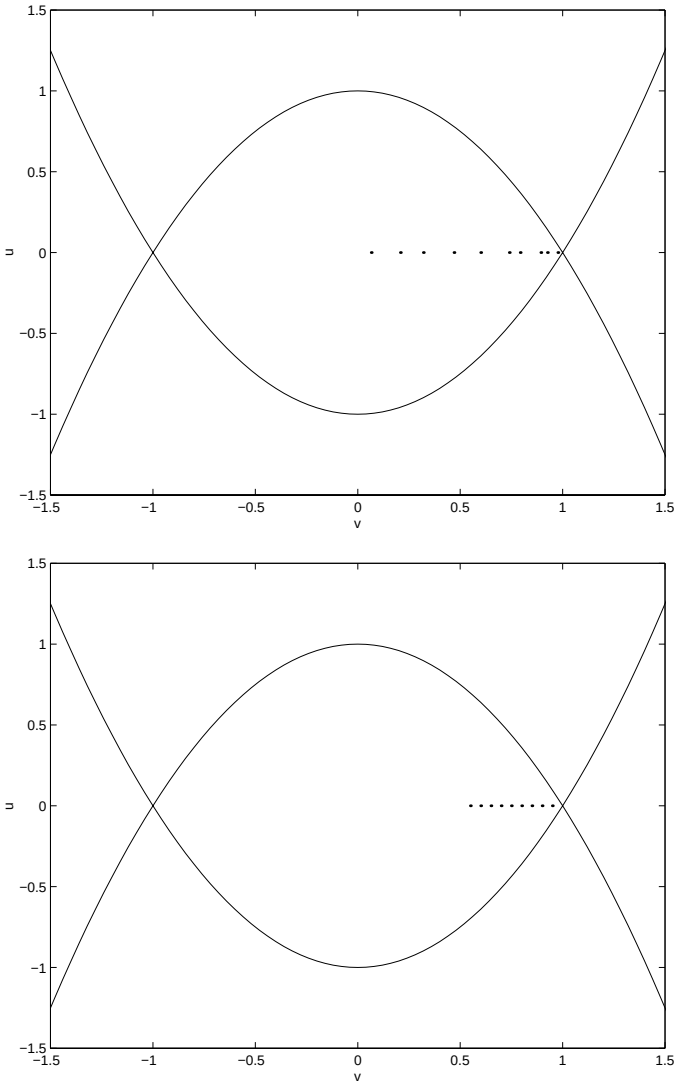

Fig. 6. The plotted points represent the amplitudes for which the experiments were carried out in the two-cycle case (*top*); The plotted points represent the amplitudes for which the experiments were carried out in the homoclinic case (*bottom*).

periods and the amplitudes (Fig. 8 (bottom)). Finally, we use the LU decomposition method to get a value of D. We have spectral curves of λ with respect to various amplitudes (Fig. 9).

The quadratic-flux model admits, for $s = 0$, a single 3-cycle solution, a 1-parameter family of 2-cycle solutions, and a 2-parameter family of homoclinic solutions, each containing a 1-parameter family of nested periodic orbits. We restrict

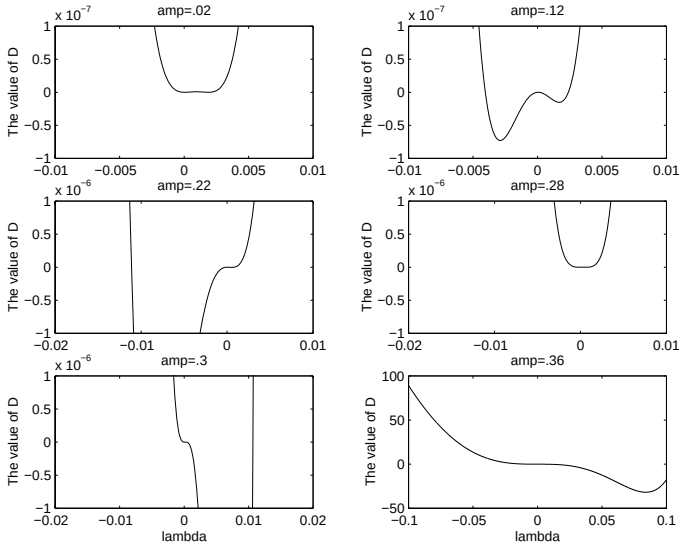

Fig. 7. Transition of the number of unstable 0-eigenvalues for the van der Waals equations, homoclinic case.

attention to the case s near zero, for which these are the only periodic solutions. The location of 3- and 2-cycles may be determined analytically; however, a new issue as compared to the van der Waals case is that the region of existence for homoclinic solutions is no longer analytically obtainable. Note: the regions of existence for two-cycles and three-cycles are analytically obtainable, as discussed in [AMPZ.3] and [GZ]. We determine the region of existence of homoclinic orbits numerically by varying (u_-, v_-) where $u_- = (-0.86, 0.86)$, $v_- \in [-0.5, 0.5)$. Figure 10 shows the break-up of the homoclinic orbit of this model. Figure 11 (top) shows the tested points (u_-, v_-) which are vertices of homoclinic orbits $(\cdot)$ and two-cycles (*), respectively. The vertices of the (unique) three-cycle are the three vertices of the surrounding triangle, the vertices of two-cycles lie on the edges, and the vertices of homoclinic orbits lie within shaded region (Fig. 11 (bottom)). For homoclinic orbits, we only need to treat the region of (u_-, v_-) inside the triangle since every outside point has a corresponding inside point yielding the same dynamical system (i.e., stationary points occur in pairs, one inside, one outside).

Inside each poly-cycle, we find several periodic orbits. To these, we apply the error analysis and the winding-number calculations as for the previous model. The same error analysis applies here as in the previous section so we shall not discuss this aspect. The maximum Rouché error over the entire region of testing was $C10^{-3}$ for some positive constant C, where in each case the winding number was greater than 1. Figures 12, 13, and 14 show the instability of each representative periodic orbit within three-cycle, two-cycle and homoclinic configurations. We see that small-amplitude orbits and also large-amplitude orbits lying near the three-cycle are unstable, as shown in Theorem 7.4, and also intermediate-amplitude orbits are

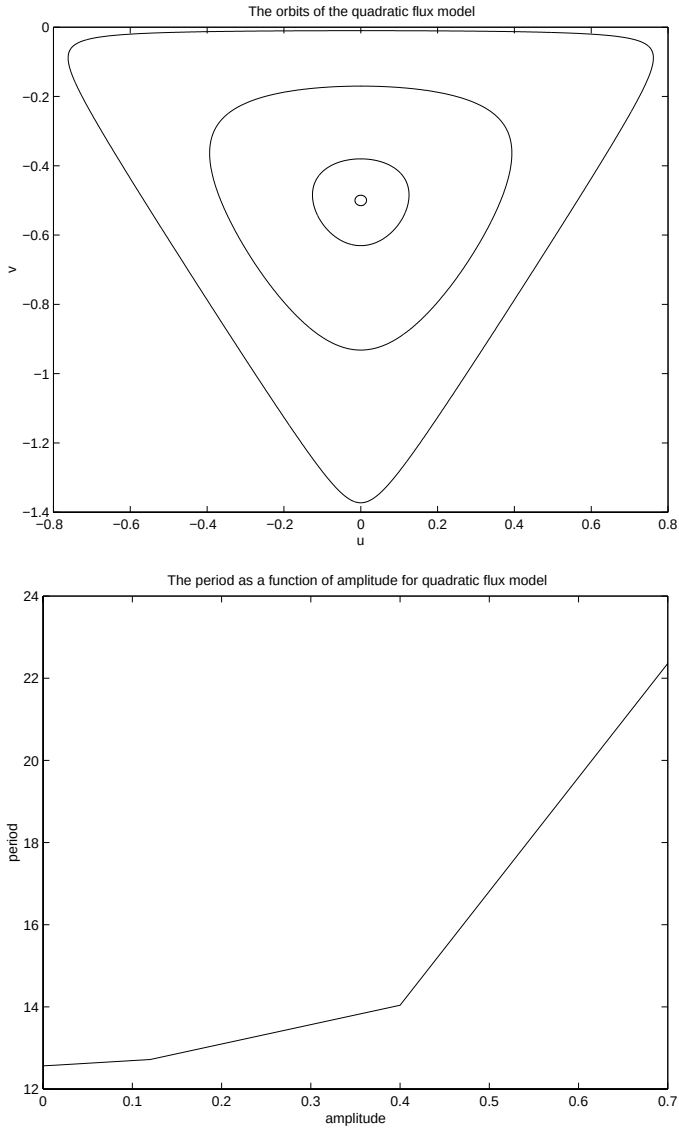

Fig. 8. Existence of periodic orbits (*top*); Period as a function of amplitude (*bottom*).

unstable. *Thus, for this model system, too, we have instability across the whole region of existence.*

Finally, similarly as in the case of the van der Waals equations, we may track the number of unstable 0-eigenvalues of the periodic waves with respect to amplitude in the homoclinic, two-, and three-cycle cases. The result in the homoclinic case is that there is a transition from zero to one unstable root as amplitude increases. In the two- and three-cycle cases, there is no such transition, indicating that waves of all

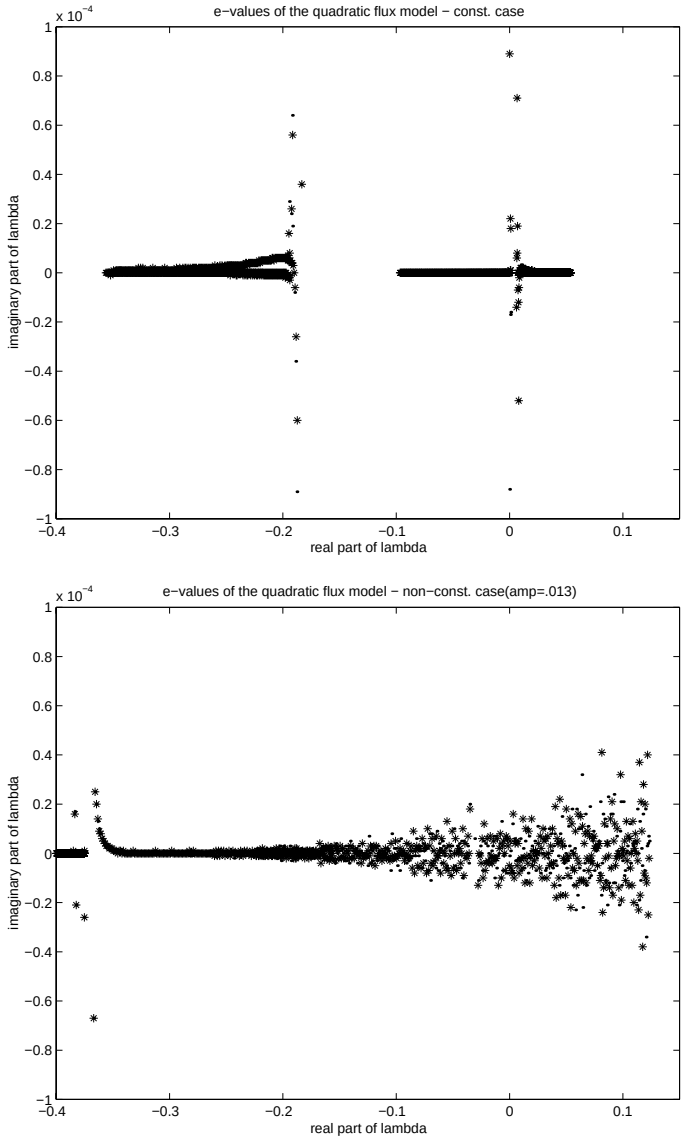

Fig. 9. The spectral curves of Evans function D; Part I.

amplitudes are stable under T-periodic perturbations, even though they are unstable under perturbations of general period. (Recall, T-periodic stability can be shown analytically for small-amplitude waves by consideration of the constant-coefficient case; see Remark 4.4.)

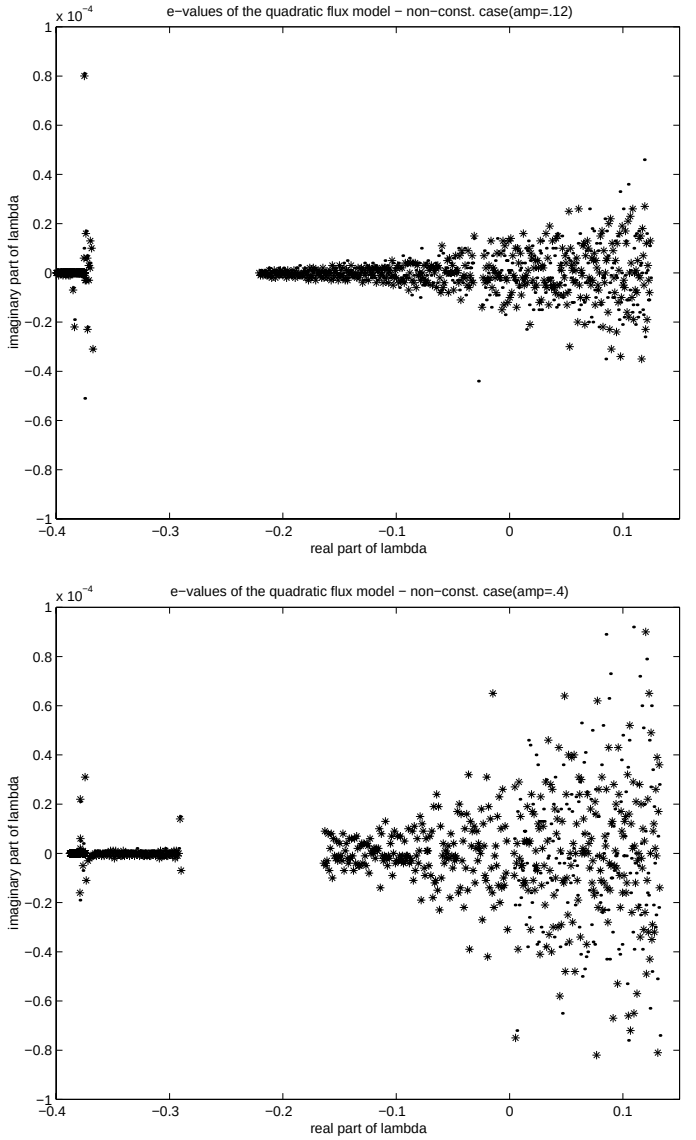

Fig. 9. The spectral curves of Evans function D; Part II.

Discussion. The instability of stationary periodic solutions of the example systems of Section 7 has been shown numerically. The code is general and easy to manipulate. It would be quite interesting, for more general systems, to either establish analytically a corresponding result of uniform instability or find a counter-example of a stable wave. Note that the code can be used also to investigate stability (for all k, not one k), though it has some difficulties near $k = 0$ due to numerical sensitivity

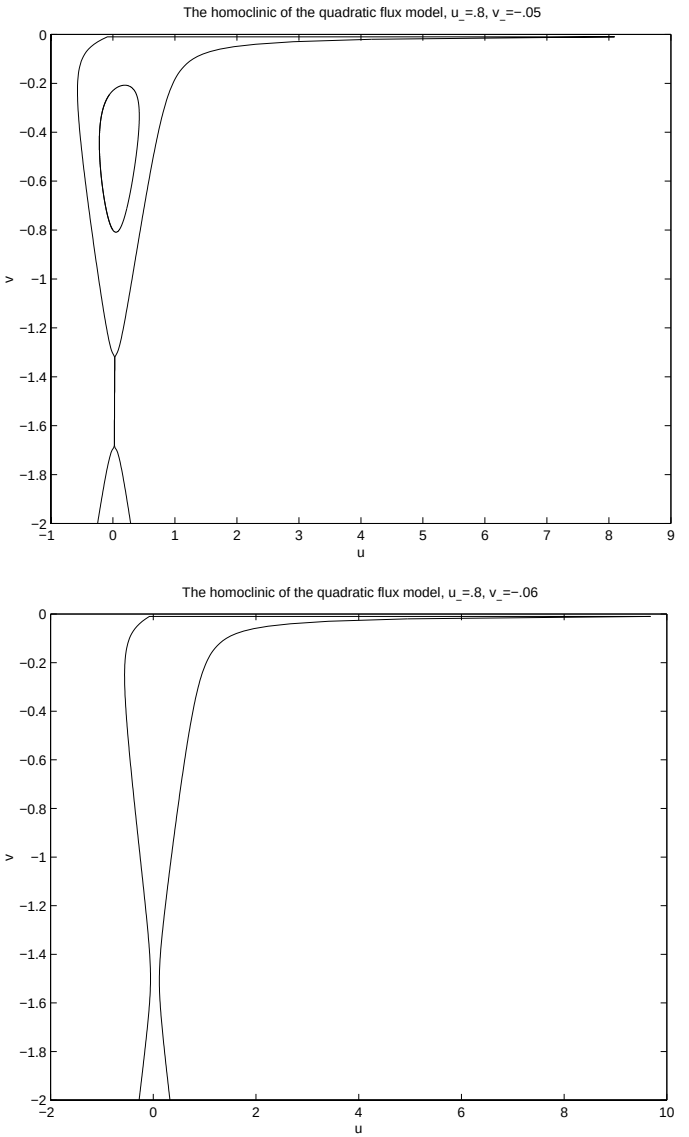

Fig. 10. The break-up of the homoclinic orbit.

associated with the multiple root in λ occurring there. This allows the systematic exploration of periodic wave stability for families of conservation laws, and also for Cahn-Hilliard and reaction-diffusion equations.

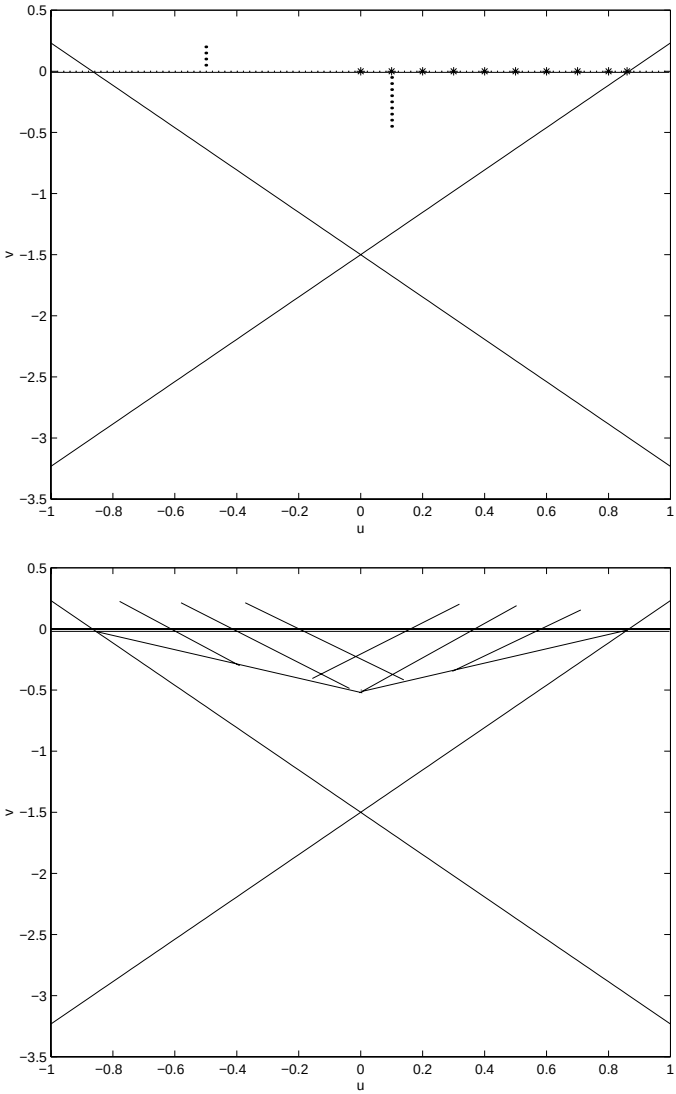

Fig. 11. The plotted points represent the vertices of one- and two-cycle for which the experiments were carried out (*top*); The region where vertices of homoclinic orbits lie (*bottom*).

Appendix B. Stationary phase approximation

In this appendix, we reproduce some unpublished computations of [AMPZ.5] referred to in the introduction, concerning the linear response under perturbation of a linearly unstable constant solution $u \equiv u_0$ of a conservation law with viscosity (1.1). Consider the linearized equation (1.4), where A and B are now constant.

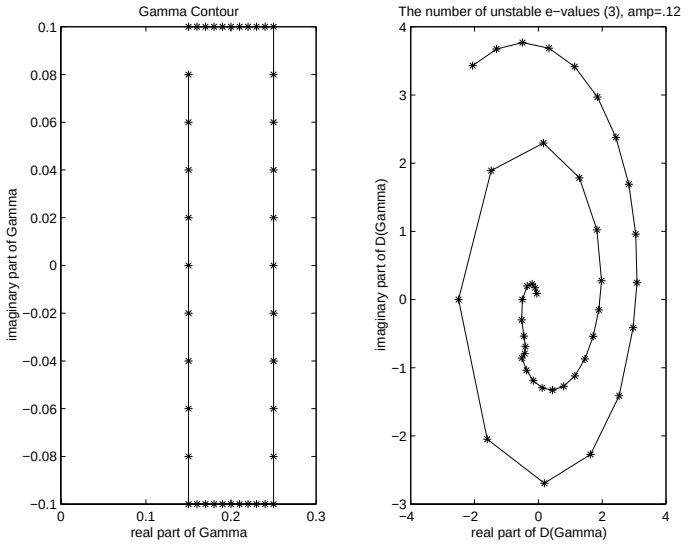

Fig. 12. The number of unstable eigenvalues, three-cycle case.

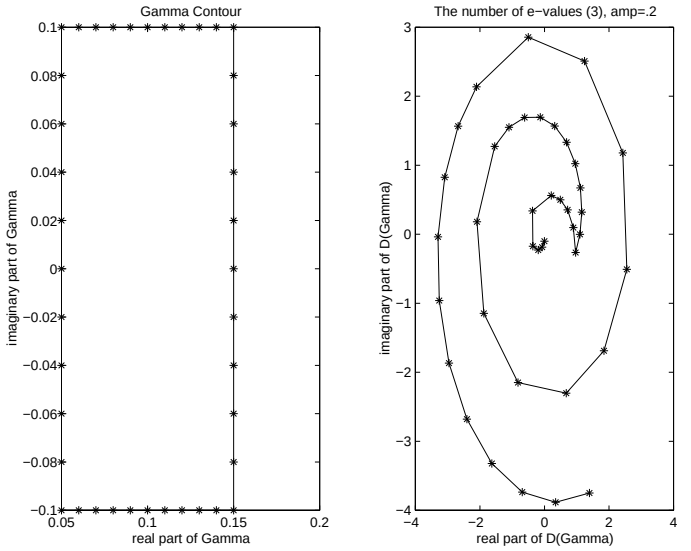

Fig. 13. The number of unstable eigenvalues, two-cycle case.

Taking the Fourier transform, we obtain

$$\hat{v}_t = P(ik)\hat{v} := (-ikA - k^2 B)\hat{v}. \tag{10.1}$$

The fundamental solution of (10.1) is clearly $\hat{\Psi}(k,t) = e^{P(ik)t}$, whence the fundamental solution of (1.4), i.e., the solution with initial data given by a Dirac delta

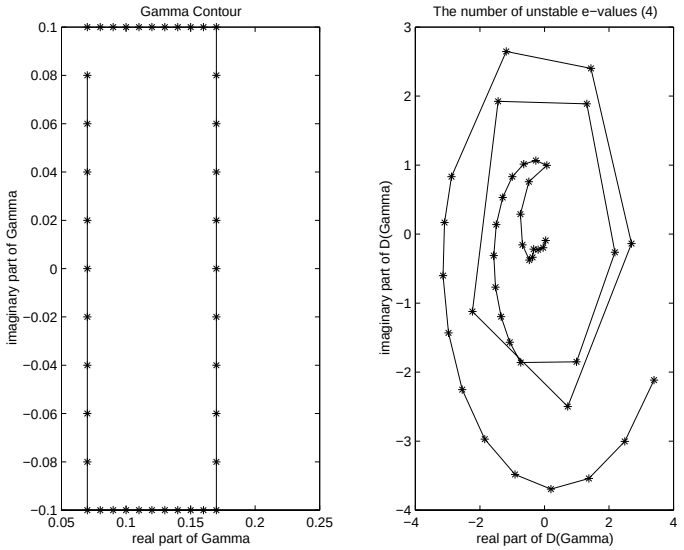

Fig. 14. The number of unstable eigenvalues, homoclinic case.

function centered at the origin, is given by the inverse Fourier transform

$$\Psi(x,t) = \frac{1}{2\pi}\int_{-\infty}^{+\infty} e^{ikx}e^{P(ik)t}\,dk, \tag{10.2}$$

and the Green function for (1.4) by $G(x,t;y) = \Psi(x-y,t)$.

The n eigenvalues of the symbol $P(ik)$ determine n dispersion relations

$$\lambda = \lambda_j(k), \quad j = 1,\dots,n, \tag{10.3}$$

with linearized stability corresponding to the condition $\operatorname{Re}\lambda_j \leqq 0$ for all $k \in \mathbb{R}$. Denote by k_j^* the critical frequency at which $\operatorname{Re}\lambda_j$ takes on its maximum value. For simplicity, we restrict attention to the generic situation where λ_j is isolated from the rest of the spectrum of $P(ik)$ at $k = k_j^*$, and $\lambda_j(k_j^*)$ is a nondegenerate maximum. Thus, λ_j admits a second-order Taylor expansion

$$\lambda_j(k) = \lambda_j(k_j^*) - i\alpha_j(k-k_j^*) - \beta_j(k-k_j^*)^2 + \cdots \tag{10.4}$$

about k_j^*, where α_j is real, and $\operatorname{Re}\beta_j > 0$. Let $R_j(k) = R_j(k_*) + \cdots$ and $L_j(k) = L_j(k_*) + \cdots$ denote right and left eigenvectors and $\Pi_j := R_jL_j^*/\langle R_j, L_j\rangle$ the spectral projection of P associated with λ_j.

Decomposing (10.2) by spectral resolution as $\Psi(x,t) = \sum_j \Psi_j(x,t)$, where

$$\Psi_j(x,t) := \sum_j \frac{1}{2\pi}\int_{-\infty}^{+\infty} e^{ikx}e^{\lambda_j(k)t}\Pi_j(k)\,dk, \tag{10.5}$$

we may estimate each of the Ψ_j by stationary phase approximation about k_j^* as

$$\begin{aligned}\Psi_j(x,t) \sim \bar{\Psi}_j &:= \frac{1}{2\pi}\int_{-\infty}^{+\infty} e^{ikx} e^{(\lambda_j(k_j^*)-i\alpha_j(k-k_j^*)-\beta_j(k-k_j^*)^2)t}\,\Pi_j(k_j^*)\,dk \\ &= \frac{1}{2\pi} e^{ik_j^* x+\lambda(k_j^*)t}\,\Pi_j(k_j^*)\int_{-\infty}^{+\infty} e^{i(k-k_j^*)x} e^{(-i\alpha_j(k-k_j^*)-\beta_j(k-k_j^*)^2)t}\,dk.\end{aligned} \tag{10.6}$$

Let us now restrict ourselves to the simplest case $B = I$. In this situation, the dispersion relations are exactly $\lambda_j(k) = -ika_j - k^2$, where a_j are the eigenvalues of A, and the associated eigenprojections Π_j are just the eigenprojections $r_j l_j^*/\langle r_j, l_j\rangle$ of A associated with a_j, where r_j and l_j denote associated right and left eigenvectors of A. Thus, linear stability is equivalent to reality of a_j, or hyperbolicity of the first-order coefficient A. By direct calculation, we find that $k_j^* = \text{Im } a_j/2$, $\alpha_j = \text{Re } a_j$, $\lambda(k_j^*) = (\text{Im } a_j/2)^2 - i\text{Re } a_j \text{Im } a_j/2$, and so

$$\alpha_j = -\text{Im } \lambda(k_j^*)/k_j^*. \tag{10.7}$$

Likewise, noting that β_j is real, we may explicitly carry out the Fourier inversion in the final factor of (10.6) to obtain

$$\begin{aligned}\bar{\Psi}_j &= e^{ik_j^* x+\lambda(k_j^*)t}\,\Pi_j(k_j^*) \times \frac{e^{-(x-\alpha_j t)^2/4\beta_j t}}{\sqrt{4\pi\beta_j t}} \\ &= e^{\text{Re } \lambda(k_j^*)t}\,\frac{r_j l_j^*}{\langle r_j, l_j\rangle} \times \frac{e^{ik_j^*(x-\alpha_j t)} e^{-(x-\alpha_j t)^2/4t}}{\sqrt{4\pi t}} \\ &= e^{(\text{Im } a_j/2)^2 t}\,\frac{r_j l_j^*}{\langle r_j, l_j\rangle} \times \frac{e^{i(\text{Im } a_j/2)(x-\text{Re } a_j t)} e^{-(x-\text{Re } a_j t)^2/4t}}{\sqrt{4\pi t}},\end{aligned} \tag{10.8}$$

where we have used (10.7) in the second equality. That is, the behavior of Φ in the jth mode is, to lowest order, that of a time-exponentially growing modulated Gaussian wave packet traveling with speed α_j, with exponential growth rate equal to the maximum real part $\text{Re } \lambda_j(k_j^*)$ of λ_j, and modulating spatial frequency equal to the critical frequency k_j^*.

In the case of a linearly stable mode $\text{Im } a_j = 0$, (10.8) reduces to the usual Gaussian "linear diffusion wave" $\frac{r_j l_j^*}{\langle r_j, l_j\rangle} \times \frac{e^{-(x-\text{Re } a_j t)^2/4t}}{\sqrt{4\pi t}}$ of [LZe]. By analogy, we might call (10.8) an "unstable linear diffusion wave." Note that unstable modes $\text{Im } a_j \neq 0$ group in conjugate pairs, with equal propagation speeds $\alpha_j = \text{Re } a_j$, and thus their diffusion waves combine to give a single real, sinusoidal diffusion wave of dimension two. The proper analogy is, therefore, to the "generalized diffusion wave" defined in [LZe] in the case of repeated real eigenvalues of A (the boundary case between strict hyperbolicity and ellipticity of A).

Example 10.1. For the equations of van der Waal gas dynamics or elasticity, we have $B = I$, and

$$A = df(u_0, v_0) = \begin{pmatrix} 0 & -1 \\ p'(v_0) & 0 \end{pmatrix}$$

has eigenvalues $a_j = \pm\sqrt{-p'(v_0)}$. Thus, linearized stability of the constant solution $(u, v) \equiv (u_0, v_0)$ is equivalent to $p'(v_0) < 0$, and failure of stability entails a pair of pure imaginary eigenvalues $a_j = \pm i\tau$. In this case, therefore, there is a single conjugate pair of *standing* unstable linear diffusion waves, $\alpha_j \equiv 0$, with time-exponential growth rate $e^{\tau^2 t/4}$ and modulating spatial frequency $e^{i\tau x/2}$.

Application to pattern formation. Now, let us consider the implications of the linear estimate (10.8) on the behavior under perturbation of solutions of the nonlinear equations, for initial data approaching a linearly unstable constant state u_∞ as $x \to +\infty$. In view of the global nonlinear structure of our models, let us make the crude approximation that nonlinear effects take over at some prescribed amplitude A, turning off the time-exponential growth and converting the sinusoidal oscillations of the linearized approximation (10.8) to a series of traveling fronts *moving with approximately zero speed* (the last assumption implies some normalization to achieve a rest frame). Looking at a single unstable mode j, the picture that emerges from this crude model on the half line $[0, +\infty)$ is an oscillatory pattern of phase transitions separated from the constant state by a modulated front whose location $x(t)$ is determined by the property that

$$|\bar{\Psi}(x_j(t), t)| \sim A, \tag{10.9}$$

i.e., ignoring the algebraic factor $t^{-1/2}$ in (10.8), travels with approximate speed σ_j determined by $(\text{Im } a_j/2)^2 t - (\sigma_j t - \alpha_j t)^2/4t = 0$. Solving, and recalling that $\alpha_j = \text{Re } a_j$, $\text{Re } \lambda(k_j^*) = (\text{Im } a_j/2)^2$, we obtain a value of

$$\sigma_j = \text{Re } a_j + |\text{Im } a_j| \tag{10.10}$$

for the approximate front speed.

Since waves under this model are "born" in the linearized regime, we can estimate the approximate wave-length inherited in the nonlinear regime by dividing the distance $d = \sigma_j t$ swept out by the front $x(t)$ from time 0 to time t, divided by the number of peaks of the linearized unstable diffusion wave (10.8) that it has crossed during that time. Working in the rest frame $x = \alpha_j t$ of the diffusion wave, we find that the number of peaks is $(\sigma_j - \alpha_j)t$ divided by the wavelength $2\pi/k_j^* = 2\pi/\text{Im } a_j/2$ of its spatial modulation, yielding an estimated wavelength of

$$T_j = \frac{\sigma_j t}{\frac{(\sigma_j - \alpha_j)t}{(2\pi/k_j^*)}}.$$

This predicts an average (Doppler-shifted) frequency for the nonlinear pattern of

$$\begin{aligned} \tilde{k}_j = 2\pi/T_j &= k_j^* \Big(\frac{\sigma_j - \alpha_j}{\sigma_j} \Big) \\ &= k_j^* \Big(\frac{|\text{Im } a_j|}{\text{Re } a_j + |\text{Im } a_j|} \Big). \end{aligned} \tag{10.11}$$

In the (standing) case $\alpha_j = \text{Re } a_j = 0$ of Example 10.1, this is just the critical frequency $k_j^* = \text{Im } a_j/2$. Note: here and above we are implicitly assuming that the

front speed σ_j is positive, i.e., the pattern is expansive. This is in fact a necessary condition for pattern formation to occur.

Numerical experiments in [AMPZ.4] showed close agreement between the predictions of (10.10) and (10.11) and behavior of actual patterns in solutions of (1.1). Likewise, the condition $\sigma_j \geqq 0$ was seen to well predict *nonlinear* instability, and the appearance of pattern formation, as model parameters (e.g., Riemann endstates) were varied.

Remark 2. In the linearly stable case, LIU & ZENG [LZe] derive also a self-similar *nonlinear* diffusion wave refining the linear estimate (10.8), by judiciously appending to an approximately diagonalized version of the linearized equations (1.4) the "diagonal" quadratic-order terms in the Taylor expansion of the nonlinear flux f. This approximation makes essential use of the small-amplitude nature of solutions. In the large-amplitude linearly unstable case, we have no such simple description of a nonlinear diffusion wave; indeed, the relevant entity seems to be the entire metastable pattern described above. We might neatly summarize the conclusions of this paper (together with those of [AMPZ.4, AMPZ.5]) as suggesting that patterns observed in dynamical phase-transitional models represent *metastable nonlinear diffusion waves* rather than *stable periodic states*.

Acknowledgements. K. ZUMBRUN thanks ROB GARDNER for several illuminating conversations regarding his foundational work on periodic stability. Thanks are also due to RICHARD LAUGESEN for pointing out the result of [Sc, LP] used in Section 7 to establish monotonicity of the period of a double-well oscillator, and to the referee for pointing out the references [BMi.1,BMi.2,M.1,M.2]. Finally, we would like to thank to EVA MARIE ELLIOT of Indiana University for her skillful and efficient typing of this manuscript. Our research was supported in part by the National Science Foundation under Grants No. DMS-9706842 and DMS-007065.

References

[AGJ] J. ALEXANDER, R. GARDNER & C. K. R. T. JONES, A topological invariant arising in the analysis of traveling waves, *J. Reine Angew. Math.* **410** (1990) 167–212.

[AMPZ.1] A. AZEVEDO, D. MARCHESIN, B. PLOHR, & K. ZUMBRUN, Nonuniqueness of solutions of Riemann problems, *Z. Angew. Math. Phys.* **47** (1996) 977–998.

[AMPZ.2] A. AZEVEDO, D. MARCHESIN, B. PLOHR & K. ZUMBRUN, Bifurcation from the constant state of nonclassical viscous shock waves, *Commun. Math. Phys.* **202** (1999) 267–290.

[AMPZ.3] A. AZEVEDO, D. MARCHESIN, B. PLOHR & K. ZUMBRUN, Capillary instability in multiphase flow models. To appear in *Z. Angew. Math. Phys.*

[AMPZ.4] A. AZEVEDO, D. MARCHESIN, B. PLOHR & K. ZUMBRUN, Long-lasting diffusive solutions for systems of conservation laws, *VI Workshop on Partial Differential Equations, Part I* (*Rio de Janeiro, 1999*), Mat. Contemp. **18** (2000), 1–29.

[AMPZ.5] A. AZEVEDO, D. MARCHESIN, B. PLOHR & K. ZUMBRUN, *private communication*, unpublished numerical computations (1996).

[BSZ] S. BENZONI-GAVAGE, D. SERRE, & K. ZUMBRUN, Alternate Evans functions and viscous shock waves, *SIAM J. Math. Anal.* **32** (2001) 929–962.

[BMi.1] T. BRIDGES & A. MIELKE, A proof of the Benjamin-Feir instability, *Arch. Rational Mech. Anal.* **133** (1995) 145–198.

[BMi.2] T. BRIDGES & A. MIELKE, Instability of spatially-periodic states for a family of semilinear PDE's on an infinite strip, *Math. Nachr.* **179** (1996) 5–25.

[Br.1] L. Q. BRIN, *Numerical testing of the stability of viscous shock waves*, Ph.D. dissertation, Indiana University, May 1998.

[Br.2] L. Q. BRIN, Numerical testing of the stability of viscous shock waves, *Math. Comp.* **70** (2001) 1071–1088.

[BZ] L. Q. BRIN & K. ZUMBRUN, Analytically varying eigenvectors and the stability of viscous shock waves. To appear, *Mat. Contemp.*

[C] S. ČANIĆ, Nonexistence of Riemann solutions for a quadratic model deriving from petroleum engineering. Preprint (1998).

[CGS.1] J. CARR, M. GURTIN, & M. SLEMROD, Structured phase transitions on a finite interval, *Arch. Rational Mech. Anal.* **86** (1984) 317–351.

[CGS.2] J. CARR, M. GURTIN, & M. SLEMROD, One-dimensional structured phase transformations under prescribed loads, *J. Elasticity* **15** (1985) 133–142.

[CL] L. CAIRO & J. LLIBRE, *Integrability and algebraic solutions for planar polynomial differential systems with emphasis on the quadratic systems*, IME/USP (Universidade de São Paulo, Brazil) Report No. 2, (1999).

[CP] S. ČANIĆ & G. PETERS, On the oscillatory solutions in hyperbolic conservation laws, *Nonlinear Anal. Real World Appl.* **1** (2000) 287–314.

[DGK] A. DOELMAN, R. A. GARDNER, & T. KAPER, A stability index analysis of 1-D patterns of the Gray-Scott Model. *Mem. Amer. Math. Soc.* **155** (2002)

[E.1] J. W. EVANS, Nerve axon equations: I. Linear approximations, *Ind. Univ. Math. J.* **21** (1972) 877–885.

[E.2] J. W. EVANS, Nerve axon equations: II. Stability at rest, *Ind. Univ. Math. J.* **22** (1972) 75–90.

[E.3] J. W. EVANS, Nerve axon equations: III. Stability of the nerve impulse, *Ind. Univ. Math. J.* **22** (1972) 577–593.

[E.4] J. W. EVANS, Nerve axon equations: IV. The stable and the unstable impulse, *Ind. Univ. Math. J.* **24** (1975) 1169–1190.

[Es] E. ESZTER, *Evans function analysis of periodic travelling wave solutions of the FitzHugh-Nagumo system*, Doctoral thesis, University of Massachussetts, Amherst, 1999.

[FreZ] H. FREISTÜHLER & K. ZUMBRUN, *Examples of unstable viscous shock waves*, unpublished note, Institut für Mathematik, RWTH Aachen, February 1998.

[FL.1] H. FRID & I.-S. LIU, Oscillation waves in Riemann problems for phase transitions, *Quart. Appl. Math.* **56** (1998) 115–135.

[FL.2] H. FRID & I.-S. LIU, Oscillation waves in Riemann problems inside elliptic regions for conservation laws of mixed type, *Z. Angew. Math. Phys.* **46** (1995) 913–931.

[G.1] R. A. GARDNER, On the structure of the spectra of periodic travelling waves, *J. Math. Pures Appl.* (9) **72** (1993) 415–439.

[G.2] R. A. GARDNER, Spectral analysis of long wavelength periodic waves and applications, *J. Reine Angew. Math.* **491** (1997), 149–181.

[G.3] R. A. GARDNER, Instability of oscillatory shock profile solutions of the generalized Burgers-KdV equation, *Phys. D* **90** (1996) 366–386.

[GZ] R. GARDNER & K. ZUMBRUN, The Gap Lemma and geometric criteria for instability of viscous shock profiles, *Comm. Pure Appl. Math.* **51** (1998) 797–855.

[GH] J. GUCKENHEIMER & P. HOLMES, *Nonlinear oscillations, dynamical systems, and bifurcations of vector fields*, (Revised and corrected reprint of the 1983 original), Springer-Verlag, New York, 1990.

[GM] M. E. GURTIN & H. MATANO, On the structure of equilibrium phase transitions within the gradient theory of fluids, *Quart. Appl. Math.* **46** (1988) 301–317.

[HK] J. HALE & H. KOCAK, *Dynamics and bifurcations*, Texts in Applied Mathematics, 3. Springer-Verlag, New York, 1991.

[He] D. HENRY, *Geometric theory of semilinear parabolic equations*, Lecture Notes in Mathematics, Springer-Verlag, Berlin, 1981.

[HP] J. Hurley & B. Plohr, Some effects of viscous terms on solutions of Riemann problems, *Mat. Contemp.* **8** (2995) 203–204.

[IR] E. Infeld & G. Rowlands, *Nonlinear waves, solitons, and chaos*, Second edition, Cambridge University Press, Cambridge, 2000.

[Ja] R. D. James, The propagation of phase boundaries in elastic bars, *Arch. Rational Mech. Anal.* **73** (1980) 125–158.

[J] C. K. R. T. Jones, Stability of the travelling wave solution of the FitzHugh–Nagumo system, *Trans. Amer. Math. Soc.* **286** (1984) 431–469.

[KS] T. Kapitula & B. Sandstede, Stability of bright solitary-wave solutions to perturbed nonlinear Schrödinger equations, *Phys. D* **124** (1998) 58–103.

[Ka] S. Kawashima, *Systems of a hyperbolic–parabolic composite type, with applications to the equations of magnetohydrodynamics*, thesis, Kyoto University, 1983

[LP] R. Laugesen & M. Pugh, Properties of steady states for thin film equations, Euro. *J. Appl. Math.* **11** (2000) 293–351.

[LF] I.-S. Liu & H. Frid, Phase mixtures in dynamics of pseudoelasticity, *Contin. Mech. Thermodyn.* **7** (1995) 475–487.

[LZe] T.-P. Liu & Y. Zeng, *Large time behavior of solutions for general quasilinear hyperbolic–parabolic systems of conservation laws*, AMS memoirs **599** (1997).

[LZ.1] T.-P. Liu & K. Zumbrun, Nonlinear stability of an undercompressive shock for complex Burgers equation, *Commun. Math. Phys.* **168** (1995) 163–186.

[LZ.2] T.-P. Liu & K. Zumbrun, On nonlinear stability of general undercompressive viscous shock waves, *Commun. Math. Phys.* **174** (1995) 319–345.

[M.1] K. Maginu, Existence and stability of periodic traveling wave solutions to Nagumo's nerve equation, *J. Math. Biol.* **10** (1980), 133-153.

[M.2] K. Maginu, Stability of periodic traveling wave solutions with large spatial periods in reaction-diffusion systems, *J. Diff. Equation* **39** (1981), 73-99.

[MP] A. Majda & R. Pego, Stable viscosity matrices for systems of conservation laws, *J. Diff. Eqs.* **56** (1985) 229–262.

[Mi] A. Mielke, Instability and stability of rolls in the Swift-Hohenberg equation, *Commun. Math. Phys.* **189** (1997) 829–853.

[OZ] M. Oh & K. Zumbrun, Stability of periodic solutions of conservation laws with viscosity: Pointwise bounds on the Green function, *Arch. Rational Mech. Anal.* **166** (2003) 167–196.

[Pa] A. Pazy, *Semigroups of linear operators and applications to partial differential equations*, Applied Mathematical Sciences **44**, Springer-Verlag, 1983.

[PW] R. L. Pego & M. I. Weinstein, Eigenvalues, and instabilities of solitary waves, *Philos. Trans. Roy. Soc. London Ser. A* **340** (1992) 47–94.

[SS.1] B. Sandstede & A. Scheel, On the stability of periodic travelling waves with large spatial period, *J. Differential Equations* **172** (2001) 134–188.

[SS.2] B. Sandstede & A. Scheel, On the structure of spectra of modulated traveling waves, *Math. Nachr.* **232** (2001) 39–93.

[Sc] R. Schaaf, A class of Hamiltonian systems with increasing periods, *J. Reine Angew. Math.* **363** (1985) 96–109.

[SSh] S. Schecter & M. Shearer, Undercompressive shocks for non-strictly hyperbolic conservation laws, *J. Dynamics Differential Equations* **3** (1991), 199–271.

[Se.1] D. Serre, Entropie du mélange liquide-vapeur d'un fluide thermo-capillaire, *Arch. Rational Mech. Anal.* **128** (1994) 33–73.

[Se.2] D. Serre, *Transitions de phase et oscillations de grande amplitude*, Qualitative aspects and applications of nonlinear evolution equations (Trieste, 1990), 172–184, World Sci. Publishing, River Edge, NJ, 1991.

[Sh.1] M. Shearer, The Riemann problem for a class of conservation laws of mixed type, *J. Diff. Eqs.* **46** (1982) 426–443.

[Sh.2] M. Shearer, Nonuniqueness of admissible solutions of Riemann inintial value problems for a system of conservation laws of mixed type, *Arch. Rational Mech. Anal.* **93** (1986) 45–59.

[Sh.3] M. SHEARER, Dynamic phase transitions in a van der Waals gas, *Quart. Appl. Math.* **46** (1988) 631–636.

[SSMP] M. SHEARER, D. SCHAEFFER, D. MARCHESIN, & P. L. PAES-LEME, Solution of the Riemann problem for a prototype 2×2 system of nonstrictly hyperbolic conservation laws, *Arch. Rational Mech. Anal.* **97** (1987) 299–320.

[Sl.1] M. SLEMROD, The viscosity-capillarity approach to phase transitions. In: *PDEs and continuum models of phase transitions* (Nice, 1988), 201–206, Lecture Notes in Phys. **344**, Springer, Berlin–New York, 1989.

[Sl.2] M. SLEMROD, The vanishing viscosity-capillarity approach to the Riemann problem for a van der Waals fluid. In: *Nonclassical continuum mechanics* (Durham, 1986), 325–335, London Math. Soc. Lecture Note Ser., **122**, Cambridge Univ. Press, Cambridge–New York, 1987.

[Sl.3] M. SLEMROD, A limiting "viscosity" approach to the Riemann problem for materials exhibiting change of phase, *Arch. Rational Mech. Anal.* **105** (1989) 327–365.

[Sl.4] M. SLEMROD, Dynamic phase transitions in a van der Waals fluid, *J. Diff. Eqs.* **52** (1984) 1–23.

[Sl.5] M. SLEMROD, Admissibility criteria for propagating phase boundaries in a van der Waals fluid, *Arch. Rational Mech. Anal.* **81** (1983) 4, 301–315.

[ST] M. SLEMROD & A. E. TZAVARAS, Shock profiles and self-similar fluid dynamic limits, *Proceedings of the Second International Workshop on Nonlinear Kinetic Theories and Mathematical Aspects of Hyperbolic Systems (Sanremo, 1994). Transport Theory Stat. Phys.* **25** (1996) 531–541.

[Sm] J. SMOLLER, *Shock waves and reaction–diffusion equations*, Second edition, Grundlehren der Mathematischen Wissenschaften [Fundamental Principles of Mathematical Sciences], **258**. Springer-Verlag, New York, 1994.

[SB] J. STOER, & R. BULIRSCH, *Introduction to Numerical Analysis*, Springer-Verlag, New York, second edition, 1992.

[Z.1] K. ZUMBRUN, Dynamical stability of phase transitions in the p-system with viscosity-capillarity, *SIAM J. Appl. Math.* **60** (2000), 1913-1929.

[Z.2] K. ZUMBRUN, *Computation of scattering coefficients for phase transitional shock patterns*, unpublished note.

[Z.3] K. ZUMBRUN, Multidimensional stability of planar viscous shock waves, *Advances in the theory of shock waves*, 307–516, *Progr. Nonlinear Differential Equations Appl.* **47**, Birkhäuser Boston, Boston, MA, 2001.

[Z.4] K. ZUMBRUN, *Stability of viscous shock waves*, Lecture notes, Indiana University, 1998.

[ZH] K. ZUMBRUN & P. HOWARD, Pointwise semigroup methods and stability of viscous shock waves, *Indiana Math. J.* **47** (1998) 741–871.

[ZPM] K. ZUMBRUN, B. PLOHR, & D. MARCHESIN, Scattering behavior of transitional waves, *Mat. Contemp.* **3** (1992) 191–209.

[ZS] K. ZUMBRUN & D. SERRE, Viscous and inviscid stability of multidimensional planar shock fronts, *Indiana Univ. Math. J.* **48** (1999) 937–992.

Department of Mathematics
Indiana University
Bloomington, IN 47405-4301, USA
e-mail: myoh@indiana.edu
e-mail: kzumbrun@indiana.edu

(Accepted March 8, 2002)
Published online December 16, 2002 –